University of Nebraska - Lincoln
DigitalCommons@University of Nebraska - Lincoln

Nebraska Department of Transportation Research Reports

Nebraska LTAP

1-2020

Feasibility Study of Development of Ultra-High Performance Concrete (UHPC) for Highway Bridge Applications in Nebraska

Flavia Ribeiro Furtado de Mendonca
University of Nebraska-Lincoln, flavia@huskers.unl.edu

Mostafa Abo El-Khier
University of Nebraska - Lincoln, maboel-khier2@huskers.unl.edu

George Morcous
University of Nebraska-Lincoln, gmorcous2@unl.edu

Jiong Hu
University of Nebraska-Lincoln, jhu5@unl.edu

Follow this and additional works at: https://digitalcommons.unl.edu/ndor

 Part of the Transportation Engineering Commons

Ribeiro Furtado de Mendonca, Flavia; Abo El-Khier, Mostafa; Morcous, George; and Hu, Jiong, "Feasibility Study of Development of Ultra-High Performance Concrete (UHPC) for Highway Bridge Applications in Nebraska" (2020). *Nebraska Department of Transportation Research Reports*. 242.
https://digitalcommons.unl.edu/ndor/242

This Article is brought to you for free and open access by the Nebraska LTAP at DigitalCommons@University of Nebraska - Lincoln. It has been accepted for inclusion in Nebraska Department of Transportation Research Reports by an authorized administrator of DigitalCommons@University of Nebraska - Lincoln.

Feasibility Study of Development of Ultra-High Performance Concrete (UHPC) for Highway Bridge Applications in Nebraska

SPR-P1(18) M072

Flavia Mendonca
Graduate Research Assistant
Department of Civil Engineering
University of Nebraska-Lincoln

Mostafa Abo El-Khier
Ph.D. Candidate
Durham School of Architectural Engineering and Construction
University of Nebraska-Lincoln

George Morcous, PE., PhD
Professor
Durham School of Architectural Engineering and Construction
University of Nebraska-Lincoln

Jiong Hu, PhD
Associate Professor
Department of Civil Engineering
University of Nebraska-Lincoln

A Report on Research Sponsored by

Nebraska Department of Transportation (NDOT)

January 2020

Technical Report Documentation Page

1. Report No SPR-P1(18) M072	2. Government Accession No.	3. Recipient's Catalog No.	
4. Title and Subtitle Feasibility Study of Development of Ultra-High Performance Concrete (UHPC) for Highway Bridge Applications in Nebraska		5. Report Date January 2020	
		6. Performing Organization Code	
7. Author/s Flavia Mendonca, Mostafa Abo El-Khier, George Morocus and Jiong Hu		8. Performing Organization Report No.	
9. Performing Organization Name and Address University of Nebraska-Lincoln, Department of Civil Engineering Peter Kiewit Institute, Omaha, NE 68182-0178		10. Work Unit No. (TRAIS)	
		11. Contract or Grant No.	
12. Sponsoring Organization Name and Address Nebraska Department of Transportation 1400 Highway 2, PO Box 94759, Lincoln, NE 68509		13. Type of Report and Period Covered	
		14. Sponsoring Agency Code	
15. Supplementary Notes			

16. Abstract

Ultra-high performance concrete (UHPC) is a new class of concrete that has superior mechanical, durability, and workability properties that far exceed those of conventional concrete. To achieve these properties, a specific mix design with a very dense internal structure, fiber reinforcement, and low water-to-binder ratio (w/b) is commonly used. The goal of this research is to develop a non-proprietary UHPC mix with constituent materials that are readily available in the state of Nebraska for bridge construction applications. In developing this mix, the particle packing model is used, and an experimental study of the impact of various design parameters on the key properties of UHPC is conducted. Multiple series of UHPC mixtures are investigated with different types and quantities of aggregate, fibers, cement, supplemental cementitious materials (SCMs), high range water reducer (HRWR), w/b, total binder content, and mixers. Mix design with type I/II cement, 8% of silica fume (by mass of binder), and 30% of slag (by mass of binder) is recommended. The developed mix exhibits sufficient flowability and stability to ensure the successful implementation in bridge components and connections. A comprehensive evaluation of mechanical properties demonstrated that the mix exhibits excellent mechanical properties, including compressive strength, modulus of elasticity, Poisson's ratio, flexural strength, splitting tensile strength, direct shear strength, slant shear strength, and bond strength. The developed mix also exhibits excellent durability properties, including mass loss of less than 1% based on freezing/thawing resistance test, very low chloride ion penetration based on surface resistivity test, and no cracking based on restrained shrinkage test. The unit cost of the developed mix is approximately $682 per cubic yard, which is approximately one-third of the current commercial products. The batching, handling, placing, and curing of the developed mix was demonstrated in a field-scale panel connection casting, which resulted in a satisfactory performance.

17. Key Words Ultra-high performance concrete, strength, durability	18. Distribution Statement		
19. Security Classification (of this report) Unclassified	20. Security Classification (of this page) Unclassified	21. No. of Pages 110	22. Price

Form DOT F 1700.7 (8-72) Reproduction of form and completed page is authorized

Table of Contents

LIST OF FIGURES

LIST OF TABLES

ACKNOWLEDGMENTS

The authors would like to thank the Nebraska Department of Transportation (NDOT) for funding the research project and providing the opportunity to study ultra-high performance concrete. Special thanks to Technical Advisory Committee members for their valuable inputs and assists throughout the project. The author would also like to thank the materials suppliers Ash Grove Cement Company, Central Plains Cement Company, GCP applied technology, Lyman-Richey Corporation, and Chryso for the kind donation of materials for this research. Furthermore, the author appreciates the help of students and laboratory technicians during the data collection process.

DISCLAIMER

The contents of this report reflect the views of the authors who are responsible for the facts and the accuracy of the data presented herein. The contents do not necessarily reflect the official views or policies of the Nebraska Department of Transportation, nor of the University of Nebraska-Lincoln. This report does not constitute a standard, specification, or regulation. Trade or manufacturers' names, which may appear in this report, are cited only because they are considered essential to the objectives of the report. The United States (U.S.) government and the State of Nebraska do not endorse products or manufacturers.

This material is based upon work supported by the Federal Highway Administration under SPR-P1(18) M072. Any opinions, findings, and conclusions or recommendations expressed in this publication are those of the author(s) and do not necessarily reflect the views of the Federal Highway Administration.

ABSTRACT

Ultra-high performance concrete (UHPC) is a new class of concrete that has superior mechanical, durability, and workability properties that far exceed those of conventional concrete. To achieve these properties, a specific mix design with a very dense internal structure, fiber reinforcement, and low water-to-binder ratio (w/b) is commonly used. The goal of this research is to develop a non-proprietary UHPC mix with constituent materials that are readily available in the state of Nebraska for bridge construction applications. In developing this mix, the particle packing model is used, and an experimental study of the impact of various design parameters on the key properties of UHPC is conducted. Multiple series of UHPC mixtures are investigated with different types and quantities of aggregate, fibers, cement, supplemental cementitious materials (SCMs), high range water reducer (HRWR), w/b, total binder content, and mixers. Mix design with type I/II cement, 8% of silica fume (by mass of binder), and 30% of slag (by mass of binder) is recommended. The developed mix exhibits sufficient flowability and stability to ensure the successful implementation in bridge components and connections. A comprehensive evaluation of mechanical properties demonstrated that the mix exhibits excellent mechanical properties, including compressive strength, modulus of elasticity, Poisson's ratio, flexural strength, splitting tensile strength, direct shear strength, slant shear strength, and bond strength. The developed mix also exhibits excellent durability properties, including mass loss of less than 1% based on freezing/thawing resistance test, very low chloride ion penetration based on surface resistivity test, and no cracking based on restrained shrinkage test. The unit cost of the developed mix is approximately $682 per cubic yard, which is approximately one-third of the current commercial products. The batching, handling, placing, and curing of the developed mix was demonstrated in a field-scale panel connection casting, which resulted in a satisfactory performance.

CHAPTER 1. INTRODUCTION

1.1 Background

Ultra-high performance concrete (UHPC) is a new class of concrete that has superior mechanical, durability, and workability properties. The very low water-to-binder ratio (w/b), high binder content, use of steel fibers, and the absence of coarse aggregate make UHPC significantly different from conventional concrete in both the fresh and hardened states. Since the use of UHPC will result in significant improvements in the structural capacity and durability of structural components, various issues, such as cracking and leakage in bridge connections, can be mitigated to a significant extent.

The superior mechanical and durability properties of UHPC are generally due to the optimized particle packing of the materials. UHPC's components are selected rigorously considering the sizes and distributions of particles to maximize their packing density (El-Tawil et al., 2016). The design of UHPC is generally based on the optimizing particle packing so that the materials in the matrix are combined in proportion to minimize voids to ensure high strength, i.e., a minimum of 17,000psi (120MPa), low permeability, and self-consolidating nature (Yu et al., 2015; Lowke et al., 2012).

Different approaches have been used to design UHPC, and particle packing models are commonly used. However, because the small particle sizes of fine powders, such as cement and supplemental cementitious materials (SCMs) used, particles are subjected to strong interparticle forces, which generally does not take into account in the models. Besides, characteristics such as particle shapes and surface textures are also not considered. Thus, while particle packing models can serve as a general guideline, experimental work is still necessary to determine the actual packing for optimum UHPC design.

The current use of UHPC in the U.S. is limited mostly to proprietary, pre-packed products provided by international suppliers because of the highly-sophisticated design of the mixture, the mixing procedure, and in some cases, the limited availability of raw materials. The high costs associated with these products, which can be as much as $2,000 per cubic yard plus the costs associated with batching, placing, and curing, have been a major impediment for the extended use of UHPC. Therefore, through the examination of the impact of different parameters on the UHPC performance, a non-proprietary UHPC mix based on local materials available in Nebraska is proposed. Since the mixing process is intense and important for the production of UHPC, a comparison study of mixtures produced with different mixers and the control of consistency during the UHPC mixing process also are presented. A comprehensive experimental study is also needed to evaluate if the overall fresh, mechanical, and durability performance of the developed non-proprietary UHPC mixes can satisfy the need for Nebraska Department of Transportation (NDOT) highway bridge applications.

1.2 Research Objectives

The overall goal of the study is to evaluate the feasibility of developing an economic non-proprietary UHPC mix(es) with locally available materials for possible use in different bridge applications in Nebraska. The specific objectives of this project are 1). To evaluate the impact of different design parameters of UHPC behavior; 2). To develop a UHPC mix(es) with local materials; 3). To evaluate the overall mechanical behavior and durability of the developed UHPC mix(es), and 4). To evaluate the technical and economic feasibility of the developed UHPC mix(es). The focus of this study is on UHPC developed for connecting precast superstructure components (e.g., deck panels and decked girders).

1.3 Organization of the Report

This report is divided into eight chapters. Chapter 1 is an introduction, where the general background and main objectives are provided. A literature review is presented in Chapter 2, which includes design, raw material usage, mixing procedure, construction practices, and properties of UHPC included in research project reports from federal and state agencies, journals and conference publications. Chapter 3 presents the experimental program, which includes the materials, mixing procedures, and the test methods used in the mixes. Chapter 4 presented mix design development and results. Chapter 5 presents the performance evaluation of the developed UHPC mixes, including fresh concrete behaviors, mechanical properties, and durability performance. Chapter 6 presented field-scale connection casting with the developed UHPC and results. Chapter 7 included the technical and economic feasibility study of the developed UHPC mixes. Chapter 8 summarizes all conclusions and provides recommendations for future studies. Five appendices were also included at the end of the report, which includes detailed results and analysis of the impact of key design parameters (Appendix A), and mixers (Appendix B), detailed mechanical test results (Appendix C), study of the impact of curing on mechanical properties (Appendix D), and impact of specimen orientation and fiber stability on mechanical properties (Appendix E).

CHAPTER 2. BACKGROUND

2.1 Introduction

During the last decade, due to the superior properties of UHPC, extensive research has been conducted to develop UHPC with different materials and different design approaches. This chapter provides a summary of the materials that are typically used in UHPC, approaches, and examples in designing UHPC, mixing and construction practices, state and federal agency specifications, and properties of the UHPC.

2.2 Background

The concept of having a high-strength and high-performance cementitious material was initiated in the 1970s based on a better understanding of hydration reactions, shrinkage, creep, and porosity, as well as the development of water reducers and advanced curing processes. The terminology related to high-strength concrete was developed in the 1980s when concrete materials with compressive strengths up to 8,702psi (60MPa) were developed using SCMs, and a low w/b. Other types of concrete, with their improved mechanical properties, durability properties, or workability, were designated as high-performance concrete. UHPC initially was introduced in the early 1990s with the application of particle packing theory, the use of fine particles, low porosity, and very low w/b. Advances in the development of chemical additives and the introduction of various fibers in the concrete also contributed to the development and use of UHPC (Naaman and Wille, 2012).

Different organizations have different requirements that characterize UHPC. ASTM C1856 (ASTM, 2017) specifies a minimum compressive strength of 17,000 psi (120 MPa), maximum aggregate nominal size of aggregate of 1/4 in (5 mm), and flow between 8 and 10 inches (200 and 250 mm) measured using the flow table test. On the other hand, Federal Highway Administration (FHWA) (Haber et al., 2018), and American Concrete Institute ACI 239 (ACI 239R-18, 2018) defines UHPC as a cementitious composite material composed of an optimized gradation of granular constituents, w/b less than 0.25, and a high percentage of discontinuous internal fibers reinforcement. The mechanical properties of UHPC include compressive strength greater than 21,700psi (150MPa) and sustained post-cracking tensile strength greater than 720 psi (5 MPa). Besides, other state agencies such as the New York State Department of Transportation (NYDOT, 2013), Georgia Department of Transportation (GADOT, 2015), and District Department of Transportation (DCDOT, 2014) require UHPC to have a minimum 28-day compressive strength of 21,000psi (145MPa). Montana Department of Transportation (Berry et al. 2017) and California Department of Transportation (CALTRANS, 2016), require a minimum 28-day compressive strength of 20,000psi (137MPa). Some other state agencies such as Iowa Department of Transportation (IADOT, 2011) and Michigan Department of Transportation (El-Tawil et al. 2018) requirements include the minimum 4-day compressive strength, with which Iowa requires 10,000 psi (68MPa) and Michigan requires 12,000psi (83MPa).

According to ACI 239 (ACI 239R-18, 2018), the high performance of UHPC is due to its discontinuous pore structure and the reduced void space in the matrix. It is implied that the level of stress transferred between particles is reduced when the contact points between particles are increased. Thus, the proper selection of materials is very important. The reduction of the level of stress improves the mechanical properties because it alleviates the formation of microcracks. Also, UHPC is expected to have a discontinuous pore structure, which reduces the ingress of liquids and significantly enhances its durability compared to conventional concrete.

2.3 Ingredients

2.3.1 Cement, cementitious materials, and filler

For non-proprietary UHPC, the commonly used ingredients are cement, pozzolanic reactive materials, i.e., SCMs and fillers, fine aggregate, superplasticizer, and fibers. Cement is the principal binder in UHPC, and the SCMs improve the particle packing, resulting in a denser structure and enhancing the strength due to the pozzolanic reactions. Sometimes, fillers also are used to improve particle packing.

Cement accounts for approximately 20% of the total volume of the concrete. The main chemical compounds of Portland cement are C_3S, C_2S, C_3A, and C_4AF. When C_3S and C_2S are hydrated, they are the main contributors to the strength of concrete. According to Sakai et al. (2008), the hydration process of C_3A occurs rapidly due to its high surface area, and this increases the water demand, which consequently affects the apparent viscosity of the fresh concrete. Thus, a low amount of C_3A can reduce the required amount of water, the formation of ettringite, and the heat of hydration (Shi et al., 2015). Therefore, cement with a C_3A content less than 8% is generally desirable in UHPC mixes. Willi et al. (2011a) also reported that cement with a lower amount of C_3A, higher amounts of C_3S and C_2S, and a moderate fineness provide better performance for UHPC. Most researchers use Type I/II Portland cement due to its low content of C_3A. There also have been reports of the use of other types of cement, such as Type III cement, because it has smaller particles than Types I/II cement. Note that because of the very low w/b, the cement in UHPC usually is not fully hydrated, the remaining unhydrated particles can be considered as a filler (Meng et al., 2017b). In addition, FHWA and other researchers used Class H oil well due to the better overall packing and its coarser particle size, which enhance later age strength (Harber et al., 2018; Muzenski, 2015; Scott et al., 2015). Other DOTs such as Michigan DOT uses a pre-blend of Type I cement and slag (Berry et al. 2017 and El-Tawil et al. 2018).

Silica fume, a byproduct from the production of ferrum-silicon alloys, is a common pozzolanic material used for the fabrication of high-strength concrete and UHPC. Due to the very fine particle size, silica fume can greatly improve the packing density of the matrix and prevent the formation of pores in the UHPC. During the pozzolanic reaction, silica fume reacts with $Ca(OH)_2$ from the hydration of cement, forming C-S-H, which is the main hydration product responsible for the strength of concrete. According to Scrivener (2004), silica fume also can improve the interfacial transition zone of the concrete by reducing its porosity at early ages. Various researchers have suggested that despite its advantages as mentioned above, silica fume can decrease the workability of the UHPC due to its high surface area and the resulting high demand for water. In different state agencies and FHWA UHPC design, the silica fume content ranges from 21% to 50% of the mass of cement (Berry et al. 2017, El-Tawil et al. 2018, Russel and Graybeal, 2013, Haber et al., 2018).

Fly ash is one of the most extensively used SCMs in concrete. It is a byproduct of coal-burning electric power plants with most of the particles in solid spheres of hollow cenospheres (Kosmatka et al., 2003). Besides the pozzolanic reactions of fly ash that can improve the mechanical properties of UHPC, fly ash can also improve the workability of UHPC due to its lubricating and ball bearing effects (Meng, 2017).

Ground granulated blast-furnace slag, also called slag, is another SCMs that is commonly used in UHPC (Meng, 2017; Yu et al., 2015; Wille et al., 2011b). Generally, the slag particles have rough and angular shapes, and, in the presence of water and cement, pozzolanic reactions of slag that can result in the denser internal structure of UHPC (Kosmatka et al., 2003).

In addition to the above- mentioned materials, some other materials, such as glass powder (Naaman and Wille, 2012) and quartz powder (Haber et al., 2018), also have been used in UHPC as they can provide better particle packing of the UHPC. Because they do not directly react with water or hydration products, they are generally considered as fillers.

2.3.2 Aggregate

Coarse aggregates are normally not used in UHPC. According to De Larrard and Sedran (1994), to achieve the high strength of UHPC, it is desirable to use only fine sand as aggregate, due to the influence of maximum paste thickness (MPT), which represents the mean distance between two aggregate particles when they are surrounded by cement paste, with thickness proportional to the diameter of the aggregate. It was found that the compressive strength decreases when MPT increases. This observation was confirmed by Graybeal (2014), who reported that, even when the UHPC design contains coarse aggregate, it tends to be smaller (less than ¼ inches (6 mm) in size) and a much lower amount compared to normal concrete. Thus, the fine aggregate usually has the largest particles in the UHPC matrix. The fine aggregate included quartz, limestone, and basalt. Graybeal (2013) recommended the use of high-quality, high-strength, low-water absorption aggregate with optimized particle packing. Silica sand also commonly is used as the fine aggregate in UHPC due to its availability and low cost. According to Meng (2017), the desirable fine aggregate to be used in UHPC should be strong and chemically stable as well as environmentally and economically desirable. Table 2.1 and Figure 2.1 provide a summary of the maximum particle sizes of aggregates that have been used in UHPC and the frequency of their usage. As shown in Figure 2.1, while different maximum sizes have been reportedly used in UHPC, approximately half of the reported aggregate usages are with maximum size between #8 (2.36mm) and #18 (1mm).

Table 2.1 Maximum aggregate particle size reportedly used in UHPC

Maximum size of aggregate	#140	#100	#35	#20	#18	#10	#8	#4
Wille et al., 2011b						YES		
Naaman et al., 2012		YES		YES				
Ambily et al., 2014		YES					YES	
Yu et al., 2014a					YES		YES	
Yu et al., 2014b					YES		YES	
Yu et al., 2015					YES		YES	
Alkasy et al., 2015	YES		YES					
Meng et al., 2016						YES		YES
Wu et al., 2016							YES	
Meng et al., 2017						YES		YES
El-Tawil et al., 2018 (MIDOT)		YES		YES				
Berry et al., 2017 (MTDOT)								YES

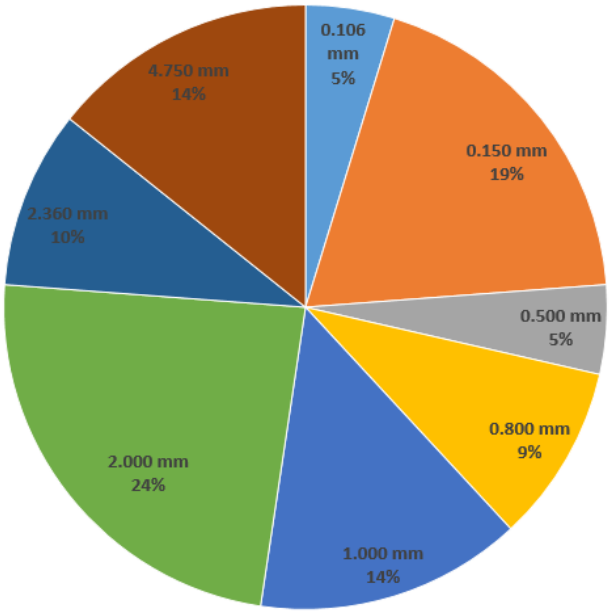

Figure 2.1 Frequency of maximum aggregate size reportedly used in UHPC

2.3.3 Chemical admixtures

The chemical admixture that is most commonly used in UHPC is the high-range water-reducer (HRWR), also known as "superplasticizer". The HRWR admixture reduces the amount of water required in the mix. Since the w/b of UHPC can be as low as 0.16, the admixture is very important to ensure the appropriate workability of the fresh concrete. According to Schrofl et al. (2008), polycarboxylate ether-based HRWR is a more effective superplasticizer for UHPC, which has been reported used in mixes from Montana DOT, Michigan DOT, and FHWA (Berry et al. 2017, El-Tawil et al. 2018 and Haber et al., 2018). Other types of HRWR, such as phosphonate-based HRWR, have also been reported. Due to the different chain lengths in HRWR, it may delay the setting time of the concrete (Wille, 2011). Therefore, accelerators are sometimes used in UHPC to ensure appropriate early age strength for construction (Graybeal, 2014).

2.3.4 Fibers

According to Graybeal (2014), the addition of fibers to the UHPC improves the hardened concrete characteristics, and it is very important when it is used in structural elements. The inclusion of fiber can increase the tensile capacity and ductility, which will, in turn, reduce the propagation of cracks. The materials, dimensions (aspect ratios), and shapes of the fibers vary depending on the availability of materials. Figure 2.2 shows some different types of steel fibers that are used in UHPC.

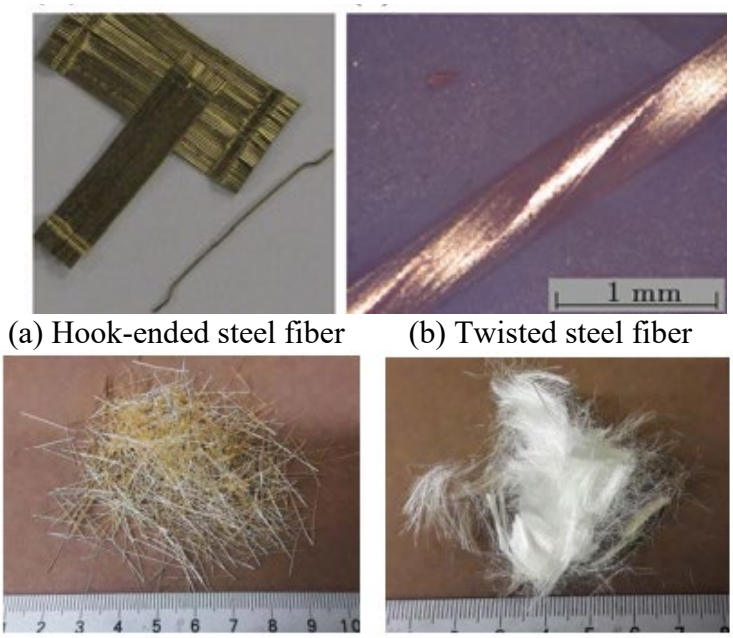

(a) Hook-ended steel fiber (b) Twisted steel fiber

(c)Straight steel fiber (d) PVA fiber

Figure 2.2 Typical fibers reportedly used in UHPC (adopted from Wille and Naaman, 2012)

Table 2.2 shows the summarized different types of fibers used in UHPC and their dimensions. The type of fibers that is used most often is steel fibers with diameters that range from 0.006 in. (0.152 mm) to 0.015 in. (0.381 mm) and lengths that range from 0.236 in. (6 mm) to 1.181 in. (30 mm). Fiber forms were reported to be with hook-ended, straight, or twisted. Among the steel fibers, the straight steel fibers with diameters of 0.008 in (0.200 mm) and lengths of 0.512 in (13 mm) are most often used for UHPC. Examples of volumes, dimensions, and forms of fibers used in agencies are 2% (by volume) of the 0.512 in (13 mm) long straight steel fibers (MTDOT), 2% of the 0.748in (19mm) long straight steel fiber (MIDOT), and 3% of the end-hooked steel fiber with 1.181 in (30mm) of length (FHWA) (Berry et al. 2017, El-Tawil et al. 2018 and Haber et al., 2018).

Besides steel fiber, Table 2.2 shows that some researchers have used PVA and polyethylene fibers in UHPC (Sbia et al., 2014; Japan Society, 2008; Khayat and Meng, 2017). The combination of different types of fibers or dimensions has also been reported as being used in UHPC to achieve the desired performance (Shi et al., 2015; Sbia et al., 2014).

Table 2.2 Types and dimensions of fibers reportedly used in UHPC

Type	Diameter (in)	Length (in)
Straight steel	0.008	0.748
	0.008	0.512
	0.006	0.236
End-hooked steel	0.015	1.181
Twisted steel	0.012	0.709
	0.005	n/a
PVA	0.002	0.472
	0.002	0.315
	0.012	n/a

1 in = 25.4 mm

Fibers are important to ensure desirable mechanical properties, particularly toughness and post-cracking tensile strength. However, since the use of fibers interference with the packing of the particles and increases the surface area of the solid particles in the mix, which leads to changes in the properties of fresh UHPC, the proportion of fibers in the concrete must be carefully controlled. Meng et al. (2017) reported that 2% of fibers by volume is considered to be the optimum fiber content for UHPC to provide the desired hardening properties.

2.4 Mixture design

2.4.1 Particle packing theory

It is well known that the particle size distribution affects both the fresh and hardened properties of concrete (Hunger and Brouwers, 2006). In UHPC, the high-density packing of particles is desired to achieve high strength and low permeability. The UHPC design is achieved when the materials of the matrix are combined in optimal proportions, and the voids between the particles are minimized (Yu et al., 2015; Lowke et al., 2012). For UHPC to have sufficient strength, the mixes generally are designed based on particle-packing theory, which is considered as the design philosophy for UHPC (El-Tawil, 2018). The particle-packing theory is based on decreasing the porosity of the concrete by filling the voids between the larger particles in the matrix with smaller particles, thereby reducing the number of voids. Figure 2.3 shows a schematic depiction of the difference between the matrix structure of conventional concrete and UHPC. The UHPC structure is packed densely with minimum voids between the particles, while the structure of conventional concrete is loosely packed.

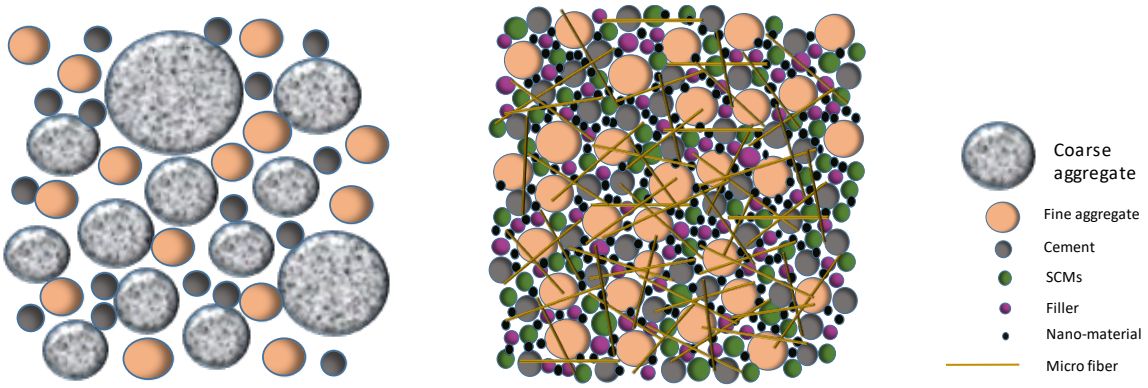

(a) Conventional concrete (b) UHPC

Figure 2.3 Schematic difference between particle packing in conventional concrete and UHPC

According to Hunger and Brouwers (2006), many particle packing models are available. The Andreasen and Andersen (A&A) theory, as shown in Equation 2.1, is the most commonly used model to design UHPC.

$$\boldsymbol{P(D) = \frac{D^q}{D_{max}^q}} \qquad \textbf{Equation 2.1}$$

where D is the particle size (μm); $P(D)$ is the volume fraction of the total solids smaller than size D; D_{max} is the maximum particle size (μm), and q is the distribution modulus. Since the A&A model does not account for the minimum particle size, a modified Andreasen and Andersen model was developed (Yu et al., 2014b), and it is considered to be more appropriate for mixtures with fine materials, such as UHPC. The modified model considers both the maximum and minimum sizes of the particles of the material. Based on the modified A&A particle packing theory, an optimum curve can be generated based on Equation 2.2.

$$\boldsymbol{P(D) = \frac{D^q - D_{min}^q}{D_{max}^q - D_{min}^q}} \qquad \textbf{Equation 2.2}$$

where D is the particle size (μm); $P(D)$ is the volume fraction of the total solids smaller than size D; D_{max} is the maximum particle size (μm); D_{min} is the minimum particle size (μm), and q is the distribution modulus. Theoretically, q should be in the range of 0 to 0.28 for fine granular blends (Hunger and Brouwers, 2006). According to Huger (2010), small q values are more suitable for finer packing, as in the case of UHPC. A q value of 0.23 was selected in this study based on the previous study by Yu et al. (2015).

Although models from the particle packing theory are often used to design UHPC, fine powders, such as cement and SCMs, are subjected to strong interparticle forces due to their high fineness, which generally is not accounted for in the models. Also, when liquid is introduced in the mix, the interaction force between fine particles (<0.004 in (100 μm)) is affected, which also generally considered (Meng et al., 2017). Other factors that could affect the degree of particle packings, such as particle shape and surface conditions, are not considered in most packing models either. Thus, while particle packing theory can serve as a general guideline, experimental work is

still necessary with the specific materials used to determine the actual packing for optimum UHPC design.

2.4.2 Other mix design approaches

In addition to particle packing theory models, different methods have been used in designing UHPC. To improve particle packing, some researchers (Wille et al., 2011; Graybeal, 2013; Meng et al., 2017) used the combinations of different aggregates. It was reported that bulk density or a particle packing model could be used to identify the best proportion of aggregates to be used.

Some researchers (Wille et al., 2011; Graybeal, 2013) used multiple stages to obtain the most promising cement paste, and then they incorporated the aggregate and the fibers to produce UHPC. First, cement pastes with the best flowability and compressive strength were identified by adjusting the cement and SCMs, w/b, and HRWR. Then, appropriate amounts and types of aggregates and fibers were introduced to obtain mixtures with promising workability and mechanical characteristics.

Their approach, however, did not evaluate the packing density of the entire UHPC matrix, i.e., the paste and aggregate together. It assumed that the best performing paste would provide the best performing UHPC. Although the paste significantly affects the workability and compressive strength of UHPC, the particle packing could be disturbed when the aggregate is introduced. The combined packing of aggregates and powder materials is a key parameter in the performance of UHPC. Therefore, even though it is a practical method, the packing density of the entire matrix, including the paste and the aggregate, should not be neglected. The energy required to mix the cementitious paste will be different from the energy required to mix UHPC, and the different mixing energies can also result in the final products having different performances.

Berry et al. (2017) defined the proportion of UHPC materials using a response surface methodology (RSM). They developed trial batches to collect sufficient data to create a model that consisted of a set of complex regression equations that can predict the behavior of each of the components of the UHPC mix. Although it was stated that the method could accurately provide responses of the behaviors and interactions of the constituents, for each specific set of ingredients, trial batches are required to build the model, and this can become impractical.

2.4.3 Representative UHPC mix designs

As previously mentioned, the UHPC design usually consists of dry constituents, i.e., cement, SCMs, filler, fine aggregate, fiber, and liquid, i.e., water, and HRWR. State agencies such as IADOT and CALTRANS, suggest the use of a commercially available UHPC (IADOT, 2011 and CALTRANS, 2015). NYSDOT and GADOT do not specify the UHPC design (NYSDOT, 2013 and GADOT, 2011). Typical examples of mix designs from the research projects FHWA, Michigan, Montana, and Missouri studies are presented in Table 2.3. In these UHPC mixes, the binder content has at an average of 1800pcy (1068Kg/m^3), and the average w/b is 0.164.

Table 2.3 Representative UHPC mix designs from federal and state agencies

Constituent	FHWA (Haber et al., 2018)	Michigan (El-Tawil et al., 2018)	Montana (Berry et al., 2017)	Missouri (Meng et al., 2017)
Cement	1328	653	1300	924
Slag	NA	653	NA	902
Fly Ash	NA	NA	371	NA
Silica Fume	518	327	279	71
Ground Quartz	367	NA	NA	NA
Fine Sand	NA	394[1]	NA	512[4]
Coarse Sand	1288	1577[2]	1556[3]	1170[5]
HRWR	23	39	60	27
Water	278	264	272	282
Steel Fibers	416	265	263	263

Note: All values are presented in pcy (1 pcy = 0.59 Kg/m^3)
1-U.S. Silica F75, max. particle size = No. 40 (0.425 mm)
2- U.S. Silica F12, max. particle size = No. 30 (0.6 mm)
3- Masonry sand, washed and dried max. particle size = No. 8 (2.36 mm)
4- Masonry sand, max. particle size = No. 10 (2 mm)
5- Missouri river sand, max. particle size = No. 4 (4.75 mm)

2.5 Construction

2.5.1. Formwork

MIDOT states that the formworks, where the UHPC will be placed, must be watertight and coated to prevent absorption of water, and it must be strong enough to resist the hydraulic pressure of the mix. Similarly, FHWA (Graybeal, 2014) affirms that the formwork should have a non-absorbent finish. CALTRANS (2017) also suggests that, before the placement of UHPC, the formwork surface must be free of dust, debris, and excess water. DCDOT (2014) requires a medium density overlay plywood formwork. Besides, DCDOT also specifies that the formwork should be pre-wetted just before the UHPC material is placed. Hand removal of formwork is also required.

2.5.2. Surface preparation

When UHPC is used to connect precast elements, the bond between the precast concrete element s and the UHPC is important to ensure a strong connection and eliminate the water infiltration and degradation of the concrete and rebar (Graybeal, 2014). Regarding surface preparation, FHWA specifies that the surface of the precast component should be pre-wet to the surface saturated condition and should also be prepared with micro and macro texture such as exposed aggregates before the UHPC placement. DCDOT (2014) affirms that the precast concrete in contact with UHPC shall have exposed aggregate finish.

2.5.3 Mixer

As stated previously, the loading sequence and mixing procedure and time of UHPC are critical to ensure uniformity and consistency. Due to the lack of coarse aggregate and the very low

w/b, the energy required to mix UHPC is higher than it is to mix conventional concrete, and longer mixing time is generally necessary to achieve the desired consistency and performance. Due to the very fine particles and low w/b in UHPC, clumps are formed easily during the mixing (El-Tawil et al., 2018). High-shear pan mixers generally are preferable to increase the efficiency of the mixing process (Graybeal, 2014). Such mixers usually have paddles that help scrape materials off from inside of mixer walls.

Different forms of paddles, dimensions of mixers, and mixing speeds provide different energy inputs. El-Tawil et al. (2018) measured the flow and turnover time (the time when the consistency of the UHPC mix was observed, i.e., when the materials start to change from powder form to liquid form) for UHPC prepared with different processes. It was observed that the mixing speed influenced the performance of the fresh concrete. As the mixing speed increased, the workability of UHPC increased slightly, and the turnover time decreased drastically. Therefore, different mixing procedures may be necessary for field mixing when the rotation speed and dimensions of mixing paddles of the mixer are different.

2.5.4 Mixing procedure

Because of the high fine particle content and the intensive energy required for mixing, the sequence of loading materials and the mixing procedure for UHPC are very important to achieve the desired fresh and hardened properties. Different researchers have different approaches for the mixing procedure, but the process generally can be separated into three steps, i.e., (1) mix the dry components, (2) add water and HRWR, and (3) add fibers. Some researchers (Yu et al., 2014, 2015; Bonneau et al., 1997; Ambily et al., 2014; Meng et al., 2016, 2017; Wu et al., 2016; Yang et al., 2009; Shi et al., 2015) have suggested that all of the powder and aggregate first should be mixed for a period 30 seconds to 10 minutes, followed by water and HRWR added to the mixture. In some cases, the liquid is divided into two portions and loaded separately into the mixer to enhance its dispersion (Yu et al., 2014, 2015; Meng et al., 2016, 2017). After the liquid is added, the total mixing time varies from 5 to 12 minutes, followed by adding fibers at the last stage. Other researchers and agencies such as MTDOT suggested dry mix silica fume and aggregate first for 5 minutes to ensure the breakdown of silica fume particles followed by cement and SCMs being added and mixed for five more minutes. After that, water and HRWR are added into the mixer and mixed until the concrete reaches the expected consistency. Finally, fibers are added and mixed for 5 minutes to ensure dispersion (Wille et al., 2011; Alkaysi, 2015; Naaman et al., 2012; Graybeal, 2013, Berry et al., 2017). In some cases, the liquid is divided into two portions and loaded separately into the mixer to enhance its dispersion (Berry et al., 2017). Based on the results of the trial experiments, this procedure was adjusted and used in this study.

Some other loading and mixing procedures are also adopted by different researchers. De Larrard and Sedran (1994) suggested mixing the powders with t liquid first until a homogenous slurry is observed, and then add the sand. According to Ferdosian and Camoes (2016), this procedure can help produce a lower viscosity mixture because of the water in contact with cement in the initial stage of mixing releases Ca^{2+} ions that subsequently are absorbed onto the HRWR chain. El-Tawil et al. (2018) affirmed that this procedure could reduce the demand for the extensive use of power for mixing during the mixture turnover stage, reducing the probability of a malfunction of the mixer. El-Tawil et al. (2018) also suggested a different procedure that involved dividing the sand into two portions, adding the first portion with the powder materials and mixing for 5 minutes, followed by the addition of the liquid, and after the concrete turnover, add the second

portion of sand and finally the fibers. It was shown that the sand helps to mix and disperse the materials, thereby shortening the turnover time of the mixture.

2.5.5 Placing and curing methods

UHPC mixes are usually very flowable with a self-consolidating characteristic and is normally placed into formwork or molds with one lift and no consolidation (Meng and Khayat, 2016). To achieve desired fiber orientation, FHWA study (Haber et al., 2018) recommended cast prims specimens with one layer from one end and allowed to flow until the other end. Haber et al. (2018) also reported using a concrete vibration table to vibrate laboratory specimens for 5 to 15 seconds in other to remove the entrapped air. Berry et al. (2017) place the concrete in the molds using two layers of approximately equal volume and consolidate specimens with a vibration table. ASTM 1856 (ASTM, 2017) requires filling cylinders using a single lift and allow to tap the cylinder molds after to consolidate specimens. Due to the high viscosity nature of UHPC, to ensure appropriate consolidation, the flow distance is sometimes limited in the field. MIDOT (2014) affirms that UHPC must not be allowed to flow farther than 24 inches during placement. They suggest pouring UHPC from one end of the joint, and once the other end is reached, start to pour in the other direction. The process should be continued until the full depth of the joint has been cast, and no vibration is necessary. FHWA (Graybeal, 2014) says that the forms that had the UHPC poured should be immediately closed after placement to minimize surface dehydration. When UHPC is placed into enclosed formworks, an exit for trapped air should be provided.

Similar to conventional concrete, moisture and temperature are both critical for the appropriate curing of UHPC. MIDOT (2014) requires that the concrete should not be placed at ambient air temperatures below 40°F (4°C) or above 90°F (32.2°C) and that the top surface of the concrete must be covered with insulating blankets. Until the initial set, it is critical to maintaining appropriate temperature and humidity since there is fast mechanical property growth at that time (Russell et al. 2013). After the initial set, the material can be cured using many different curing regimes such as standard curing room, water storage, heat-curing treatment, steam curing, and autoclave curing regimes.

As silica fume is generally a part of UHPC, heat-treatment (176°-194°F (80°-90°C)) can be effectively used and can contribute to enhancing the strength (Choi et al., 2016). Heat treatment usually consists of storing concrete specimens in 176°- 194°F (80°-90°C) water after 24-hour, for a period that can vary from 24 hours to 7 days. Precast/Prestressed Concrete Institute (PCI) quality control manual (PCI, 1999) suggests for the heat treatment that the heat shall be applied after concrete sets in a controlled rate which ensure the heat gain not to exceed 36°F (20 °C) per hour and the maximum curing temperature not to exceed 180°F (82°C). The cooling rate should also be controlled at 50°F (27.8°C) per hour to prevent surface crazing. Moreover, Meng and Khayat (2016) reported that they heat-cured UHPC specimens at 194°F (90°C) for 24 hours, after 24-hour initial curing with wet burlap and plastic sheets at room temperature for 24 hours. .Although the UHPC under heat curing frequently presents a higher compressive strength (Meng et al., 2017; Shi et al. 2015; Ozylidirim, 2011; Russel et al., 2013), it is considered impractical in the field (Wille et al. 2011). Therefore, the standard curing method is more practical in the field for cast-in-place concrete than heat curing. The standard curing consists of covering the concrete immediately after casting with plastic sheets and keeping the surface wet after the removal of forms or molds.

As for lab curing, the most common practice immediately following demolding at appropriately 24 hours, immerse UHPC specimens in lime-saturated water and maintain the temperature at 73°F (23°C)) until the day of testing (El-Tawil et al., 2018). Some researchers use

multiple curing processes until the concrete reaches 28 days (Meng and Khayat, 2016; Bonneau et al., 1997; Ozyildirim 2011; Wan et al., 2016).

2.5.6 Surface grinding

IADOT suggests that the concrete achieves a minimum of 10ksi of compressive strength prior to performing surface grinding. In addition, they also specified that if fibers pull out is observed during the grinding process, the operation should be suspended and not resume until approval of the engineer. Due to the very high strength of UHPC, the delay of the grinding process can cause challenges in effective grinding and extensive wear out of grinding plate, no maximum compressive strength for grinding was reported.

2.5.7 Mockup

Due to the unique workability behavior of UHPC, a mockup section is generally encouraged. According to IADOT, the mockup shall be cut transversely at locations determined by the engineer to allow the visual inspection of the joint interface and material bond.

2.6 Properties of UHPC

2.6.1 Fresh concrete properties

Due to its high flowability, the control of the fresh properties of UHPC requires consistent measurements of the workability. The properties of fresh UHPC normally are determined using the flow table test (Naaman and Wille, 2012; Meng et al., 2017; Choi et al., 2016), which consists of filling a small cone-shaped mold atop a standard flow table, raising the mold from the mixture, and measuring the spread. However, different procedures are suggested by different specifications. For instance, according to ASTM C1437 (ASTM, 2015), the test consists of dropping the table 25 times in 15 seconds and calculating the average of the diameters measured from the four lines scribed on the top of the table, which is sometimes reported as the "dynamic" flow. FHWA (Haber et al., 2018) suggested a different approach that involved allowing the concrete flow by itself until no movement is detected and then calculating the average of the diameters measured from the four lines scribed in the flow tabletop, which is sometimes reported as the "static" flow. The new ASTM C1856 (ASTM, 2017) standard for UHPC states that the material must be allowed to spread by itself for 2 minutes, after which the average between the maximum and minimum diameters is to be calculated and reported. MIDOT (El-Tawil et al., 2018) follows the ASTM C1856 procedure described while MTDOT (Berry et al., 2017) measures the flow of the concrete after the concrete spread shows no more movement on top of the flow table. Different states and federal agencies have been using a 7 to 10 in (179 to 250 mm) flow as the criterion for UHPC flow, while ASTM 1856 requires 8 to 10 in (200 to 250 mm). Table 2.4 summarizes UHPC flow criteria from different agencies.

In addition to the flow table tests, other tools, such as rheometers (Dils et al., 2013) and mini V-funnels (Meng, 2017; Dils et al., 2013), have been used to evaluate the workability and rheological behavior of UHPC. However, their use is limited significantly due to the lack of availability of the instruments.

Table 2.4 UHPC flow requirement of state agencies and organizations

Agency/Organization	Flow requirement (in.)
ASTM C1856 (ASTM, 2018)	8 to 10
FHWA (Graybeal et al., 2014)	7 to 10
IADOT, 2011	7 to 10
NYDOT, 2013	7 to 10
CALTRANS, 2017	7 to 10
GADOT, 2015	7 to 10
MIDOT, 2014	7 to 12

2.6.2 Hardened concrete properties

Different agencies and organizations have specified different minimum compressive strengths for UHPC. Table 2.5 presents some of the requirements. Graybeal et al. (2014) and Caltrans (2015) stated that ideally, the structure could not be open for the traffic of live loads, and formworks should not be stripped until UHPC reaches a 14ksi (97MPa) of compressive strength. While different requirements are specified, the 28-day compressive strength of non-proprietary UHPC reported by different agencies and researches varies from 11,300 psi to approximately 30,000 psi (77.9 MPa to 206 MPa). While FHWA (Haber et al., 2018) reported a 28-day compressive strength of 18,000psi (124 MPa), MIDOT reported a 28-day compressive strength of 21,700 psi (150MPa) and MTDOT reported a 28-day compressive strength of 19,200 psi (132MPa).

Table 2.5 UHPC compressive strength requirements from agencies and organizations

Agency/Organization	$f'_{c,4}$	$f'_{c,28}$
ASTM C1856 (ASTM, 2017)	n/a	≥ 17 ksi (120 MPa)
FHWA (Graybeal et al., 2014)	> 14 ksi (97 MPa)	≥ 21.7 ksi (150 MPa)
IADOT, 2011	≥ 10 ksi (68 MPa)	n/a
NYDOT, 2013	≥ 12 ksi (83 MPa)	≥ 21 ksi (145 MPa)
CALTRANS, 2017	≥ 14 ksi (97 MPa)	≥ 20 ksi (137 MPa)
GADOT, 2015	≥ 12 ksi (83 MPa)	≥ 21 ksi (145 MPa)
MIDOT, 2014	≥ 12 ksi (83 MPa)	n/a

Flexural strength of UHPC is greatly enhanced due to the addition of the fibers that are commonly used in UHPC, and the reported 28-day flexural strength varies from 1,800psi to 5,000psi (12.4MPa to 34.4MPa).

2.6.3 Concrete shrinkage and durability properties

While some argues that the shrinkage of UHPC is expected to be higher than conventional concrete due to the high amount of cement in its design, this is not always the case mainly because of the very low w/b and presence of fibers that can internally restrain the cementitious matrix from shrinking (Harber et al., 2018). FHWA evaluated the drying shrinkage of non-proprietary UHPC mixes following ASTM C1856 (ASTM, 2017), and results showed a drying shrinkage value of approximately 400 με (Harber et al., 2018).

The dense matrix improves not only the mechanical properties but also the durability of UHPC (Harber et al., 2018). The lower permeability of UHPC, when compared to conventional

concrete, makes the water percolation difficult giving exceptional durability properties to the concrete. The durability of UHPC is evaluated with various tests including freezing/thawing resistance per ASTM C666 (ASTM, 2015), rapid chloride permeability test per ASTM C1202 (ASTM, 2019), and surface resistivity following AASHTO TP95 (AASHTO, 2014). The freezing/thawing resistance test allows observing if the concrete can resist stresses caused by expansion and contraction of the water to ice transformation. Results showed that UHPC usually shows no to very minimum mass loss and retains the dynamic modulus of elasticity, showing very little change during the test (Haber et al., 2018). As an indirect measurement of concrete permeability, the rate of chloride ion can be used to evaluate the internal structure of the concrete and to predict its durability. The capacity of UHPC to resist the chloride ion penetration is generally evaluated using the rapid chloride ion penetration test and surface resistivity test. It should be noted that both tests are electrical tests, and the inclusion of steel fibers in UHPC can interfere in the results. When steel fibers contact each other, it can create a conductive path possibly resulting in non-representative values (Harber et al., 2018). Due to this reason, most agencies specify to evaluate the rapid chloride penetration, and surface resistivity with specimens excludes steel fibers. Due to the very low permeability, the resistivity of UHPC is expected to be high.

Table 2.6 shows the durability requirement of federal and different state agencies.

Table 2.6 UHPC durability requirements from federal and state agencies

	Chloride ion penetration, 28 days	Freezing/ thawing resistance	Free shrinkage, 28 days	Scaling resistance	Abrasion resistance	Alkali-silica reaction
FHWA (Graybeal, 2014)	≤ 250 coulombs	RDM ≥ 95% after 300 cycles	≤ 800 με	n/a	n/a	n/a
NYDOT, 2012	≤ 250 coulombs	RDM >96% for 600 cycles	≤ 766 με	< 3	<0.025 oz. lost	Innocous
CALTRANS, 2015	≤ 350 coulombs	RDM ≥ 95% after 300 cycles	n/a	n/a	n/a	16 days (0.15% max expansion)
GADOT, 2015	≤ 250 coulombs	RDM >96% for 600 cycles	≤ 766 με	< 3	<0.025 oz. lost	Innocous

Some states include the watertight integrity test that consists of flooding the deck where UHPC joints were placed. Observation will then be made under the joints during the flooding and after the supply of water has stopped, to identify if there is any water leakage. The joint shall be considered watertight if no dripping water or water droplets are visible at the underdeck areas along the full length of joint (IADOT, 2011; NYDOT, 2013; DCDOT, 2014).

2.7 Summary

This chapter presents the results of the literature review that was conducted for this research. Based on the literature review, preliminary materials were selected for further analysis. The loading sequence and mixing procedure used in this research for the production of UHPC was also identified based on the findings from the literature review.

Although different approaches have been reported for the design of UHPC, all of them have different limitations. The most commonly used particle packing model that was used to design UHPC, namely the modified A&A model, only considers dry particles yet does not account for the interaction force between fine particles in dry and wet conditions. Also, the shapes and textures of the particles were not taken into account. Other approaches optimize the paste of the UHPC independently of the aggregate, but they disregarded the overall matrix packing density of UHPC. Instead, the packing density of the paste was optimized separately from the optimization of the aggregate matrix, and the two materials were combined later. Besides the concern of the particle packing density, the energy used to mix the paste portion can be different from the energy required to mix UHPC, which, consequently, results in a different performance of the final product. It is important to implement a better method that simultaneously accounts for the cementitious materials paste, the aggregate, and the fibers.

The fresh, mechanical, and durability properties of UHPC and related requirements are summarized in this chapter. The chapter also includes test methods most used to evaluate each property.

CHAPTER 3. EXPERIMENTAL PROGRAM

3.1 Introduction

The objective of this chapter is to present the materials investigated and test methods used in this research to characterize the developed UHPC. The different types of cement, SCMs, aggregates, fibers, and chemical admixtures used in the study are presented. Most of the materials presented were selected based on a review of the literature and their availability in Nebraska.

This chapter also includes details of test methods that were used to evaluate the fresh, hardened, and durability properties of UHPC, such as flowability, compressive strength, and freezing/thawing resistivity. The tests of flowability and compressive strength are essential to determine whether the UHPC mixes that were developed are acceptable according to the requirements per ASTM 1856 (ASTM, 2017).

3.2 Materials

3.2.1 Cementitious materials

Because of the much higher binder content compared to conventional concrete, cementitious materials used for UHPC should be selected rigorously due to their contribution to the fresh, hardened, and durability properties of the final product. The workability and the strength of UHPC depend largely on the type of binder and its content. While fresh properties of the cement paste control the workability of UHPC, the hydration of the cement and the pozzolanic reactions of SCMs determine the properties of the hardened product.

3.2.1.1 Cement

In this research, four different types of cement were used in the development of UHPC, i.e., Type I/II and Type III Portland cement (both of which meet ASTM C150 (ASTM, 2018)), Type IP Portland cement that meets ASTM C595 (ASTM, 2018), and Class H Oil Well cement that meets American Petroleum Institute API – Spec 10A (API, 2010). Type I/II, III, and IP cement were collected from Ash Grove Cement Company (Louisville, NE), and Oil Well cement was collected from Ash Grove Cement Company (Seattle, WA).

3.2.1.2 Supplemental Cementitious Materials and Filler

Various SCMs products were used for the study, which includes class C fly ash that meets ASTM C618 (ASTM, 2017) from Boral Materials (Denver, CO), Force 10,000 densified micro-silica (silica fume) from Grace Construction Products (Cambridge, MA), and un-densified silica fume that meet ASTM C1240 (ASTM, 2015), and ground, granulated blast-furnace slag that meets ASTM C989 (ASTM, 2018) shipped from Skyway Cement Company (Chicago, IL). A quartz powder also was used in the study as a filler material.

The chemical composition and particle size distribution for the different types of cement and SCMs used in the study are shown in Table 3.1 and Figure 3.1, respectively.

Table 3.1 Chemical composition of cement and SCMs used in the study

Substance	Content (%)							
	Type I/II Cement	Type IP Cement	Type III Cement	Class H Oil Well Cement	Fly ash	Silica Fume	Slag	Quartz Powder
Silicon Dioxide (SiO_2)	20.4	-	19.50	21.90	42.46	92.50	-	99.40
Silicon trioxide (SiO_3)	-	-	-	-	-	0.52	0.04	-
Aluminum Oxide (Al_2O_3)	4.10	-	4.60	4.20	21.00	-	-	0.26
Iron Oxide (Fe_2O_3)	3.10	-	3.20	5.00	4.78	-	-	0.031
Sulfur Trioxide (SO_3)	2.70	3.10	3.40	2.40	1.12	-	-	-
Calcium Oxide (CaO)	63.80	-	62.3	64.20	20.34	-	-	0.01
Magnesium Oxide (MgO)	2.30	2.45	4.00	1.10	3.69	-	-	0.02
Sodium Oxide (Na_2O)	0.12	-	-	0.09	1.43	-	-	<0.01
Potassium Oxide (K_2O)	0.71	-	-	0.66	0.62	-	-	0.03
Carbon dioxide (CO_2)	1.70	-	1.90	-	-	-	-	-
Limestone	4.30	-	4.50	-	-	-	-	-
$CaCO_3$ in Limestone	88.00	-	94.00	-	-	-	-	-
Titanium dioxide	-	-	-	-	-	-	-	0.01
Chlorine (CL^-)	-	-	-	-	-	0.14	-	-
C_3S	60.00	-	51.00	52.00	-	-	0.84	-
C_2S	13.00	-	17.00	24.00	-	-	55.30	-
C_3A	6.00	-	7.00	3.00	-	-	7.90	-
C_4AF	9.00	-	10.00	15.00	-	-	8.80	-
Loss-on-Ignition	-	1.00	2.50	1.10	0.75	3.39	-	0.30

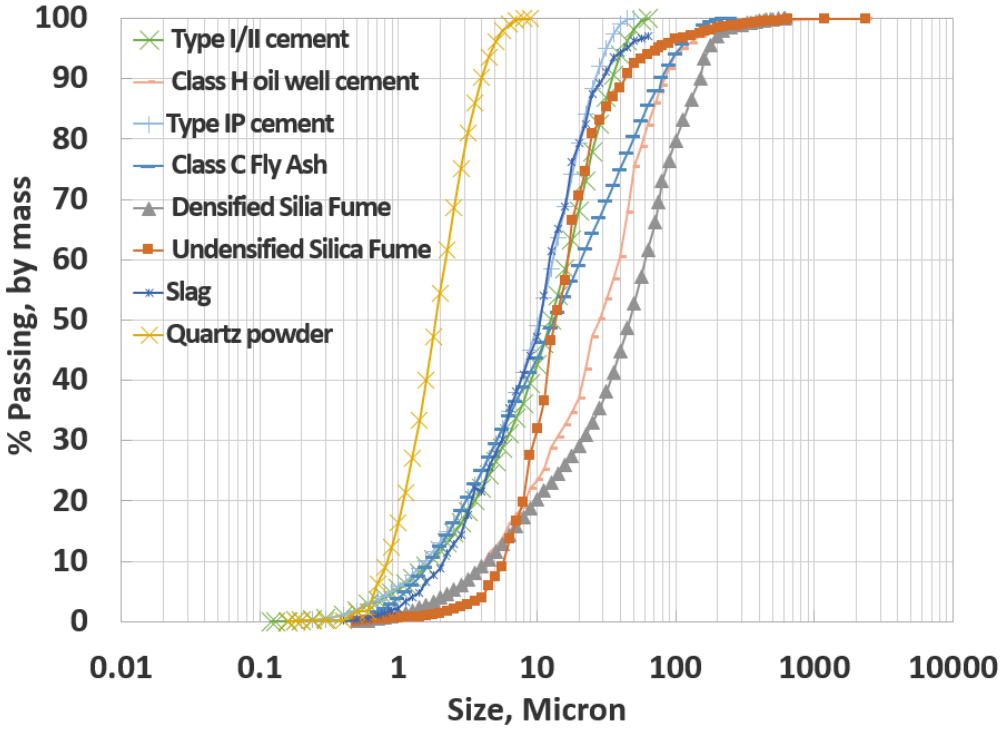

Figure 3.1 Particle size distribution of cement and SCMs used in the study

It was observed that, because silica fume has a very fine particle size and strong surface charge, the particles of densified silica fume were agglomerated, showing a coarser particle size distribution than other SCMs. A large portion of the agglomerates was expected to be dispersed after mixing. Thus, the particle size distribution of un-densified silica fume was used in the analysis of the overall particle size distribution because it was believed that it better represented the gradation of the material in the UHPC mix. Note that, while a portion of the agglomerates was expected to be dispersed after mixing, a substantial amount still could remain in the mixture (Diamond and Sahu, 2006).

3.2.2 Aggregate

To ensure economically feasible UHPC mixes, the main aggregate used in this concrete mixture was fine silica sand from Lyman-Richey (Omaha, NE), which had a maximum size of No. 10 (2.00 mm). Three other aggregates, i.e., a commercially available fine silica sand (F75), a local limestone sand (Unical L), and local river sand also were used to evaluate the feasibility of further improving the design of the mix through the optimization of the aggregate gradation. Sieving analyses were performed according to ASTM C136 (ASTM, 2014), and Figure 3.2 presents the gradation curves of the four aggregates.

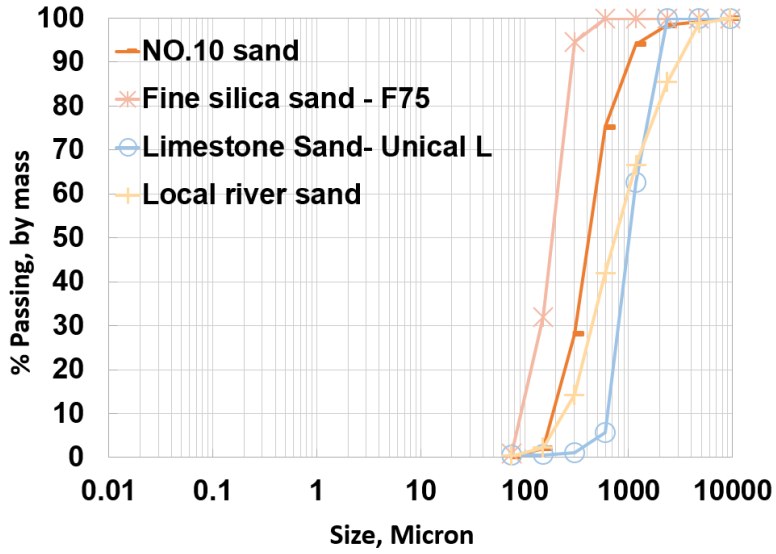

Figure 3.2 Particle size distribution of aggregates used in the study

3.2.3 Chemical admixtures

Due to the very low w/b and high flowability requirements, HRWR is important to ensure the success of the UHPC development. In this study, three types of HRWR admixtures, including a modified polycarboxylate based (Premia 150, from CHRYSO), two polycarboxylate based HRWR admixtures (Adva 198 and Adva 140M, both from GCP) that met ASTM C494 (ASTM, 2017) Type A and F admixtures were used. Besides, during the preliminary study, two other polycarboxylate based admixtures were also used (MasterGlenium 7500 and MasterGlenium 7920, both from BASF). Also, a workability-retaining admixture (MasterSure Z60, from BASF) and an air detrained admixture (MasterSure 1390, from BASF) were used in selected mixtures to control the workability loss and air respectively.

3.2.4 Fibers

Four different types of fibers that were used in the study, i.e., a straight stainless steel micro-fiber (SS) from Bekaert, two twisted steel fibers (TS13 and TS25) from Helix, and a synthetic fiber-glass (SG) fiber from Owens Corning as shown in Figure 3.3.

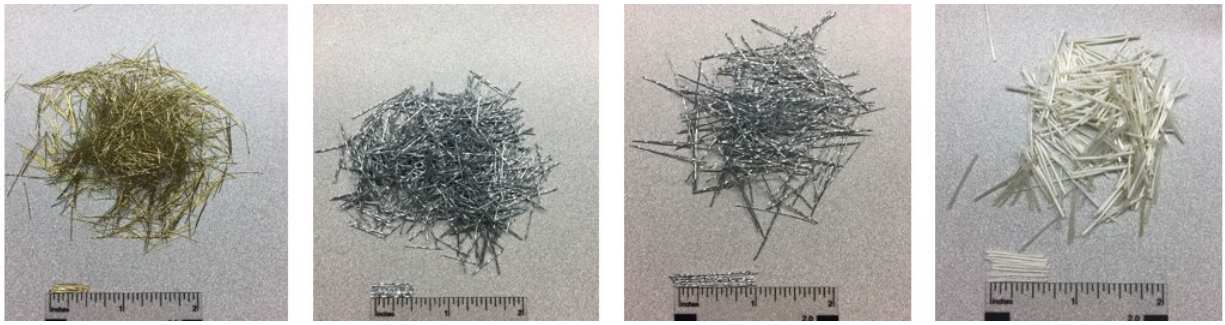

(a) SS (b) TS13 (c) TS25 (d) SG

Figure 3.3 Fibers used in the study

Table 3.2 provides the details of the physical and mechanical characteristics of the four fibers.

Table 3.2 Physical and mechanical properties of fibers used in the study

	SS	TS13	TS25	SG
Specific Gravity	7.800	7.800	7.800	2.000
Length (in)	0.510	0.510	0.980	0.750
Diameter (in)	0.078	0.020	0.020	0.020
Modulus of Elasticity (ksi)	29,000	29,000	29,000	6,092
Tensile Strength (ksi)	399	247	247	247

1 in. = 25.4 mm
1 ksi = 6.89 MPa

3.3 Mixing Procedures

Because of the very fine particle sizes, the elimination of the coarse aggregate, and the very low w/b, higher mixing energy generally is needed for UHPC, which results in a longer mixing time than conventional concrete to ensure good distribution of all of the particles (Wille et al., 2011). Since UHPC's ingredients are composed of very fine particles, and they are likely to agglomerate and form chunks, mixing these particles in the dry condition is critical to reducing the shear force required to break the pieces.

The process of mixing UHPC can be very peculiar and specific for the different mixers used and the volumes of the materials that are being mixed. In this study, two different mixers were used, and the results were compared. Since UHPC requires higher mixing energy, a lower volume than the recommended capacity of the mixer was used. A 20-qt capacity Vollrath (0.5 HP) benchtop mixer with three different speeds was used for all the batches with 0.16 ft^3 (0.0045 m^3) of UHPC (small batches). Selected mixes also were prepared using a 16 ft^3 (0.45 m^3) capacity Imer Mortarman 750 mixer (5 HP) with batch sizes of approximately 2ft^3 (0.06 m^3) (large batches). The mixing process generally can be separated into three main steps, i.e., mix the dry components; (2) add water and superplasticizer; (3) add the fibers. Generally, the final product consistency can be

first determined by visual examination of the fresh material, of which UHPC should have a flowable and viscous consistency. Note that because of the different paddle configurations, dimensions, and speed, the mixing time will differ depending on the mixer and the volume of the batch.

The mixing procedures used in this study were developed based on the literature (Naaman and Wille, 2012; Graybeal and Hartmann, 2003; Alkaysi and El-Tawil, 2015) and adjusted based on consistency changes during the mixing of the trial batches. Figure 3.4 shows the procedures for the two different mixers and batch sizes that were used in this study. The powder materials were separated in different containers and were not combined before the mix starts. All the sand was air-dried to a moisture content ranging from 0.07% to 0.25%. The water and admixture were proportioned in small containers and were premixed before being loaded into the mixer.

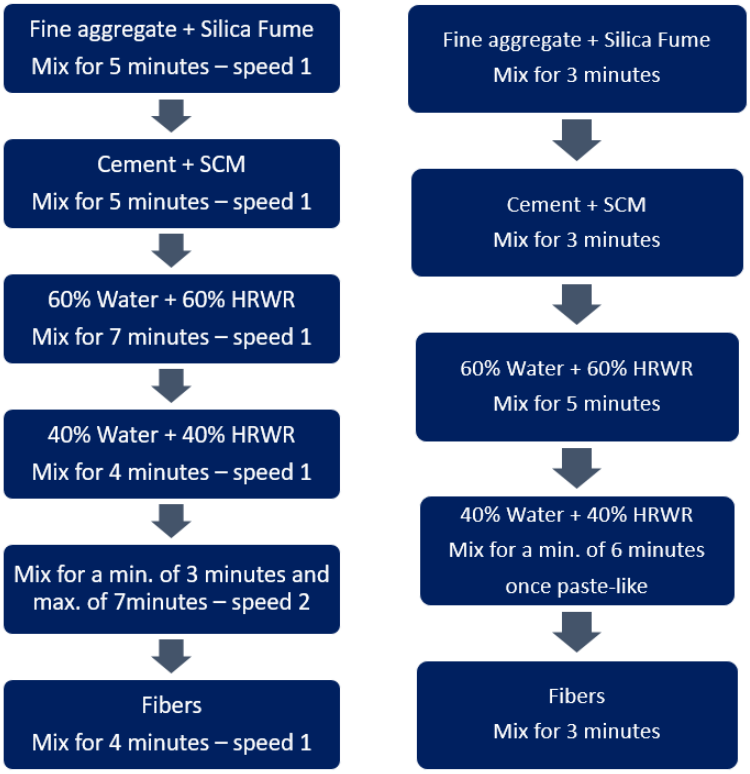

(a) Small batch (b) Large batch

Figure 3.4 Flow charts of the batching and mixing procedures for different sizes of batches

Figure 3.5 shows the appearance of mixtures at the different mixing stages, as described above in the flow chart for the small mixer (top figures) and large mixer (bottom figures). In Figure 3.5, photograph (1) represents right after the mixing of aggregate the silica fume; photograph (2) represents after introducing cement and fly ash; photograph (3) represent after introducing the first portion of the premixed liquid; photograph (4) represents after introducing the second portion of the premixed liquid; photograph (5) represents the final product after the fibers were loaded.

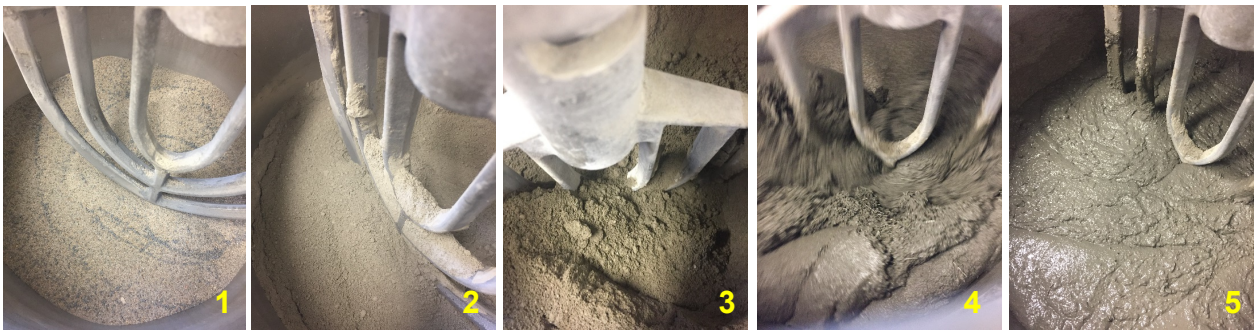

(a) Small batch

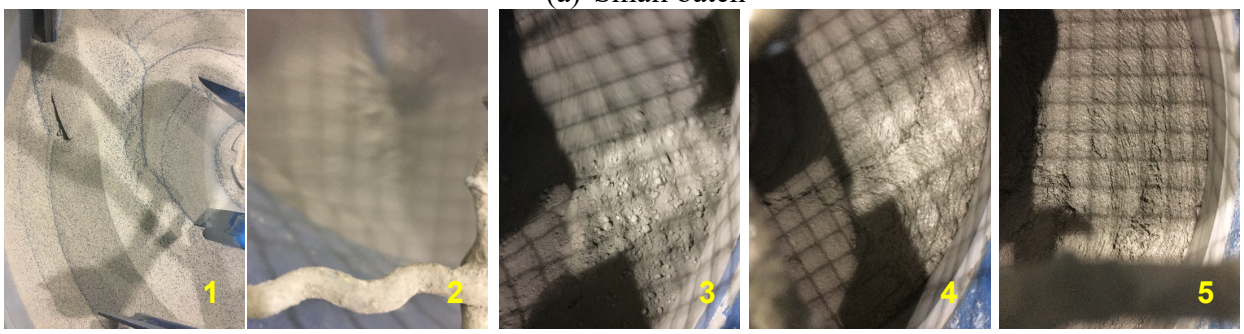

(b) Large batch

Figure 3.5 Consistency changes in the mixers during mixing

3.4 Test Methods

3.4.1 Fresh concrete properties

3.3.1.1. Workability

Figure 3.4 shows the standard flow table with a diameter of 10 in. (254 mm), as specified in ASTM C230 (ASTM, 2014), that was used for fresh UHPC workability measurement in the study.

Figure 3.6 Flow table test apparatus

The flow table test was conducted following ASTM C1856 (ASTM, 2017). The test procedure consisted of filling the cone mold with UHPC without tamping, followed by lifting the

mold, and measuring the diameter of the spread after 2 min ± 5sec of flow. The average of the maximum and minimum diameters measured was reported as the flow value.

3.4.1.2. Fresh Unit weight

The fresh unit weight of the UHPC was determined by filling a 0.25 ft^3 volume cylindrical container made of steel. The cylinder is tilted in about 45 degrees while concrete is poured to ensure a better consolidation and minimum of trapping air as neither internal vibration nor rodding is applied. The steel cylinder with the concrete inside is weighted, and unit weight was calculated and reported.

3.4.2 Early age properties

3.4.2.1. Setting time

The setting time test was conducted following two methods, namely penetration resistance test per ASTM C403 (ASTM, 2016) and Vicat needle test per ASTM C191 (ASTM, 2018). ASTM C403 test procedure consists of placing the concrete in a 6×6 in. (152×152 cm) cylinder, finishing the surface and measuring the force needed to penetrate 1 in. (25.4 cm) of needles with different diameters in it. The penetration resistance for each measurement is calculated based on the area of the needle needed and the applied penetration force. A plot of penetration resistance versus elapsed time is made, and the initial and final setting times are obtained when the resistance reaches 500 psi (3.4 MPa) and 4,000 psi (27.5 MPa), respectively. For the Vicat needle test, each test specimen was prepared by placing the UHPC in a cone shape mold and finishing the surface. The initial and final setting times are obtained based on the measure of the depth at which the Vicat needle of known weight can penetrate the sample. A plot of penetration depth versus elapsed time is made, and the initial and final setting times are obtained based on the time when the penetration depth equals 1 in. (25mm) and when the needle cannot penetrate nor leave a notable mark on the surface of the sample. Figure 3.7 shows the test setup for the two tests.

(a) Penetration resistance test (b) Vicat set time test

Figure 3.7 Set time test apparatus

3.4.2.2. Heat of hydration

As the cement hydration process generates heat, the measurement of hydration heat can provide insights into the hydration process, particularly at an early age. The heat of hydration was measured with an isothermal conduction calorimeter (Calmetrix I-CAL 8000). The calorimeter was set at a constant temperature of 70±2ºF (21±2ºC). The test consists of measuring the heat generated by the hydration process during the first 96 hours. Immediately after the mixing was completed, a 110±10 g of UHPC specimen is placed in a small plastic cup. The plastic cup is then moved to the calorimeter, and the test is initiated. Figure 3.8 shows the calorimeter and an example of the data obtained. The area under the curve obtained represents the heat generated during the measured period.

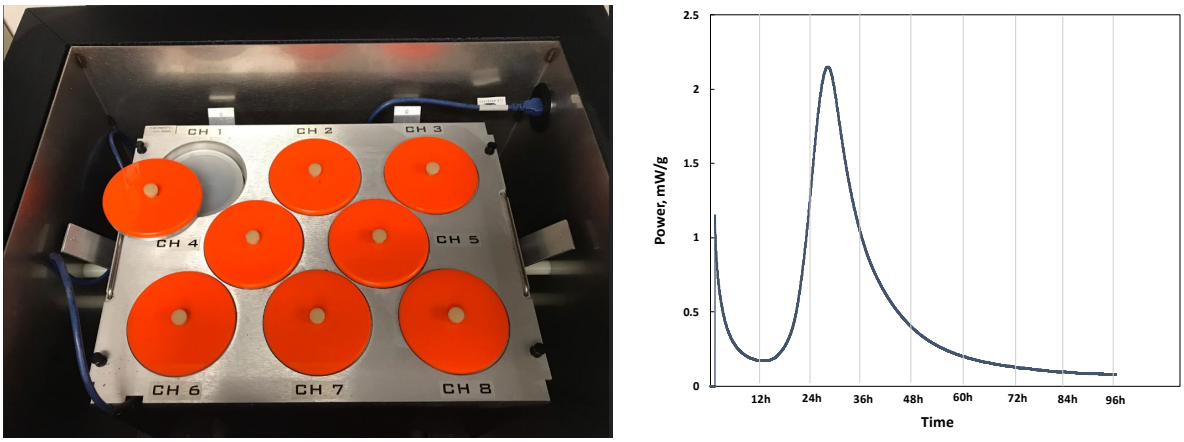

(a) Calorimeter (b) Example of heat of hydration curve

Figure 3.8 Heat of hydration test setup and example results

3.4.3 Mechanical properties

3.4.3.1. Compressive strength

According to ASTM C1856 (ASTM, 2017), 3×6in. cylinders were casted and used to determine the compressive strength of UHPC mixes at the ages of 4, 7, 28, and 56 days. The cylinders were cast on an angle of 45º and then tapped on the side to minimize the entrapped air inside the specimens. The cylinders were stripped out of the molds after 24 hours and had standard curing procedure. Cylinder ends were ground using a cylinder end grinder manufactured by Marui Co., LTD., as shown in Figure 3.9, to ensure flat and level surface at both ends and the consistency of test results.

According to ASTM C1856, a load rate of 150 psi/sec. was applied on the test cylinders using an axially loaded compression machine till failure. A minimum of three specimens was used for each test, and the average value was reported as compressive strength at each specific age.

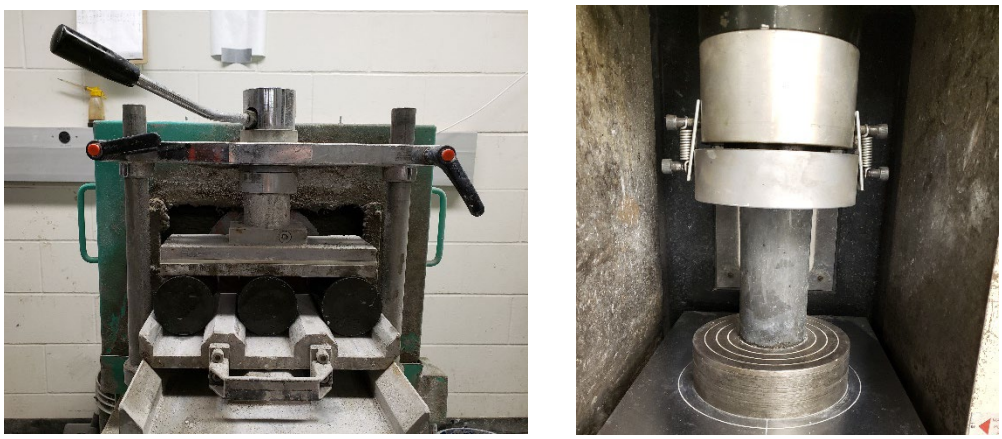

Figure 3.9 Cylinder end grinding and compressive strength test setup

3.4.3.2. Modulus of Elasticity and Poisson's Ratio Test

4×8in. cylinders from each UHPC mix were casted and used for modulus of elasticity (MOE) and Poisson's ratio tests according to ASTM C469 (ASTM, 2014), specified by ASTM C1856 (ASTM, 2017). The cylinder ends were ground using end grinder machine to insure flat and level surface. Figure 3.10 shows the Compressometer/Extensometer cage attached to a specimen that was placed in an axially loaded compression machine. Each cylinder was loaded to approximately 40% of its compressive strength. Modulus of elasticity is calculated based on the ratio of stress over longitudinal strain corresponding to 40% of the ultimate load. Poisson's ratio is calculated based on the ratio of transverse strain at the mid-height and longitudinal strain.

Figure 3.10 Modulus of elasticity test setup

3.4.3.3. Flexural strength test

According to ASTM C1856, the flexural strength UHPC was measured according to ASTM C1609 (ASTM, 2019) for the flexural performance of fiber-reinforced concrete. As the steel fibers used had a length of 0.5 in., a cross-section for flexure specimen of 3×3in. was used. Three 3×3×14 in. prisms from each mix were used for flexure strength test according to ASTM C1609 using four-point loading as shown in Figure 3.11. A Tinius Olson testing machine was used

to apply compression load on the specimens to failure. According to ASTM C1609, a displacement rate up to 0.003 in./min was applied until a mid-span deflection of L/900 and, then, increased gradually up to 0.008 in./min. until a mid-span deflection of L/150. The specimen mid-span deflection was captured using two LVDTs connected to the steel base and pointing to a steel frame attached to the specimen top in the middle section. The width and depth of each prism were measured to calculate the flexural strength accurately.

Figure 3.11 Flexure strength test setup

3.4.3.4. Splitting tensile strength test

The splitting strength test was performed according to ASTM C496 (2017) to determine the splitting tensile strength of each mix. Three 4×8 in. cylinders were used to conduct the splitting tensile test instead of 6×12 in. cylinders as UHPC has high compressive strength. A load rate of 300 lb/sec. was applied using a compression machine until failure, as shown in Figure 3.12(a). A typical failure mode of the developed mixes is shown in Figure 3.12(b). The splitting tensile strength was obtained based on the maximum applied load and the dimension of specimens according to ASTM C496.

(a) Test setup (b) Typical failure mode

Figure 3.12 Splitting tensile strength test setup and typical failure mode

3.4.3.5. Direst tensile strength test

Three 2×2×24 in. prismatic specimens were prepared and tested for each UHPC mix to determine the direct tensile strength based on FHWA report (Graybeal and Baby, 2019). The specimens were placed in lime saturated water till the day before testing. Then, Aluminum grip plates covering one-third of the specimen from both ends were installed using a thin layer of epoxy to prevent failure at the ends due to the machine clamping force. The tension specimen was then placed inside a 400 kips capacity Tinius Olsen testing machine and aligned vertically with the machine clamps. Two LVDTs were attached to the tension specimen to measure the vertical displacement within the middle third of the specimen. The direct tension test setup is shown in Figure 3.13. An axial tension load rate of 700 lb/min. was applied until specimen failure. The strain was calculated by dividing the measured vertical displacement by the distance between LVDTs fixation points. The direct tensile strength was calculated by dividing the applied tension load by the cross-section area of the specimen.

(a) specimen preparation (b) setup (c) typical failure mode

Figure 3.13 Direct tension test specimen preparation, setup, and typical failure mode

3.4.3.6. Direst shear strength test

A direct shear test was conducted to evaluate the interface shear resistance of monolithic UHPC. Based on Haber et al. (2017), 2×2×6 in. prismatic specimens were cut from a longer specimen cast from one end to align the fibers with the specimen length. A steel loading frame was used to apply double shear loading to the specimens as shown in Figure 3.14. A displacement-controlled loading rate of 0.05 in./min. was applied until failure. The direct shear strength was obtained as an average of a minimum of three specimens for each UHPC Mix. All the specimens exhibited a double shear failure. The obtained direct shear strengths were calculated by dividing the applied load by the double shear areas.

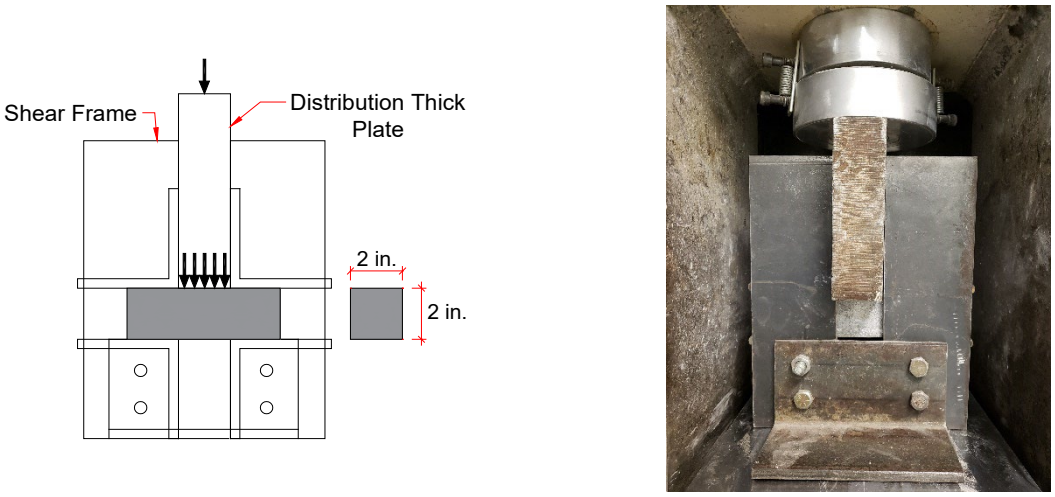

Figure 3.14 Direct shear test setup

3.4.3.7. Slant-shear bond strength test

A slant shear test was performed based on ASTM C882 (2013) to evaluate the interface shear resistance of fresh UHPC cast on hardened conventional concrete (CC). Sections of 4×8 in. cylinders instead of sections of 3×6 in. cylinders were used to allow the use of CC as a substrate. Hardened CC cylinders were sawed cut diagonally at a 60° angle with the horizontal axis after been cured for 28 days in lime-saturated water. The compressive strength of CC at 28 days was approximately 8 ksi. Figure 3.15 shows the two different textures applied to interface shear surface, i.e., as-cut (as cut by wet saw with no additional surface preparation) and deep grooved (1/4 in. depth at 1 in. interval). The interface surface was pre-wetted directly before casting UHPC. The composite section specimens were stripped out of the form after one day and submerged in lime-saturated till the day of testing. Both ends of the composite specimen were ground prior to being tested under a compression load rate of 300 to 400 lb/sec, following ASTM C39 for compressive strength testing of CC, till failure, as shown in Figure 3.16.

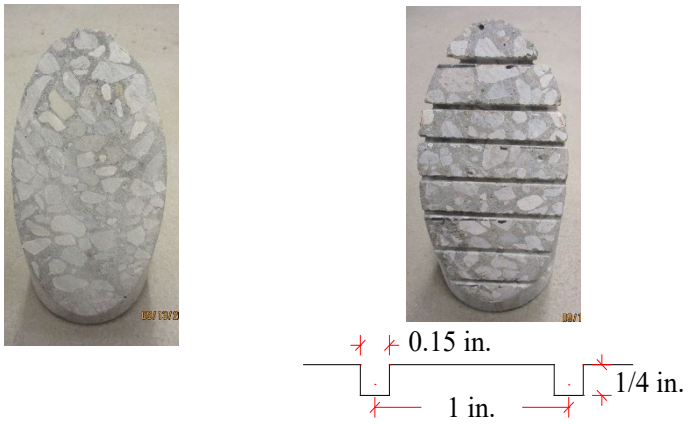

(a) As-Cut (b) Deep grooved

Figure 3.15 Interface textures of substrate concrete for slant-shear bond strength test

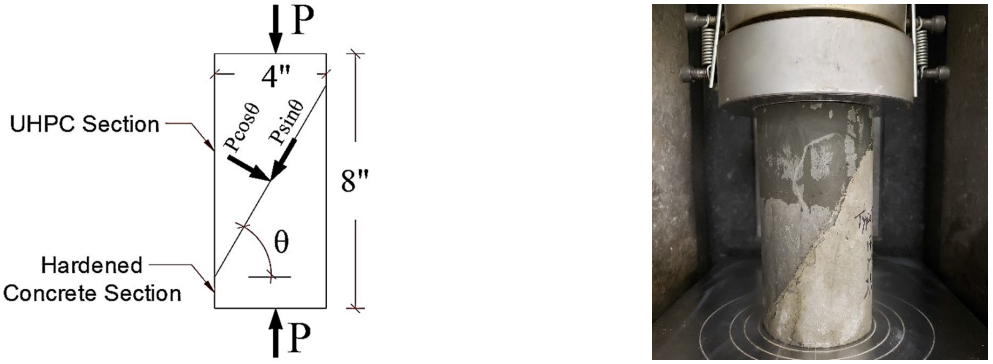

(a) Test specimen **(b) Test setup**

Figure 3.16 Slant shear test specimen and test setup

3.4.3.8. Rebar development length test

The FHWA-HRT-14-090 report (Graybeal and Baby, 2019) recommended a minimum embedment length of $8d_b$ and a minimum side cover of $3d_b$ to attain a deformed bar by achieving the lesser of the bar yield strength or 75 ksi before bond failure. The rebar development length test was conducting using UHPC blocks with two embedded steel bars aligned along the same axis as shown in Figure 3.17 (Roy et al., 2017). The longer embedded bar (support bar) has a larger diameter (No. 6) compared to the pullout bar (No. 4 anchorage bar) to ensure the failure will happen first at the pullout bar side. The two No. 4 bars at the sides prevent the concrete block from monolithic tensile failure at the mid-section. Three concrete blocks, with dimensions of 8×9×3in. that meet the minimum FHWA recommendation (Graybeal and Baby, 2019), were cast using commercial and the final UHPC mixes. The commercial and final UHPC mix specimens were tested under an axial tension load rate of 1500 lb/min. until failure using a 400 kips capacity Tinius Olsen testing machine and a lab-made testing frame with hydraulic jack as shown in Figure 3.18. With the lab-made testing set up, a steel frame was used, and tension load was applied using hydraulic ram attached to the pullout bar (No. 4). The anchorage bar (No. 6) was fixed using a coupler resting on steel plate against the frame Two LVDTs are attached to the pullout bar to capture the bar slippage after subtracting the bar elongation.

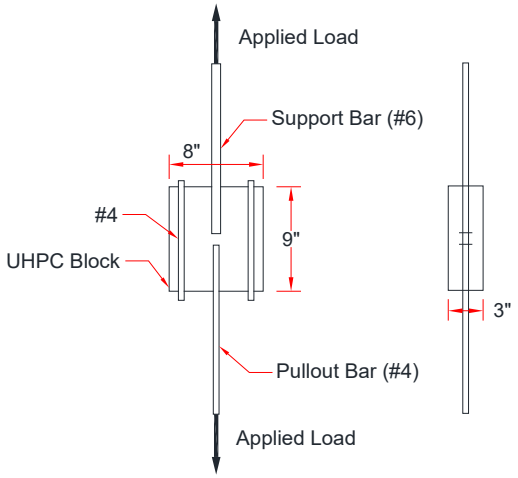

Figure 3.17 Rebar bond strength specimen dimensions

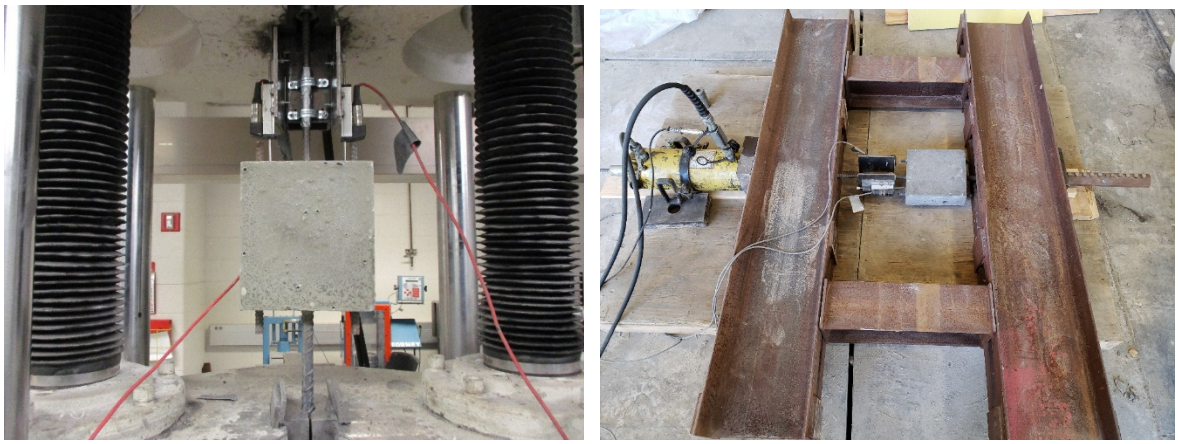

Figure 3.18 Rebar bond strength test setups

3.4.4 Durability

3.4.4.1. Freezing/thawing resistance

The resistance to freezing/thawing cycles was measured following ASTM C666 (ASTM, 2015) with the appropriate modifications as described in ASTM 1856 (ASTM, 2017). The test consists of subjecting 3×4×14in. test prisms to a freezing and thawing condition and measuring the dynamic modulus of elasticity and the mass loos after a certain number of cycles. The initial reading was taken after 14-day curing in lime saturated water at room temperature. After that, test samples are placed in molds full of water inside a freezing and thawing chamber (as shown in Figure 3.19) where temperature varies from 0ºF (-18ºC) to 40ºF (4.4ºC), exposing the concrete to an accelerated freezing and thawing cycling environment. Specimens were removed from the chamber every 30±5 freezing/thawing cycle to have the dynamic modulus of elasticity and the mass measured, then returned into the chamber. The specimens were subjected to a total of 600 cycles, which is doubled compared to the recommended 300 cycles as recommended by ASTM C666.

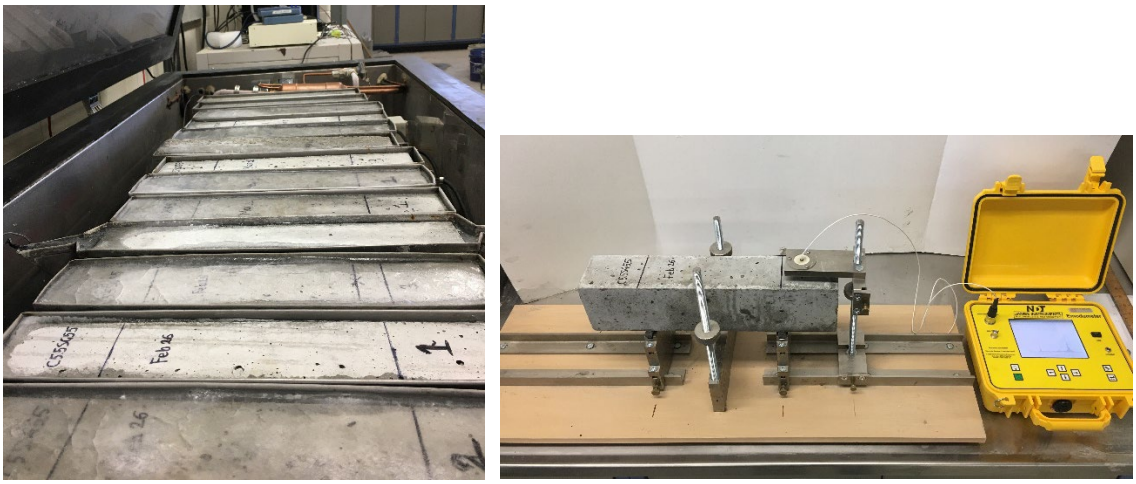

(a) Freezing/thawing chamber (b) E-meter

Figure 3.19 Freezing/thawing resistance test setup

3.4.4.2. Surface and bulk resistivity

The resistance to chloride ions penetration of the UHPC was measured using a non-destructive test capable of measuring the surface electrical resistivity, follows AASHTO TP95 (AASHTO, 2014). 4×8 in. (101.6×203.2 mm) cylinders were used for surface resistivity measurement by applying a current flow into the concrete from the outer pins while the inner pins receive it. With the current applied and the potential difference between the two inner pins, the resistivities of the test specimens were calculated and reported. Similarly, bulk resistivity was also measured with two testing plates contacting the two ends of ground cylinders. Figure 3.20 shows the resistivity apparatus for both surface and bulk resistivity measurements.

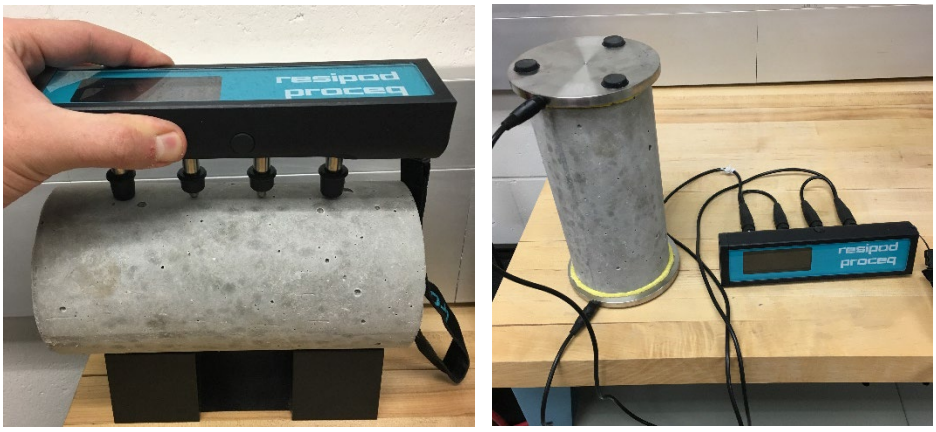

(a) Surface resistivity (b) Bulk resistivity

Figure 3.20 Resistivity test setup

3.4.4.3. Restrained shrinkage

The cracking potentials of the developed UHPC mixes were measured based on monitoring the age of crack initiation with the restrained shrinkage test following ASTM C1581 (ASTM, 2009). A 1.5 in. thick concrete ring was placed in a circular mold around a 0.5 in. thick steel ring where strain gages were installed, as showed in Figure 3.21. The shrinkage of the concrete causes a strain in the inner steel ring, and a sudden decrease in the strain indicates a concrete crack.

(a) Test specimen (b) strain gauge attached to the inner steel ring

Figure 3.21 Restrained shrinkage test setup

3.4.4.3. Free shrinkage

The drying deformation of UHPC was measured using a length change apparatus following ASTM C157 (ASTM, 2008) with the appropriates modifications as described in ASTM C1856 (ASTM, 2017). The test was conducted with three 3×3×11.25in. (76.2×76.2×285.8 mm) prisms. The initial (0-day) length and mass were measured after 24-hour curing. The specimens were then submerged in lime saturated water at room temperature for 28 days. After the 28th day, the specimens were moved to a controlled temperature and humidity environmental chamber with a temperature of 73±1ºF (23±0.5ºC) and 50±4% of relative humidity. Length and mass changes were measured after 4, 7, 14, and 28 days of air drying in the environmental chamber, with a length comparator (as shown in Figure 3.22) and a digital scale with a sensitivity of 0.1g.

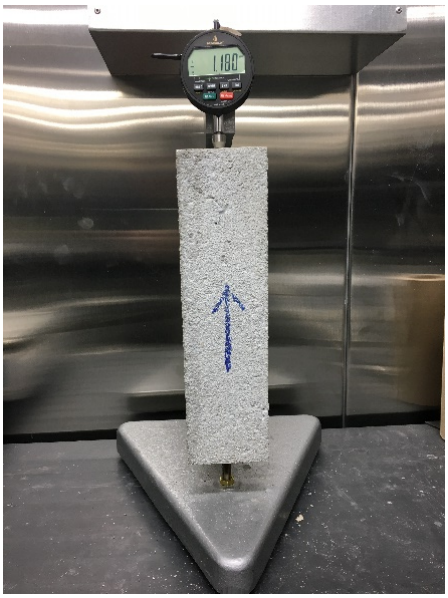

Figure 3.22 Length comparator used in the free shrinkage test

3.5 Summary

This chapter presented sources and key characteristics the raw ingredients, including cement, SCMs, fine aggregate, HRWR, and fibers, selected for UHPC development. The chapter also includes details of mixing procedure for UHPC preparation and test methods conducted, include measurements for fresh concrete, hardened concrete, and durability properties.

CHAPTER 4 MIX DESIGN DEVELOPMENT AND RESULTS

4.1 Introduction

Chapter 4 presents the process of identifying promising UHPC mixtures. The methodology of proportioning the materials was based on an experimental study on the impact of different parameters on key UHPC characteristics, including flow, compressive strength, and tensile toughness.

This chapter presents the impact of design parameters in multiple phases. First, void content test on the different aggregate candidates and combinations was used to identify the best locally available aggregate. Then, flexural strength and toughness of UHPC prepared with different fibers, along with the consistency of mixes with different types of HRWR, were used to determine the most promising fiber and HRWR, respectively. The workability and compressive strength of mixes prepared with different types of cement, types, and content of SCMs, total binder content, and HRWR content were compared. Designs with the most promising fresh and hardened concrete properties were identified as final UHPC mixes for further performance evaluation, which is to be presented later in Chapter 5.

4.2 Mixture Development

As previously summarized in Chapter 2, most UHPC designs are based on particle packing theory, which is intended to reduce the porosity of the concrete matrix by filling the voids among larger particles with smaller particles. Theoretically, the optimum proportion and performance of a UHPC design can be obtained by using the appropriate particle packing model. The modified Andreasen and Andersen particle packing model was used in this study. An optimum particle packing curve was created using Equation 2.2 with a q value of 0.23, based on the previous study by Yu et al. (2015).

The theoretical optimum particle packing curve and examples of particle size distribution curves of preliminary mixes prepared with different combinations of binders are showing in Figure 4.1.

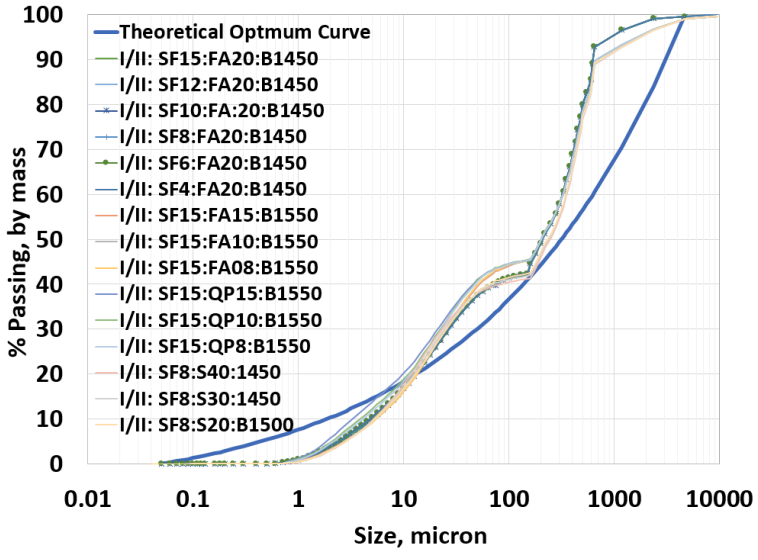

Figure 4.1 Particle packing curve of mixes with different binder combinations

A preliminary laboratory study showed that, unlike what was predicted based on the particle packing model, mixes with the best performances were those that had higher total binder content. The difference that was observed is likely due to the interference of parameters that the model does not account for, such as the surface charges between fine particles in combination with the use of water and admixtures in the mixes that can affect the interparticle forces among fine particles. Moreover, the particle shape and surface conditions were not considered in the model. It was concluded that the theoretical packing of the particles does not necessarily result in a UHPC with the highest flow and compressive strength. It is worth noting that besides the platform portion between 50 and 200 microns in the particle packing curves, which is the gap of particle sizes between the fine aggregate and binders used in this study, the particle packing curves also significantly skewed away from the optimum packing curve toward the maximum particle size. While there is only a small portion (5% to 10%) of particles larger than 0.6mm, presumably all from the No. 10 sand, the particle packing curves can be significantly different. Therefore, in this study, the particle packing theory was only used to guide the UHPC design at the initial stage. However, further development of UHPC was based more on experimentally identifying mixes with the best performance through the study of the impact of various design parameters.

In this study, UHPC design development was based on a systematic plan that can be divided into three phases. Phase I consists of materials screening. The performance of the UHPC with different types of fine aggregates, fibers, and HRWRs was investigated in this phase. Once the most appropriate types of these materials were selected, the study proceeded to Phase II. In this phase, the impact of the types of cement, the types and contents of the SCMs, content of HRWR, and total the binder on the performance of the UHPC were studied. The combination of materials that provide acceptable flow, and the highest compressive strength was selected. Finally, Phase III consisted of the performance evaluation of selected mixes. Figure 4.2 shows the sequence of the phases described, including the parameters analyzed in this study.

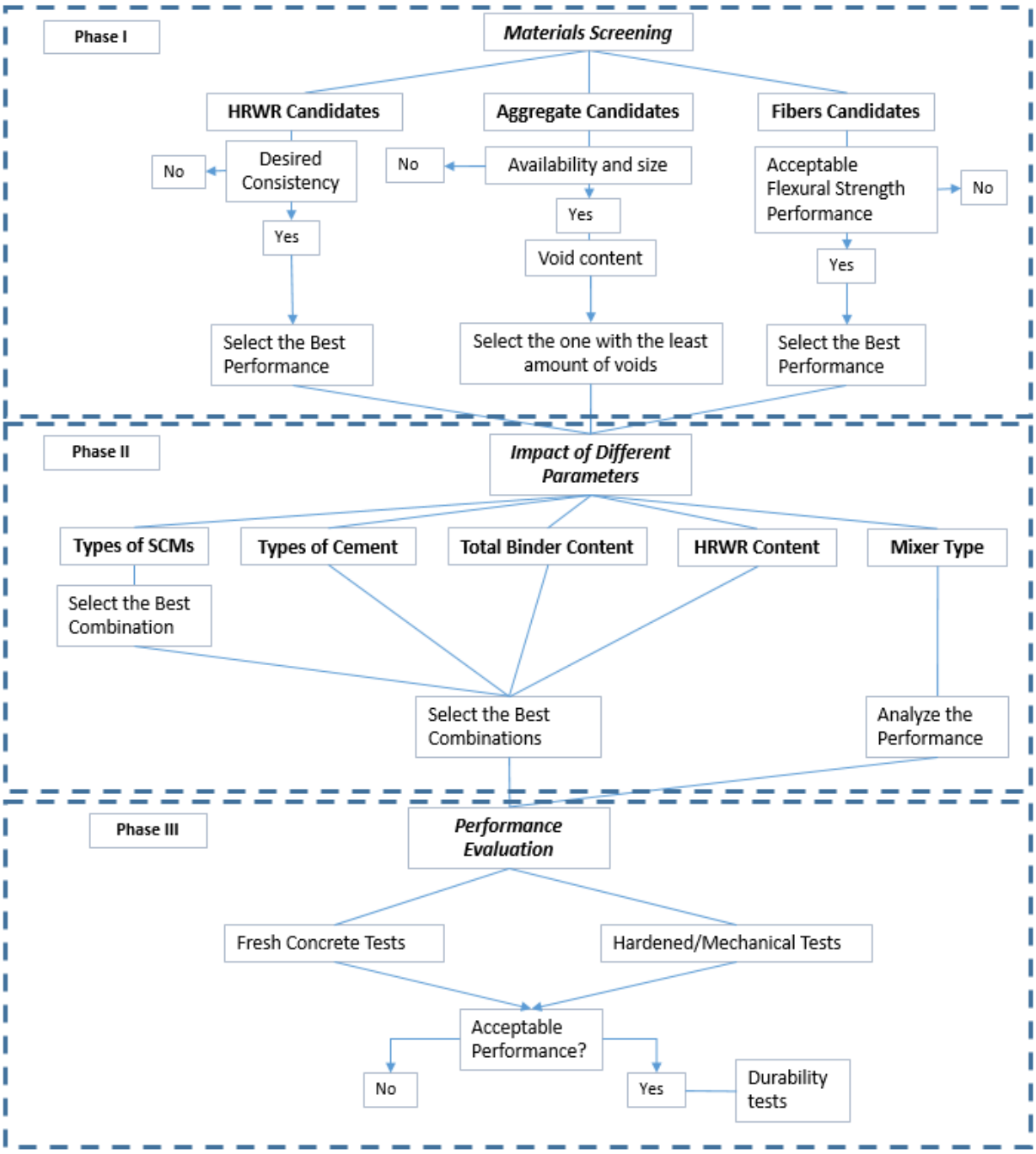

Figure 4.2 Sequence of mixture development phases

Since it is generally believed that the mixer and the volume of material mixed can influence the mixing procedure and, consequently, the performance of the UHPC, additional experimental work was conducted to evaluate the impact of the mixers on the performance of the fresh and hardened UHPC.

For this study, the identification of the mix began with the type of cement, followed by a letter that refers to the other type of binder, a number that indicates the percentage of the additional binder based on its mass fraction of all of the binder. To identify the type of cement, IP stands for

IP cement, I/II stands for Type I/II cement, III stands for Type III cement, and OWH stands for class H oil well cement. For the type of binder, SF stands for silica fume, FA stands for Class C fly ash, S stands for slag, and QP stands for quartz powder. Finally, after the letter(s) refer to binder type(s), the total binder content rounded to the nearest 50 pcy was identified followed the letter "B". As an example, I/II:SF19:FA16:B1500 uses Type I/II cement, 19% silica fume, and 16% fly ash in the total mass of the binder. The mix does not contain slag or quartz powder. The total binder content is approximately 1500 pcy.

When the impact of fibers was evaluated, the mixture identification had two additional letters at the end, representing the type of fiber used. The following letters indicate the types of fibers, i.e., SS (straight steel fiber), TS13 and TS25 (the two twisted steel fibers), and SG (synthetic fiberglass fiber). When the impact of the amount of HRWR was evaluated, the mixture identification had "HRWR" followed by the percentage of the chemical by the total mass of binder used. When the mixes were mixed in a large batch, "LB" was added at the end of the mixture identification. The designs of the mixes presented in this chapter are presented in pcy, and it is adjusted based on the hardened unit weight of the samples. The aggregate masses were all presented in the SSD condition.

4.2.1 Phase I: Material screening

4.2.1.1 Aggregate

As mentioned earlier in this chapter, one of the main focuses of the phase I study was to select an appropriate aggregate for the development of UHPC. Aggregates account for the largest fraction in UHPC design. To ensure cost-effectiveness, aggregates candidates were identified based on their availability in the state of Nebraska. In the preliminary stage of the study, locally available riversand and limestone sand (a commercial product name Unical L) were considered. However, particle size distribution results showed that the particle size is significantly larger than binder materials particles, which lead to a lower packing degree due to the large gap in particle size. The finding is consistent with the information, as shown in Chapter 2, that aggregates with finer particles, i.e., the maximum size below sieve size No. 8, are desirable in the UHPC matrix. Also, a preliminary study also demonstrated that the resulting strength of concrete made with river sand and limestone could not achieve sufficient strength for UHPC development, the two materials were excluded from further study. The focus on aggregate selection was therefore focused only on a locally available No. 10 sand, also classified as masonry sand. To determine the feasibility of further improve particle packing with the No. 10 sand, a commercial fine silica sand, was also introduced. The commercial fine silica sand, namely F75, was reportedly used by other researchers as well. A void content test based on ASTM C1252 (ASTM, 2006) was performed with different aggregates and aggregate combinations to identify the aggregates matrix that provides the least amount of voids. In addition, to account for the high fineness of the materials, a compacted voids test was also conducted, as suggested by De Larrard (1999). Since the surface charge of the fine particles may result in repulsion forces among fine aggregate particles, compaction can minimize the interaction force among the fine particles and provide a more meaningful evaluation of the voids. The compacted void test consists of filling a $0.25ft^3$ ($0.03m^3$) container with the aggregate or combination of aggregates and vibrating them for 1 minute using a vibrating table. During the vibration, an external pressure of 1.45 psi (10 KPa) was applied to the specimens with a consistent weight applied on top of the aggregate specimen. The percentage of voids was calculated based on the bulk volume of the aggregate inside the testing container after vibration, according to Equation 3.1.

$$Void\% = \frac{(SG \times UW_{water}) - \frac{W}{V}}{(SG \times UW_{water})} \qquad \textbf{Equation 4. 1}$$

where SG is the specific gravity of the aggregate or combination of aggregates, UW_{water} is the unit weight of the water, W is the mass of the aggregate, and V is the volume occupied by the aggregate. The specific gravity of the combination of aggregates SG_{comb} was calculated using Equation 3.2.

$$SG_{comb} = \frac{1}{(\frac{P1}{SG1} + \frac{P2}{SG2})} \qquad \textbf{Equation 4. 2}$$

where P_1 and P_2 are the percentages of aggregate 1 and aggregate 2, respectively, and SG_1 and SG_2 are the specific gravity of aggregate 1 and aggregate 2, respectively. The specific gravity and absorption of aggregates were obtained following ASTM C128 (ASTM 2015).

Figure 4.3 shows the results of the uncompacted and compacted void content of No. 10 sand and matrix of No. 10 sand being partially replaced by the F75 fine silica sand.

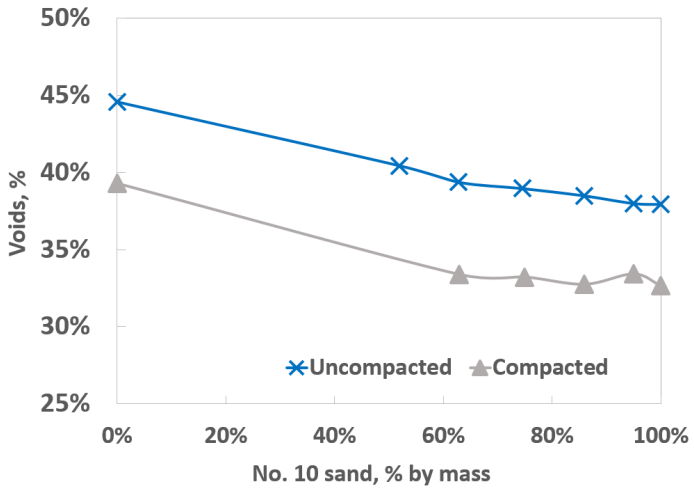

Figure 4.3 Uncompacted and compacted void contents of aggregates in No. 10 sand matrix

Results, as shown in Figure 4.3, indicate that, when the F75 fine silica sand was introduced into the No.10 sand matrix, the particle packing was disturbed slightly, resulting in an increase in the uncompacted and compacted voids in the matrix. Figure 4.3 also shows that when the F75fine silica sand was evaluated individually, the void content is higher than that of No. 10 sand. The results indicate that a single-aggregate system with only No. 10 sand should be selected in the UHPC mixes, considering that it is locally available and the least amount of voids is desirable to achieve a denser structure in the UHPC matrix. Per ASTM C128 (ASTM, 2015), the specific gravity and absorption of the No. 10 sand were measured at 2.63 and 0.38%, respectively.

4.2.1.2 Fibers

To determine the most effective type of fiber to be used, specimens were prepared with a representative design that had the same volume fraction (2%) but different types of fibers. The type that provided the highest flexural strength and toughness was selected. As mentioned earlier, four different types of fibers were studied, i.e., a straight stainless steel fiber (SS), two twisted steel fibers (TS13 and TS25), and a synthetic fiberglass fiber (SG). The performance of the UHPC

mixtures was evaluated with a flexural strength test per ASTM C1609. Table 4.1 shows the design of mixes that were prepared with different fibers.

Table 4.1 Mix design of mixes prepared with different fibers

Mix ID	Cement	Silica Fume	Fly ash	Water	Sand	Fiber	HRWR	w/b
I/II:SF6:FA20:B1450:SS	1076	87	294	250	2132	260	47.7	0.195
I/II:SF6:FA20:B1450:TS13	1074	87	293	244	2107	260	47.6	0.191
I/II:SF6:FA20:B1450:TS25	1080	87	295	243	2134	260	47.9	0.189
I/II:SF6:FA20:B1450:SG	1070	86	292	243	2109	68	47.7	0.191

Note: All units are in pcy (1 pcy = 0.59 Kg/m^3)

Figure 4.4 shows the 28-day load-displacement relationship of specimens with mixes from the four different types of fibers.

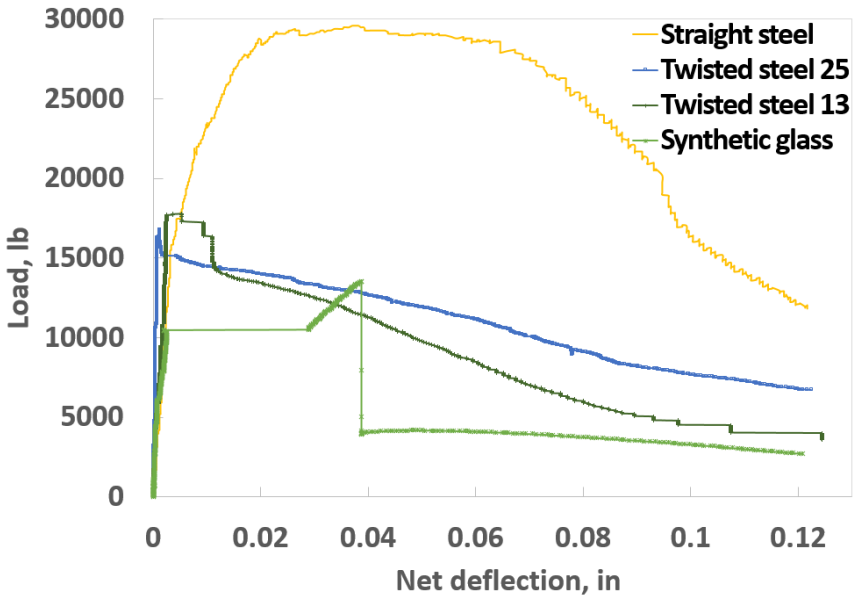

Figure 4.4 Load-displacement relationship of flexural behavior of UHPC with different types of fibers

The flexural behavior, as shown in Figure 4.4 suggests the selection of micro straight steel (SS) fibers due to their much higher modulus of rupture and toughness compared to the other three types of fibers. The mix with SS fibers provided a modulus of rupture and toughness that were comparable to the commercial UHPC product.

4.2.1.3 HRWR

Since the significantly low w/b of UHPC makes the use of HRWR essential, mixes with a representative design but different HRWRs were prepared to identify the most effective HRWR for the developed UHPC mixes. At the low w/b used in the design, the selected HRWR is expected to provide sufficient flowability to ensure good consistency and self-compaction capability during casting.

Table 4.2 shows the mix design of mixes prepared with different HRWRs. The mix identification has a number (1, 2, or 3) added after "HRWR," and the numbers indicate the three different HRWR used. HRWR#1 was a modified polycarboxylate based HRWR (Premia 150 from CRYSO), HRWR#2, and HRWR#3 were two polycarboxylate based HRWRs that met ASTM C494 (ASTM, 2017) Type-A and F (ADVA 198 from GCP) and Type I (ADVA 140M from GCP) respectively. Note that two other polycarboxylate based HRWRs (MasterGlenium 7500, and MasterGlenium 7920 from BASF) were also used in preliminary mixes, but were not selected for further study due to the resulted substantially-low workability.

Table 4.2 Mix design of mixes prepared with different HRWRs

Mix ID	Cement	Silica Fume	Slag	Water	Sand	Fiber	HRWR	w/b
I/II:SF11:S34:B1400:HRWR1	884	117	427	239	2131	266	50.0	0.192
I/II:SF11:S34:B1400:HRWR2	880	117	426	238	2124	266	49.9	0.192
I/II:SF11:S34:B1400:HRWR3	880	117	426	238	2124	266	49.9	0.192

Note: All units are in pcy (1 pcy = 0.59 Kg/m^3)

Based the evaluation of flowability of developed UHPC mixes, HRWR #1 (Premia 150 from CRYSO) was chosen to be used in the UHPC mixes as it provided a flowable mix with approximately 9.6 inches of flow and reasonable compressive strength with $f'_{c,4}$ at approximately13,000 psi and $f'_{c,28}$ at approximately 17,200 psi. The other two HRWRs (#2 and #3) did not provide the desired consistency, as determined by visual examination of the mixtures at the fresh stage. Figures 4.5a and 4.5b show examples of the UHPC with the desired consistency and poor consistency, respectively. Noted that for clearer demonstration, the pictures were taken prior to fiber be added into the mixture.

(a) Desired consistency (b) Unacceptable consistency

Figure 4.5 Examples of UHPC mixtures with desired and unacceptable consistencies

4.2.2 Phase II: Key design parameters evaluation

In Phase II, the performance of UHPC mixes with different types and contents of binders, different contents of HRWR, and mixers were studied. The modified A&A particle packing theory model was used as the initial guide for deciding the proportions of the materials. However, as the impact of binder composition (cement and SCMs type, and relative content), as well as the total binder content on particle packing, workability, and strength development of UHPC are often interrelated, there is no practical way to obtain the optimum binder composition and content directly. The approach of this study is, therefore, to identify the best binder combination and content based on the evaluation of UHPC performance with the adjustment one component at a time. This stage consisted of ternary binder mixes using and different types and quantities and cement of binders, with each parameter being analyzed separately, while other parameters, including fiber, aggregate, HRWR, remained the same. Figure 4.6 shows a summary of the cement and SCMs and the quantities evaluated. The amounts presented for each of the SCMs are in the volume fraction of the whole binder content.

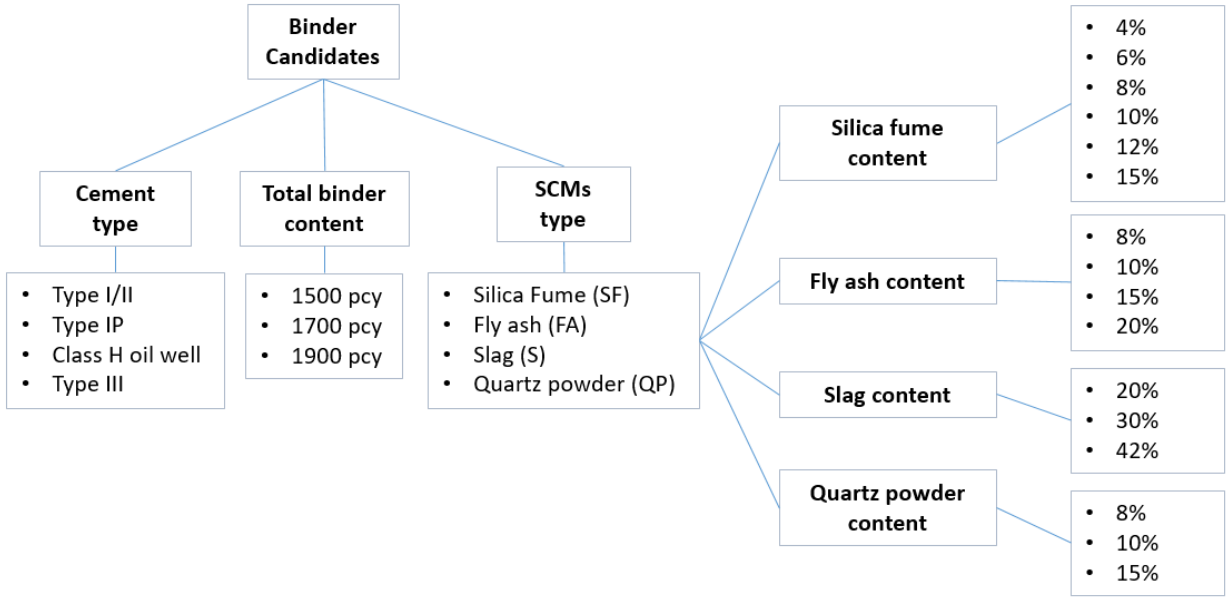

Figure 4.6 Cement and SCMs types and quantities included in Phase II study

Overall, this stage can be divided into multiple series. Series 1 evaluated different types of cement to be used in the UHPC mixes. Series 2, series 3, series 4, and series 5 investigated different silica fume, fly ash, slag, and quartz powder contents, respectively. The impacts of the types and quantities of binders were analyzed within each series and between the series. Series 7 evaluated the impact of total binder content. Furthermore, the impact of HRWR content on UHPC performance was evaluated in Series 8. Furthermore, selected mixes were prepared with two different mixers and batch sizes, and the performance of the mixes was evaluated in Series 9.

The investigation of phase II involved the evaluation of the key characteristics of fresh and hardened concrete, namely flow and 28-day compressive strength. Table 4.3 summarises the mix design for mixes in all the series prepared in this phase, as well as the resulted flow and compressive strength.

Based on results from the Phase II study, Type I/II cement was determined to provide the best workability and strength characteristics. It was also found that 8% of silica fume (by mass of binder) was the optimum amount that provides the highest strength yet economic UHPC mix. While fly ash and quartz powder did not provide positive impacts on UHPC performance, 30% of slag (by mass of the binder) was found to provide the best performance of UHPC. The total binder content of approximately 1900pcy provided a UHPC with better performance when compared to the other binder contents analyzed. Detailed results and discussions of the impact of different parameters on the performance of UHPC are presented in Appendix A and Appendix B.

Table 4.3 Mix design and results from mix design development phase II study

Series	Mix ID	Cement	Silica fume	Fly ash	Slag	Quartz powder	Water	Sand	Fiber	HRWR	w/b	Flow, in	$f'_{c,28}$, ksi
1	I/II:SF8:S30:B1450	884	117	0	427	0	239	2131	266	50.0	0.192	8.5	12.94
	IP:SF8:S30:B1450	902	120	0	436	0	244	2176	266	51.1	0.192	9.45	14.46
	OWH:SF8:S30:B1500	921	123	0	446	0	229	2222	266	52.0	0.178	6.84	15.28
	III: SF11:FA22:S0:QP0	1119	125	314	0	0	240	1687	265	54	0.189	8.28	16.16
	I/II: SF11:FA22:S0:QP0	986	110	277	0	0	229	2004	261	51	0.192	9.62	14.46
2	I/II:SF4:FA20:B1450	1108	58	295	0	0	247	2130	264	46.4	0.191	8.27	15.24
	I/II:SF6:FA20:B1450	1076	87	294	0	0	250	2123	260	47.7	0.195	7.52	16.73
	I/II:SF8:FA20:B1450	1049	117	294	0	0	247	2132	261	51.2	0.194	7.65	17.44
	I/II:SF10:FA20:B1450	997	143	287	0	0	233	2081	260	46.4	0.186	6.25	16.61
	I/II:SF12:FA20:B1450	987	175	293	0	0	236	2119	260	63.4	0.193	7.79	16.70
	I/II:SF15:FA20:B1450	928	215	288	0	0	230	2098	260	65.7	0.193	7.18	15.41
	I/II:UndSF8:FA20:B1450	1050	118	295	0	0	244	2135	250	51.3	0.191	9.93	16.13
	I/II:UndSF8:S42:B1400	691	118	0	586	0	234	2130	266	48.9	0.192	9.64	14.38
3	I/II:SF15:FA8:B1550	1183	232	130	0	0	261	1980	265	56.0	0.194	7.63	15.39
	I/II:SF15:FA10:B1550	1157	231	154	0	0	260	1977	265	56.0	0.194	7.71	15.18
	I/II:SF15:FA15:B1550	1086	233	233	0	0	262	1988	265	56.0	0.194	6.87	14.84
	I/II:SF15:FA20:B1450	928	215	288	0	0	230	2098	260	65.7	0.193	7.18	15.41
4	I/II:SF8:S20:B1500	1064	119	0	299	0	245	2164	250	51.9	0.190	8.89	16.51
	I/II:SF8:S30:B1450	906	117	0	427	0	239	2131	266	50.1	0.192	9.57	17.26
	I/II:SF8:S42:B1450	711	121	0	603	0	240	2200	266	50.3	0.192	9.39	16.83
5	I/II:SF15:QP8:B1550	1202	236	0	0	132	265	2021	265	50.0	0.191	6.27	14.60
	I/II:SF15:QP10:B1550	1159	232	0	0	155	261	1980	265	50.0	0.191	6.36	14.91
	I/II:SF15:QP15:B1550	1075	230	0	0	230	259	1968	265	50.0	0.192	6.19	16.06
6	I/II:SF7:S23:QP16:B2000	1175	138	0	388	327	278	1637	266	58.0	0.157	10.00	16.98
	I/II:SF13:S21:QP16:B1900	1025	242	0	341	316	259	1582	266	58.0	0.156	10.00	15.26
	I/II:SF17:S20:QP17:B1900	958	319	0	319	319	256	1597	266	58.0	0.155	9.39	15.99
7	I/II:SF8:S30:B1450	884	117	0	427	0	239	2131	266	50.1	0.192	8.50	12.94
	I/II:SF8:S30:B1650	1035	138	0	501	0	280	1863	266	58.7	0.192	8.47	13.73
	I/II:SF8:S30:B1900	1175	156	0	569	0	318	1559	266	66.6	0.192	10.00	13.45
	IP:SF8:S30:B1450	902	120	0	436	0	244	2176	266	51.1	0.192	9.45	14.46
	IP:SF8:S30:B1700	1065	141	0	516	0	288	1862	266	60.3	0.192	10.00	15.96
	IP:SF8:S30:B1900	1182	157	0	573	0	319	1498	266	67.0	0.191	10.00	16.58

	OWH:SF8:S30:B1500	921	123	0	446	0	229	2222	266	52.2	0.178	6.84	15.28
	OWH:SF8:S30:B1750	1094	145	0	529	0	238	1913	266	62.0	0.159	10.00	16.81
	OWH:SF8:S30:B2050	1281	171	0	621	0	278	1624	266	72.6	0.159	10.00	17.47
8	I/II:SF8:S30:B1900:HRWR3.4%	1179	157	0	571	0	301	1565	266	64.6	0.182	10.00	14.04
	I/II:SF8:S30:B1900:HRWR2.8%	1172	156	0	576	0	300	1498	266	54.0	0.177	10.00	13.65
	I/II:SF8:S30:B1900:HRWR2.3%	1156	154	0	560	0	295	1534	266	42.9	0.174	0.00	0.00
	IP:SF8:S30:B1900:HRWR3.5%	1182	157	0	573	0	319	1498	266	67.0	0.191	10.00	16.58
	IP:SF8:S30:B1900:HRWR2.4%	1185	158	0	574	0	320	1502	266	45.7	0.184	10.00	13.84
	OWH:SF8:S30:B2050:HRWR3.5%	1281	171	0	621	0	278	1624	266	72.6	0.159	10.00	17.48
	OWH:SF8:S30:B2100:HRWR2.9%	1291	172	0	626	0	289	1638	266	61.4	0.159	10.00	17.07
	OWH:SF8:S30:B2050:HRWR2.4%	1277	170	0	617	0	293	1619	266	49.2	0.159	10.00	16.22
9	I/II:SF8:S30:B1450:HRWR3.5%	884	117	0	427	0	239	2131	266	50.1	0.192	8.50	12.94
	I/II:SF8:S30:B1800:HRWR3.5%	1107	147	0	536	0	299	1991	266	62.7	0.192	10.00	15.33
	I/II:SF8:S30:B1900:HRWR3.4%	1179	157	0	571	0	301	1565	266	64.6	0.182	10.00	14.77
	I/II:SF8:S30:B1900:HRWR2.8%	1172	156	0	576	0	300	1498	266	54.0	0.177	10.00	13.65
	I/II:SF8:S30:B1450:HRWR3.9%:LB	885	117	0	428	0	242	2133	266	55.0	0.196	10.00	13.86
	I/II:SF8:S30:B1800:HRWR3.5%:LB	1070	143	0	518	0	289	1925	266	60.6	0.191	10.00	16.82
	I/II:SF8:S30:B1900:HRWR3.4%:LB	1207	161	0	585	0	309	1603	266	66.1	0.182	10.00	17.70
	I/II:SF8:S30:B1900:HRWR2.8%:LB	1214	162	0	588	0	310	1612	266	55.6*	0.178	10.00	16.49

* I/II:SF8:S30:B1900:HRWR2.8%:LB had 1.4pcy addition of air detrainer admixture

4.3 Summary

This chapter presented the details of the experimental program to investigate the impact of different types of materials, including aggregates, fiber, HRWR, cement, SCMs on UHPC performance. Impacts of the different combinations of binders, different total binder quantity, different HRWR quantity, and different mixers were also evaluated.

While detailed results and discussions can be found in Appendix A and Appendix B, the chapter includes the results of the flow and compressive strength of the UHPC mixes included in this study as well as the final selection of materials and mix design. The aggregate and fiber selected for the UHPC were No.10 sand, and micro straight steel fiber, respectively. The HRWR that provided UHPC with the best performance was a modified polycarboxylate-based HRWR (Premia 150 from CRYSO). Based on results from the impact of the cement, SCMs, and their contents, Type I/II cement was determined to provide the best flow and compressive strength. With regard to silica fume content, it was found that 8% (by mass of binder) was the amount that provides the highest strength yet maintains good workability. While fly ash and quartz powder did not provide positive impacts on UHPC performance, a 30% (by mass of the binder) of slag was found to provide the best performance of UHPC. The total binder content of approximately 1900 pcy provided a UHPC with better performance when compared to the other binder contents analyzed. Based on the test results, three mixes were chosen for further performance evaluation, which will be detailed in Chapter 5.

CHAPTER 5 PERFORMANCE EVALUATION

5.1 Introduction

Based on results from Phase I and Phase II study, three developed UHPC mixes, UNL UHPC 1450, UHPC 1700, and UHPC 1900, were selected for further performance evaluation. Table 5.1 presents the mix design of the three selected mixes, together with a commercial UHPC product. This chapter presents a comprehensive evaluation of fresh and early age, mechanical, and durability properties of the three developed UHPC mixes. All UHPC mixes listed in Table 5.1 were prepared with large laboratory quantities at approximately 2.5 ft^3 to simulate field batching.

Table 5.1 Mix proportions of developed and commercial UHPC mixes

Constituent	Mass (lb/yd^3)			
	UNL UHPC 1450	UNL UHPC 1700	UNL UHPC 1900	Commercial
Type I/II Cement	878	1070	1214	Pre-bagged
Silica Fume	117	143	162	
Slag	425	518	588	
#10 Sand	2119	1925	1612	
Water and Ice	241	289	310	219
HRWR (Premia 150)	55	61	56	51
Fiber	267	283	266	263
w/b	0.196	0.192	0.178	< 0.200

5.2 Fresh and Early Age Concrete Properties

5.2.1 Flowability and setting time

Results of the flow of the three developed UHPC mixes are shown in Table 5.2. As shown in the table, all three developed UHPC mixes had satisfactory flow according to ASTM C1856 requirement of 8 to 10 in. (ASTM, 2017) and FHWA acceptance criteria of 7 to 10 in. (FHWA, 2014). The setting time of mix UNL UHPC 1900 was measured based on ASTM C403 (ASTM, 2016) and ASTM C191 (ASTM, 2018). Both tests present similar results, and the initial set and final set time are both reasonable for field construction.

Table 5.2 Results of fresh and early age concrete behaviors of final UHPC mixes

Property	UNL UHPC 1450	UNL UHPC 1700	UNL UHPC 1900	
Flow	8.70 in.	10+[1] in.	10+[1] in.	
Initial set	n/a	n/a	2.5 hr	2.2 hr
Final set			5.5 hr	6.0 hr

[1] Mixes flowed out of the flow table within 2 minutes, and the flow values are reported as higher than 10 in.

Detail results from the two set time tests are shown in Figure 5.1.

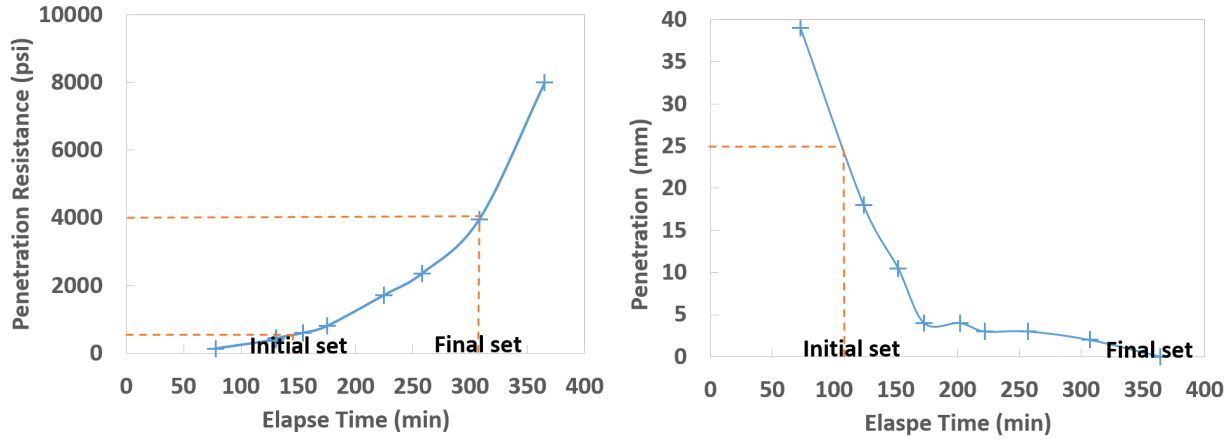

(a) ASTM C403 test method (b) ASTM C191 test method

Figure 5.1 Set time results of the developed UNL UHPC 1900 mix

5.2.2 Heat of hydration

Figure 5.2 shows the heat of hydration results of the first 96 hours for the three developed UHPC mixes. As the three mixes have the same relative silica fume and slag contents, and differ mostly only on total binder content, as expected, the heat generated per gram of binder of each mix does not differ much from each other.

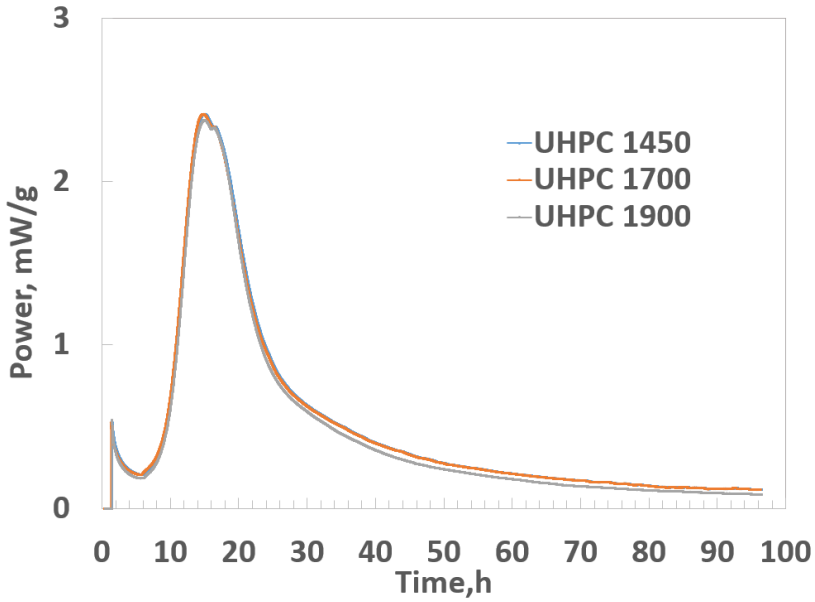

Figure 5.2 Heat of hydration results of the developed UHPC mixes

5.3 Mechanical Properties

Methods, sizes, and numbers of specimens used in evaluating different mechanical properties are summarized in Table 5.3.

Table 5.3 Mechanical properties testing matrix

Test	Reference	Specimen	Number
Compressive strength	ASTM C1856	Cylinders 3″x6″	9
Modulus of elasticity & Poisson's ratio	ASTM C469	Cylinders 4″x8″	3
Flexural Strength	ASTM C1856 & ASTM C1609	Prism 3″x3″x14″	3
Splitting tensile strength	ASTM C496	Cylinders 4″x8″	3
Direct tensile strength	FHWA-HRT-17-053	Prism 2″x2″x 24″	3
Direct shear strength	Haber, et al. (2017)	Prism 2″x2″x6″	4
Slant shear test	ASTM C882	Cylinders 4″x8″	6
Rebar bond strength	Roy, et al. (2017)	Prism 8″x9″x3″	3

5.3.1 Compressive strength

Figure 5.3 shows the average compressive strength versus the age of the three developed UNL UHPC mixes, together with a commercial UHPC product. Detailed testing results are available in Appendix C.

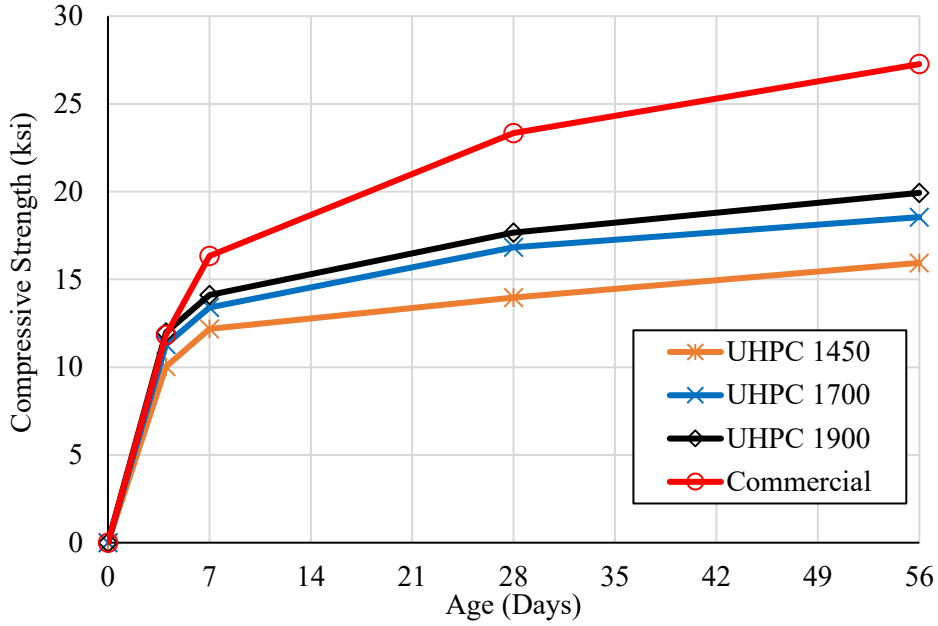

Figure 5.3 Compressive strength of developed and commercial UHPC mixes at different ages

Results showed that while the compressive strengths of the three UNL UHPC mixes are lower than the commercial product, UHPC 1900 mix achieved a compressive strength of 17.8ksi at 28-day of age and UHPC 1700 achieved 17.2ksi at 56-day which both satisfies the ASTM C1856 requirement of 17ksi. UHPC 1900 mix showed a good agreement with the FHWA (2018) report as it reached 20.0ksi at 56-day with standard curing.

5.3.2 Modulus of elasticity and Poisson's ratio test

The average modulus of elasticity (MOE) and Poisson's ratio for the commercial and three developed UHPC mixes are presented in Figures 5.4 and 5.5, respectively. Detailed testing results are available in Appendix C. Results showed that while there is no significant difference among the modulus of elasticities of the three developed UHPC mixes, they are slightly lower than that of the commercial UHPC. Also, the Poisson's ratio values for UHPC mixes showed no significant difference, but slightly higher than that of the commercial product.

According to AASHTO LRFD Bridge Design Specification (2017), MOE can be calculated with the following equation for conventional concrete with design compressive strength up to 15 ksi and unit weight between 0.090 to 0.155 kcf:

$$E_c = 120000 K_1 w_c^{2.0} f_c'^{\,0.33} \qquad \textbf{Equation 5.1}$$

where E_c *is the* modulus of elasticity (ksi), K_1 is the correction factor for the source of aggregate (to be taken as 1.0 unless determined by a physical test, and as approved by the owner), w_c is the unit weight of concrete (kcf), and f'_c is the compressive strength of concrete for the use in design (ksi).

Based on *FHWA-HRT-18-036*, the modulus of elasticity can be calculated with the following equation:

$$E_c = 1430 \sqrt{f_c'} \qquad \textbf{Equation 5.2}$$

The obtained modulus of elasticity for the three developed mixes were compared to predicted values by AASHTO LRFD 2017 and report No. *FHWA-HRT-18-036* as shown in Figure 5.5. The measured MOE showed good agreement with FHWA-HRT-18-036 predicted values. However, the AASHTO LRFD 2017 predicted values gave higher MOE as the prediction equation was designed for conventional concrete.

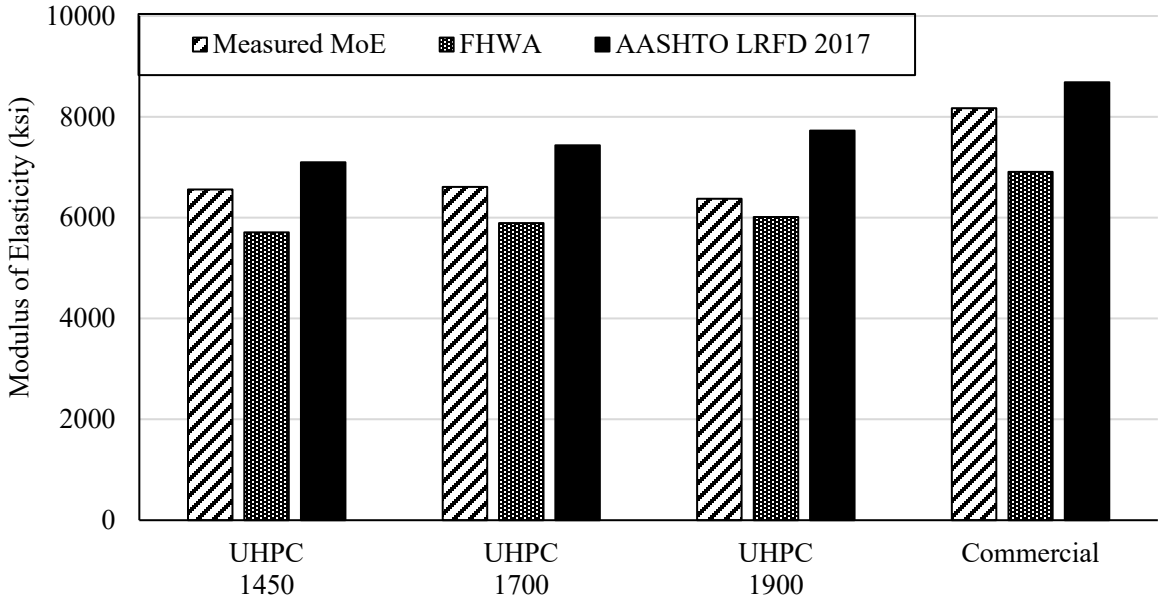

Figure 5.4 Modulus of elasticity of the developed and commercial UHPC mixes and comparison to predicted values

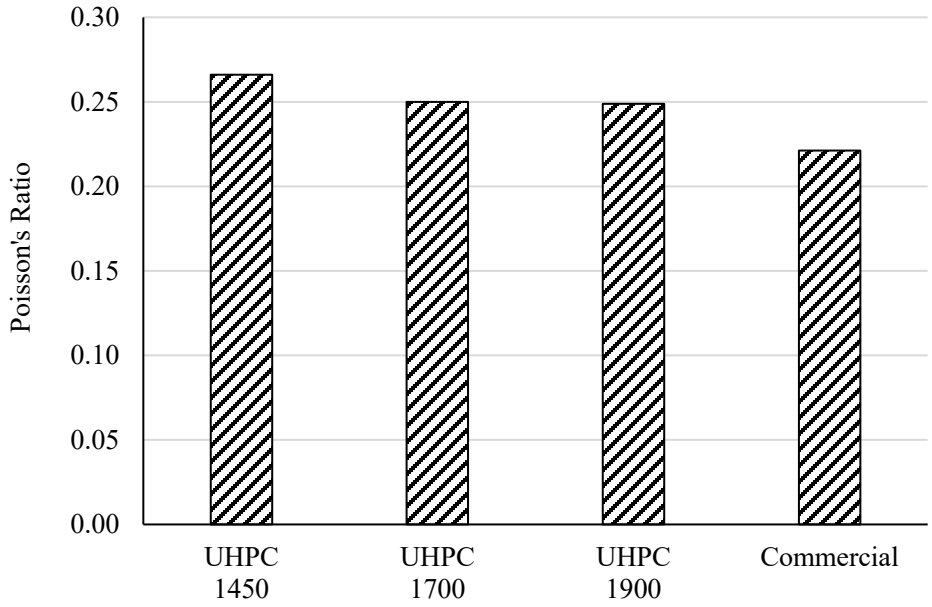

Figure 5.5 Poisson's ratio of developed and commercial UHPC mixes

5.3.3 Flexural strength test

Figure 5.6 shows the flexural strength test results of the developed UHPC mixes and their comparison to ACI limits based on ACI 319-19. Detailed testing results are available in Appendix C. UHPC 1900 mix flexural curve, and first crack and peak crack strengths showed good agreement with the commercial UHPC mix and satisfying ACI-318-19 limits.

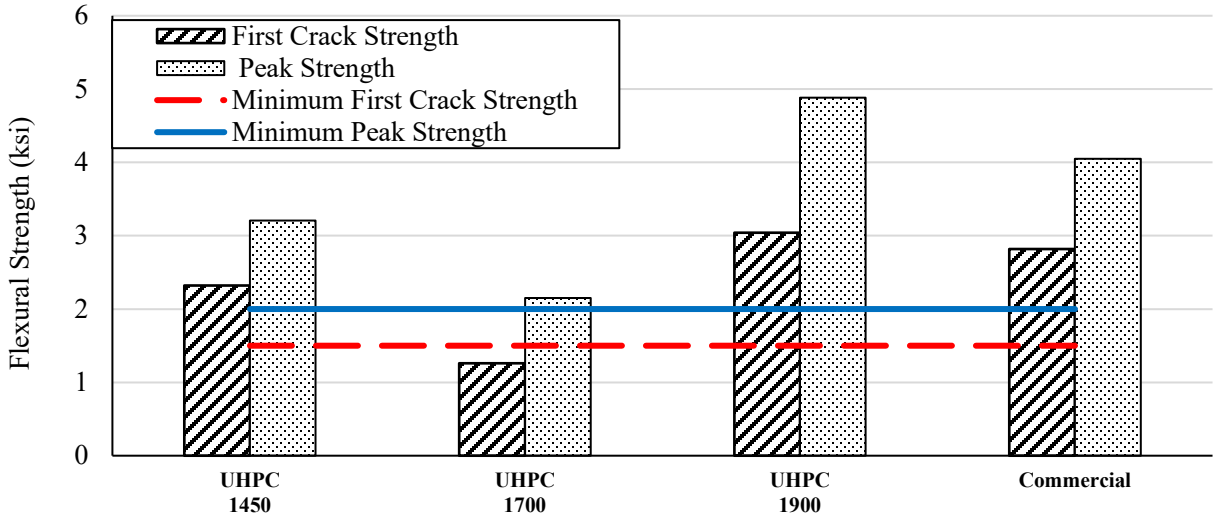

Figure 5.6 Flexural strength of the developed and commercial UHPC mixes and their comparison to ACI-318-19 limits

5.3.4 Splitting tensile strength test

According to AASHTO LRFD (2017), the tensile strength may be determined by splitting tensile strength test and may be estimated by the following equation for normal concrete with design compressive strength up to 10 ksi.

$$f_t = 0.23\sqrt{f_c'} \qquad \textbf{Equation 5.3}$$

Where f_t is the direct tensile strength (ksi), and f'_c is the compressive strength of concrete for use in design (ksi).

The average splitting tensile strength of each of the developed UHPC and commercial UHPC mixes and their comparison to AASHTO LRFD 2017 are presented in Figure 5.7. Detailed testing results are available in Appendix C. The obtained splitting tensile strength of UHPC mixes showed no significant difference. However, it was lower than the commercial UHPC. The high variance of the measured and predicted splitting test results indicated that splitting tensile test equation from AASHTO LRFD is not adequate for predicting the tensile strength of UHPC.

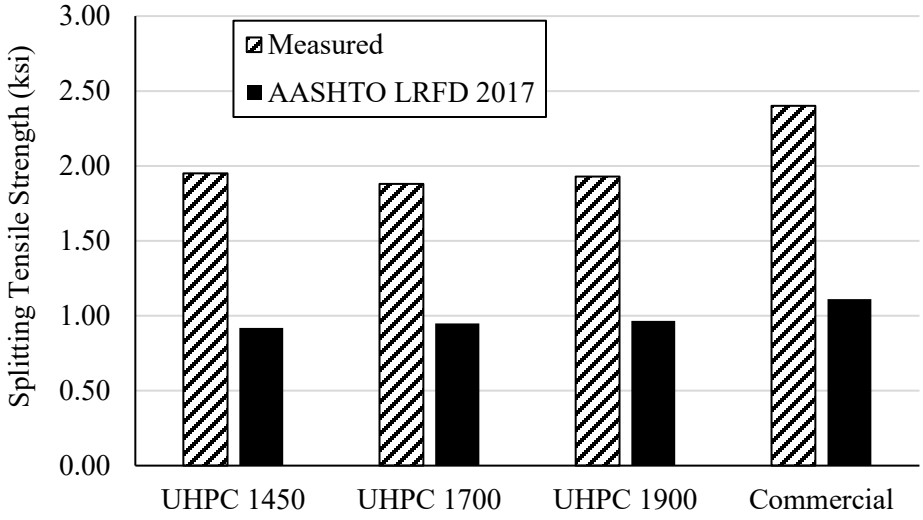

Figure 5.7 Splitting tensile strength of the developed and commercial UHPC mixes and their comparison to AASHTO LRFD 2017

5.3.5 Direct tensile strength test

The direct tensile strength test was conducted for only three UHPC specimens made of the commercial mix and not any of the specimens made of UNL UHPC due to malfunction of the testing equipment. Therefore, no test results are available for this report. However, an inverse analysis was conducted to convert the flexural strength test results to the equivalent tensile strength. In this analysis, the simplified stress-strain relationship of UHPC in compression and tension proposed by Fehling and Leutbecher (2011) were used. Different values of the tensile strength were assumed and the corresponding flexural strength values were calculated using strain compatibility. A straight line relationship between the two properties was developed, which yield a conversion factor of approximately 2.5. For example, a 4 ksi flexural strength using the 3”x3”x12” prism would results in 1.6 ksi tensile strength for an 18 ksi compressive strength.

5.3.6 Direct shear strength test

The average direct shear strength of the developed and commercial UHPC mixes is shown in Figure 5.8. All the specimens exhibited a double shear failure. Detailed testing results are available in Appendix C. The three developed UHPC mixes showed good agreement with the direct shear strength from the commercial product and the range reported by the FHWA study (Haber et al., 2017).

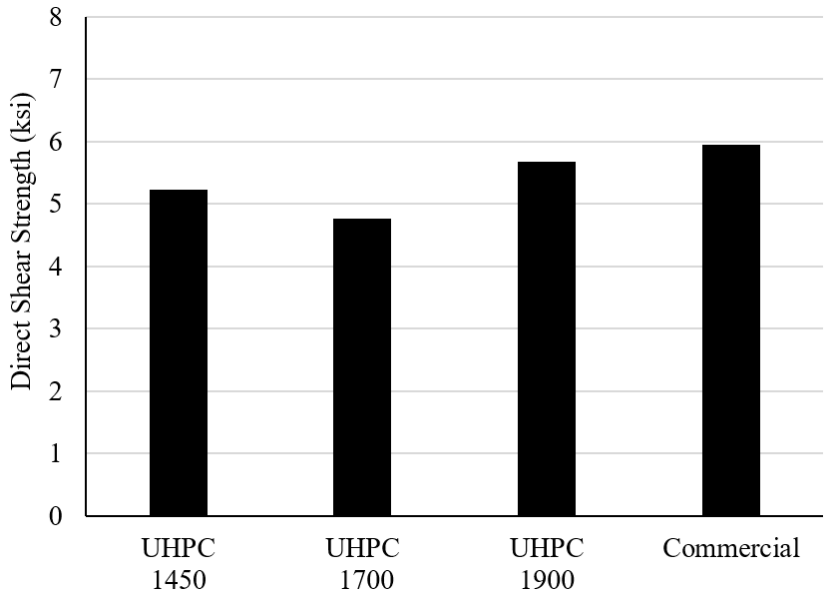

Figure 5.8 Direct shear strength for the developed and commercial UHPC mixes

5.3.7 Slant shear test

With the slant shear specimens tested, two different failure modes were observed, depends on the surface textures. It was observed that all the specimens with a smooth interface surface had a bond failure, as shown in Figure 5.9 (a). However, specimens with a deep grooved interface surface had a failure in the CC portion as shown in Figure 5.9 (b). The interface shear resistance and normal stress were calculated by dividing the applied load components at the interface surface, based on the interface angle, as shown in Figure 3.16, by the interface surface area (25.1 in.^{2}). Figure 5.10 presents the average interface shear resistance of three identical specimens for the three developed UHPC and commercial UHPC mixes. Results indicate that there is no significant difference in the interface shear resistance of different UHPC mixes with deep grooving surface texture as it depends on the compressive strength of CC. Detailed testing results are available in Appendix C.

(a) Bond failure (b) CC failure

Figure 5.9 Slant shear specimen failure modes

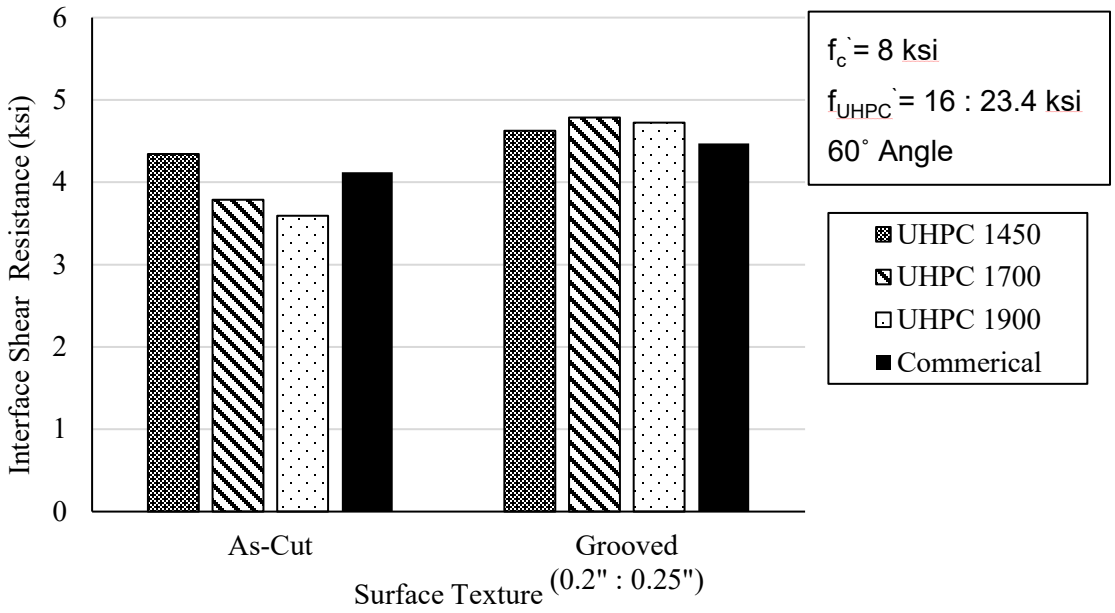

Figure 5.10 Interface shear resistance of UHPC with different surface textures

5.3.8 Bond strength test

Figure 5.11 and Figure 5.12 show the results of the commercial and the developed UHPC 1900 mix. All specimens exhibited splitting failure mode in the UHPC block, as shown in Figure 5.13, except the first UHPC 1900 specimen as it was tested twice for anchorage bar slippage out of the coupler. All the specimens achieved maximum bar tensile strength higher than 60 ksi before exhibiting bond failure and before 0.1in. bar slippage. The UHPC 1900 mix satisfied the recommendations of *FHWA-HRT-14-090*. Detailed testing results are available in Appendix C.

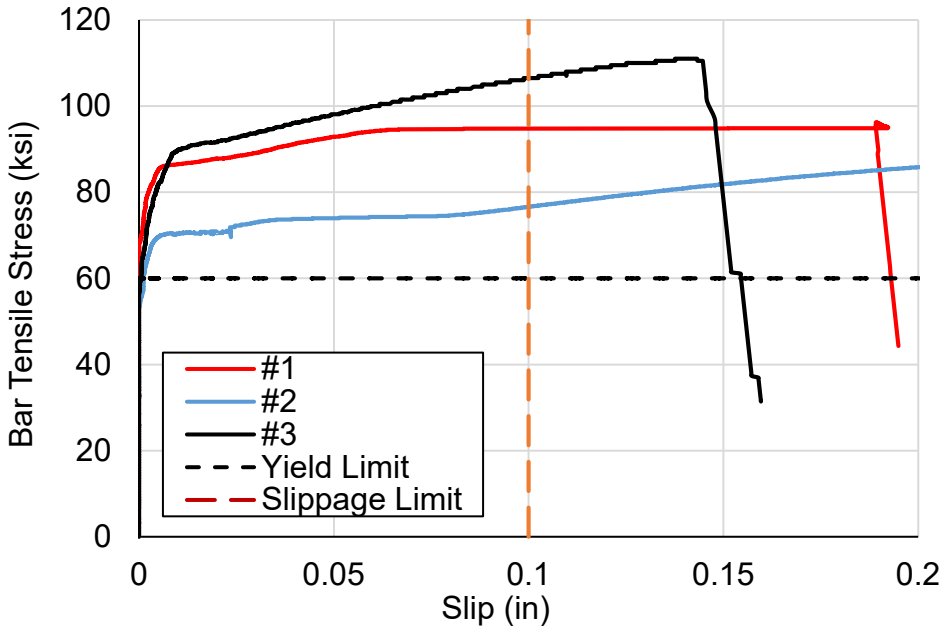

Figure 5.11 Bond test results of commercial UHPC mix

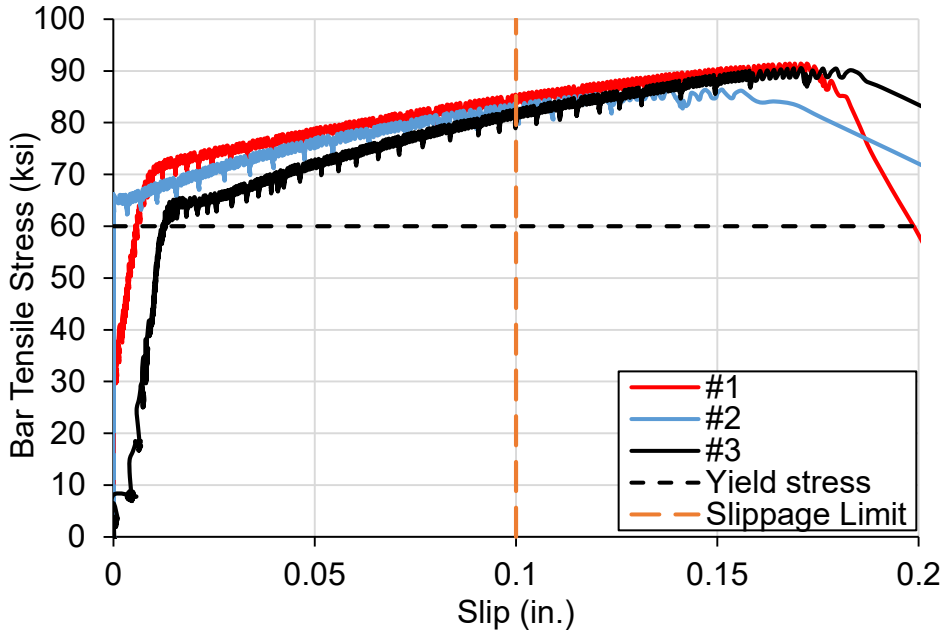

Figure 5.12 Bond test results of UHPC 1900 mix

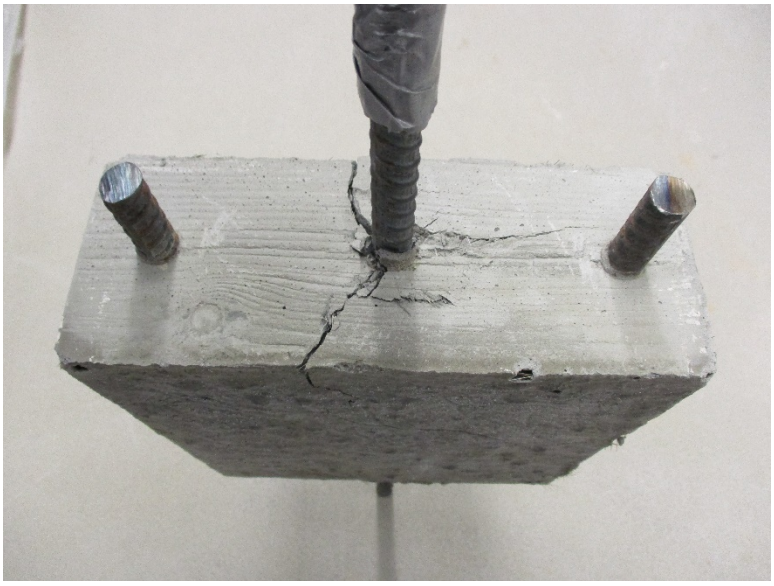

Figure 5.13 Bond test splitting failure mode

5.4 Durability

5.4.1 Freezing/thawing resistance

The freezing/thawing resistivity results for the three developed UHPC mixes, together with conventional concrete (standard NDOT 47B) are presented in Figure 5.14. Results showed that, likely owing to the high strength and low permeability, the three developed UHPC mixes exhibit almost no apparent deterioration caused by freezing/thawing cycles for up to 600 cycles.

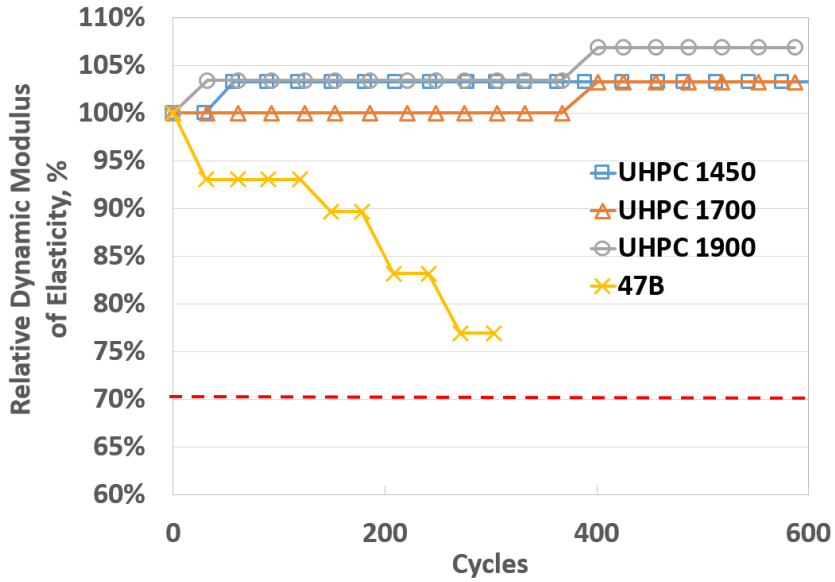

(a) Relative dynamic modulus of elasticity

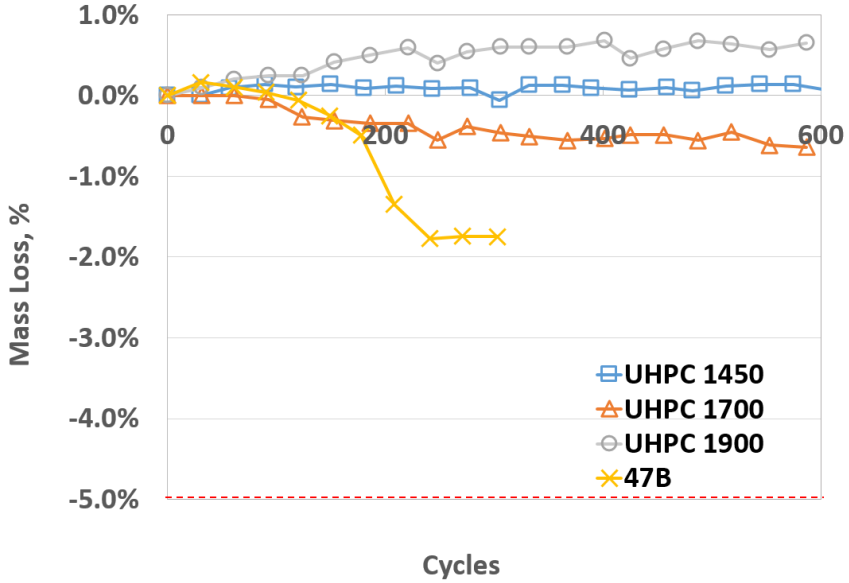

(b) Mass loss

Figure 5.14 Freezing/thawing resistivity results of the developed UHPC mixes

5.4.2 Surface resistivity

The surface resistivity test was performed with the UHPC 1900 mix using specimens prepared with and without fibers. It is believed that, due to the high conductivity, steel fibers can influence the surface resistivity results if they connect to each other inside the concrete matrix. As presented in Figure 5.15, results show that the developed UHPC 1900 mix exhibit much higher surface resistivity compared to the conventional concrete (standard NDOT 47B), with the chloride ion penetration fall into the "very low" range at 28-day.

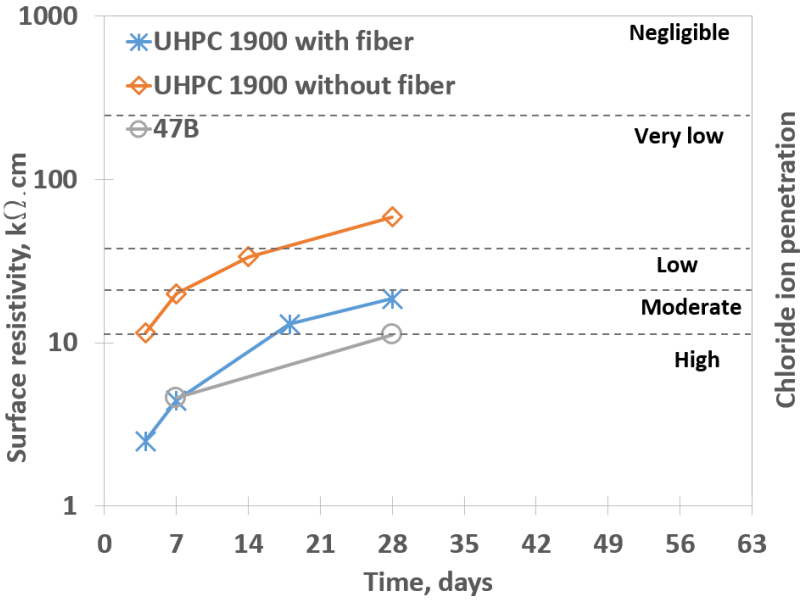

Figure 5.15 Surface resistivity results of the developed UHPC 1900 mix and standard NDOT pavement mix

5.4.3 Restrained shrinkage

Restrained shrinkage results from the developed UHPC 1900 mix, together with a conventional NDOT pavement mix (47B) and bridge deck (47BD) mix are shown in Figure 5.16. Results show that compared to the two conventional mixes, the UHPC mix exhibits a higher level of microstrain compared to conventional concrete, likely due to the high binder content and the elimination of coarse aggregate. However, the steel fibers embedded inside the UHPC mix appear to prevent the concrete from cracking, as no cracking was observed till 28-day of the required testing period, while cracks were observed at approximately 6 and 10 days for the 47BD and 47B mix respectively.

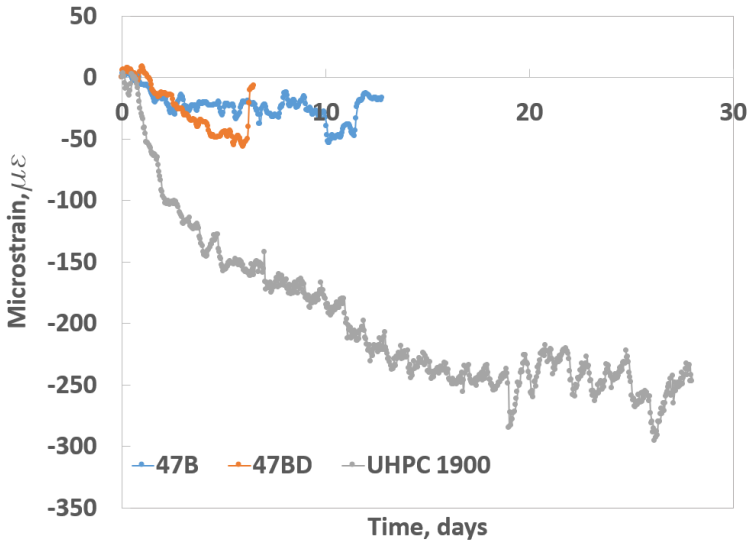

Figure 5.16 Restrained shrinkage results of the developed UHPC and standard NDOT pavement and bridge deck mixes

5.4.4 Free shrinkage

The free shrinkage results of UHPC are shown in Figure 5.17. Noted that a specimen dimension of 1×1×11 in. (2.54×2.54×27.94 cm) was used for UHPC 1450 and UHPC 1700 while a specimen dimension of 3×3×11in. (7.65×7.62×27.94cm) was used for UHPC 1900, and the conventional concrete (47B) mixes.

Results showed that even with the much higher binder content, the developed UHPC mixes exhibit almost the same level of shrinkage compared to conventional concrete, at approximately 500 microstrains till the age of approximately 120-day.

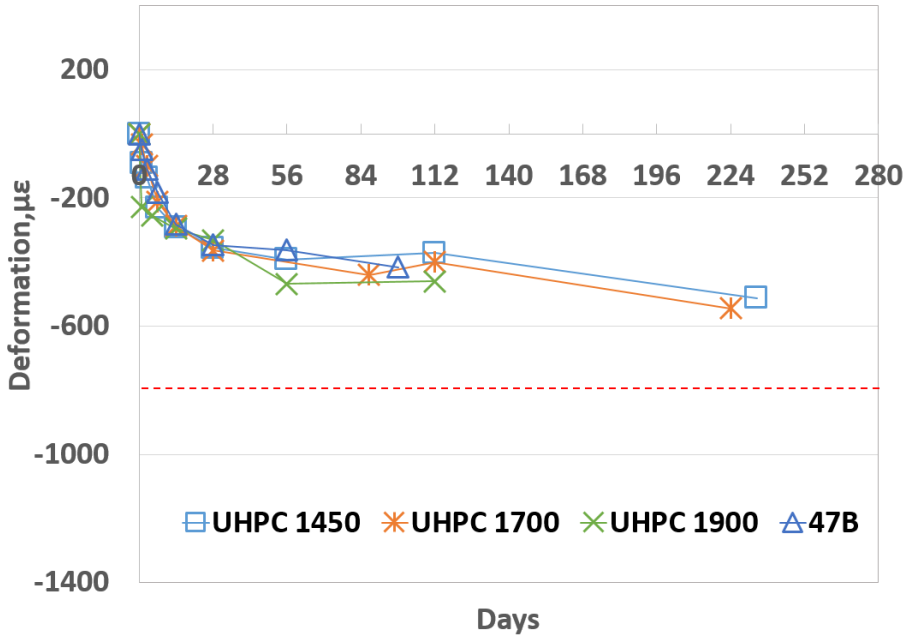

Figure 5.17 Drying shrinkage results of the developed UHPC mixes and standard NDOT pavement mix

5.5 Summary

The summary of the performance evaluation of the mixes along with the requirements of ASTM C1856 and FHWA and results of FHWA non-proprietary UHPC, is presented in Table 5.4. Detailed information is shown in Appendix C. Results showed that the developed UNL UHPC 1900 mix has acceptable fresh and hardened concrete properties that satisfy ASTM and FHWA criteria for workability, mechanical, and durability performances.

Table 5.4 Requirements and results of the performance evaluation of the developed and commercial UHPC mixes

Property	ASTM C1856 requirement	FHWA acceptance criteria (2014)	FHWA results U-A (2017)	Commercial	UHPC1900
Flow (in.)	8 to 10	7 to 10	5.75	10+	10+
Setting time (initial, hr/final, hr)	n/a	n/a	>9/<15	n/a	2.5/5.5
Compressive strength, 28d (psi)	17,000	21,000	18,000	23,300	17,670
Modulus of elasticity, 28d (ksi)	n/a	7	6 : 8	8.17	6.38
Poisson's ratio, 28d	n/a	n/a	0.15	0.22	0.26
Flexural strength at first crack, 28d (ksi)	n/a	1.3	n/a	2.82	3.04
Peak flexural strength, 28d (ksi)	n/a	n/a	n/a	4.05	4.88
Splitting tensile strength, 28d (ksi)	n/a	1.3 (Cracking Strength)	2.57*	2.4	1.93
Direct tensile strength, 28d (ksi)	n/a	1.2 (Cracking Strength)	1.35*	2.41	N/A
Direct shear strength, 28d (ksi)	n/a	n/a	n/a	5.95	5.67
CC-UHPC interface resistance, as-cut texture, 28d (ksi)	n/a	n/a	n/a	4.12 (Bond Failure)	3.59 (Bond Failure)
CC-UHPC interface resistance, grooved texture, 28d (ksi)	n/a	n/a	n/a	4.47 (CC Failure)	4.72 (CC Failure)
Rebar development length	Satisfied the FHWA-HRT-14-090 recommendation ($L_d=8d_b$ and Cover= $3d_b$) Bar Yield before Bond Failure				
Freezing/thawing, 600 cycles	n/a	≥95%	≥95%	n/a	>95%
Surface resistivity, 28 days	n/a	n/a	Negligible	n/a	Very low, Mix w/o fiber
Chloride ion penetration (coulombs)	n/a	≤ 250	302@28d, 53@56d	n/a	280@41d, 25@180d 47@3d w/ heat curing
Restrained shrinkage	n/a	n/a	n/a	n/a	No Crack
Free shrinkage, 112days	n/a	≤ 800 με	-400 με	n/a	-460 με

**29-day with 3% fiber content*

CHAPTER 6 FIELD SCALE CONNECTION CASTING AND TESTING

6.1 Introduction

This chapter presents a field-scale experimental work performed in the laboratory to evaluate the feasibility and effectiveness of placing a UHPC connection between two bridge deck panels with the developed UHPC mix. Details of the construction practices for the joint of two single-tee sections are described. Results from the structural test from the single-point load test are also presented.

6.2 Test Setup

The structure set up for the joint connection was two single-tee sections to be connected using UHPC, simulating a bridge structure. The UHPC was used to bond the two pieces together with the help rebar, as shown in Figure 6.1.

Figure 6.1 Field-scale connection setup

The wood formwork was set under the connection space and on the sides, as shown in Figure 6.2. Due to the high flowability of the UHPC mix, special attention was made to ensure formwork is strong enough to support the mix and do not leak during construction.

Figure 6.2 Field-scale connection formwork setup

6.3 Mixing

The volume of UHPC needed to fill the connection was approximately 5ft^3. Due to the relatively large batch size, the mix was prepared using an Imer Mortarman 120+ mixer with batch sizes of 1.5 ft^3 and an Imer Mortarman 750 mixer with batch sizes of 3.5 ft^3. To ensure good consistency, the two batches were prepared simultaneously.

The two batches were prepared following the procedure, as detailed in chapter 3. Figure 6.3 presented details during the preparation of the large batch.

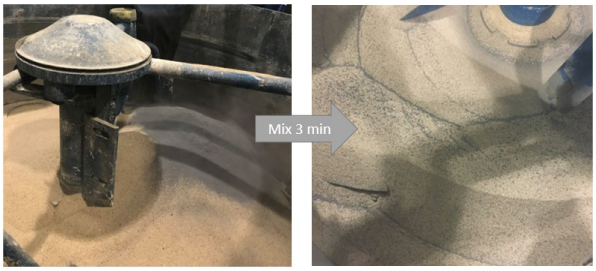

(a) Mixing of sand and silica fume

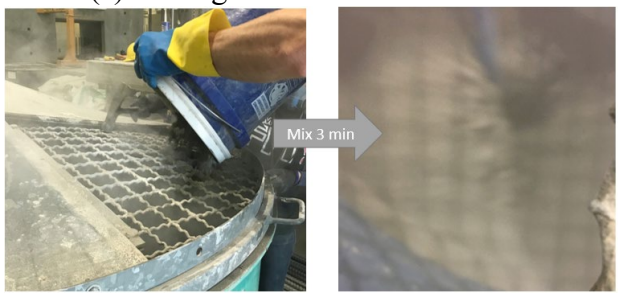

(b) Loading cement and other SCMs

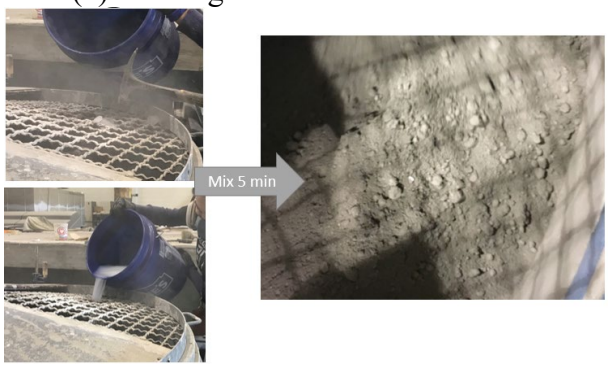

(c) Introducing 60% of liquid (water, ice, and HRWR)

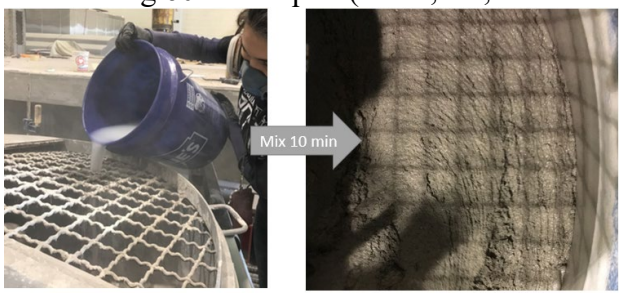

(d) Introducing the remaining 40% of liquid (water, and HRWR)

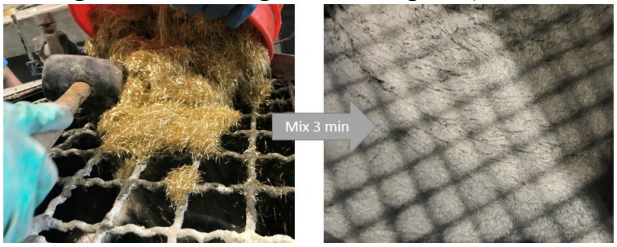

(e) Introducing fibers

Figure 6.3 Field-scale connection UHPC mixing procedure

During the mix preparation, the medium batch (1.5 ft^3) overloaded the Imer Mortarman 120+mixer during the turnover time. The turnover time is defined as when a UHPC mix consistency started to be observed, i.e., when the materials start to change from powder form to liquid form. As this stage is the most energy and power demanding for the mixer, due to the relatively small engine power of the mixer, the volume of UHPC material appears to exceed the mixer, which caused an overload and engine stoppage. The research team has to remove the material from the medium batch mixer was transferred into the large batch mixer and continue the mixing procedure there. Both mixers were at the same stage of mixing. Figure 6.4 shows the process or transferring materials from one mixer to the other, as explained above.

Figure 6.4 Issues occurred during field-scale connection trial

6.4 Placing and Curing

As shown in Figure 6.4, the formwork and reinforcement were cleaned and pre-wet prior to the start of the mixing process. Moist towels were used to cover the form to keep them moistened until the mix was ready to be placed.

Figure 6.5 Field-scale connection preparation

Upon the completion of mixing, UHPC was transported with 5-gallon buckets and placed roughly from the two ends of the connection. Neither vibration nor surface finishing was applied. Figure 6.6 presents some details of the casting process.

Figure 6.6 Field-scale connection UHPC placement

As shown in Figure 6.7, upon the completion of the casting, the connection was covered using wet towels until the test day. The average maximum and minimum temperature during this curing period was 73°F (22°C) and 57°F (14°C) respectively.

Figure 6.7 Field-scale connection UHPC curing

6.5 Mechanical Test

The structural test of the two slabs connected with the UHPC joint was conducted 16 days after casting. As shown in Figure 6.8, the testing rig was set up for a three-point bending test with a hydraulic ram placed in the middle of the specimen and supports at the two ends of the specimen. The hydraulic loads were applied in a small increment during testing until there was a significant drop in load, and the specimens were under rotation.

Figure 6.8 Field-scale connection mechanical test setup

While the load was applied using a hydraulic pump, displacement was measured through string potentiometers placed next to the shear key in both sides at the location of loading point, quarter-point, and at supports.

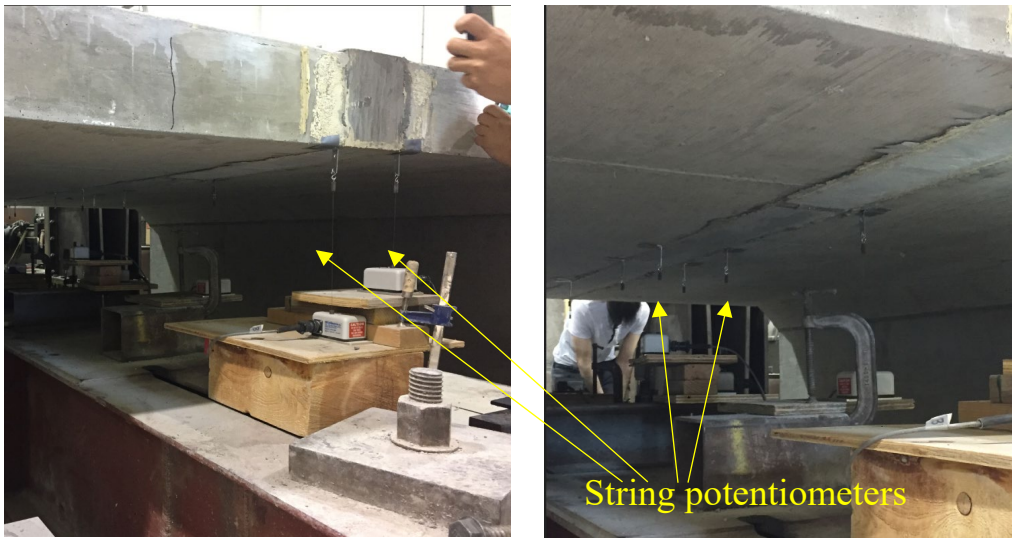

Figure 6.9 Field-scale connection string potentiometers setup

Figure 6.10 shows the test results, the maximum load was 85 kips and the maximum displacement was approximately 1.6 in. After testing reached this maximum load, the load did not increase and remained at the peak level while rotation was taking place. The test was terminated due to the steel plates beginning to punch through the concrete. Results showed that the developed UNL UHPC mix provided comparable structural capacity for the joint connection compared to the commercial UHPC product.

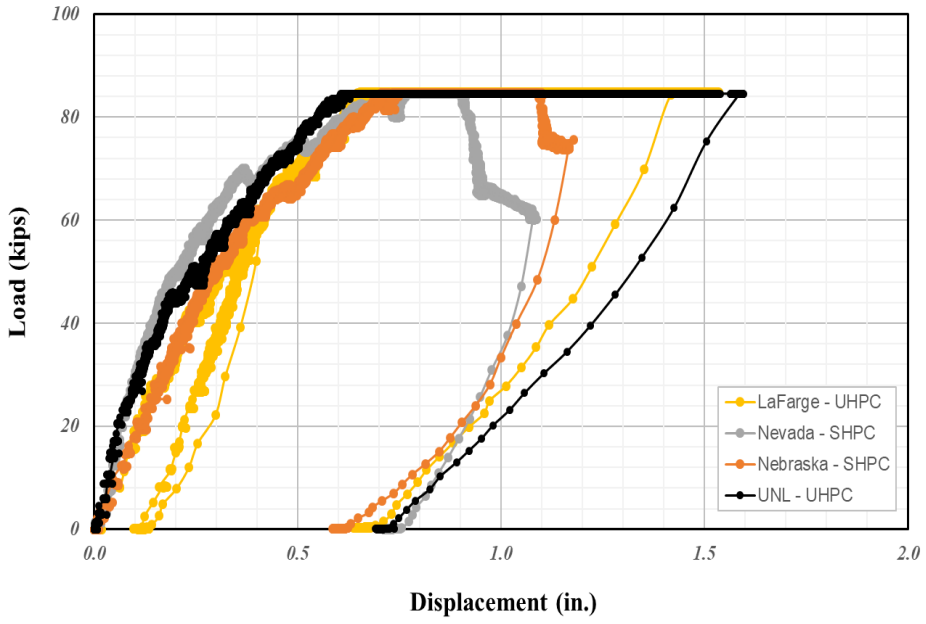

Figure 6.10 Field-scale connection test results

6.3 Summary

Results from the field-size connection casting and testing demonstrated that not only does the developed UNL UHPC mix have excellent workability for successful joint placement, the mix also demonstrated comparable structural capacity compared to the commercial UHPC product.

CHAPTER 7 ANALYSIS OF FEASIBILITY AND COST-EFFECTIVENESS AND RECOMMENDATION FOR UHPC PRACTICE

7.1 Introduction

Chapter 7 presents a cost analysis of the developed UHPC mixes. The chapter also covers the technical feasibility of developing a local UHPC mix for NDOT and recommended practice for preparing and handling the material.

7.2 Cost-Effective Analysis

As the prohibitory cost of proprietary UHPC products greatly limits its application, the main purpose of this study is to develop non-proprietary UHPC mixes with good performances using locally available materials. With the identified raw materials sources and mixture designs of the developed UHPC mixes, a cost analysis was performed based on raw material costs. The result showed that with the use of local materials, the material cost is significantly reduced, compared to proprietary UHPC products.

7.2.1 Methodology

Table 7.1 summarizes the source and location, as well as the unit cost of the different raw materials used for the developed UHPC mixes. Note that the unit cost was decided based on the inputs from local producers, and are subjected to change, depends on the availability.

Table 7.1 Unit cost of raw materials selected for the recommended UHPC mix

	Materials	Source and location	Unit cost $/ton
Sand	No.10 sand	Lyman-Richey Corporation Omaha, NE	10
Cement	Type I/II	Ash Grove Cement Company Louisville, NE	105
Slag	Grade 100 Slag	Central Plains Cement Company Omaha, NE (terminal)	123
Silica fume	Force10,000 densified microsilica	GCP Grace Construction Products	1080
Fiber	Dramix OL 13/.20 micro steel fiber	Bekaert	2600
HRWR	Premia 150	Chryso	18.5*

* in $/gallon

7.1.2 Results

According to the unit cost of raw materials and the final mix designs, the cost of the developed UNL UHPC 1900 mixes is approximately $682 per cubic yard, which is approximately one-third of the cost of proprietary commercial products. Note that the unit costs of materials are subjected to change, thus the actual cost depends on the location and availability of raw materials at the time of construction.

7.3 Feasibility Analysis

As discussed in Section 7.1, as the non-proprietary UHPC mixes were developed mostly using local materials, the unit cost of the mixes are less than $700 per cubic yard, which is

economically feasible for highway bridge construction. Also, as demonstrated in the panel joint connection construction, the construction process is practical and feasible with appropriate handling and mixing. To ensure sufficient mixing energy, a high shear pan mixer is necessary to produce the concrete. The product has a satisfactory performance with good workability without the need of internal vibration, mechanical properties, and durability.

UHPC is a very sensitive material. To ensure mix uniformity, the fine aggregate should be air-dried and the moisture content needs to be adjusted in the mix design. As the fibers selected to be used are similar to needles and can be hard to handle without an appropriate glove, it is suggested to wear a rip-resistant latex industrial nitrile glove under the normal work glove when handling fibers and fresh concrete. To achieve the appropriate performance, materials selection, as well as loading and mixing sequence and time, should be rigorously followed. Furthermore, the fresh concrete behavior is time-sensitive and if the UHPC is allowed to rest for an extended period of time (as short as 3 to 5 minutes), the internal structure of the concrete will start to build up and it can lose the ability to self-consolidate and flow. Continue mixing prior to placing is therefore recommended. And if the mix does exhibit loss of workability due to resting, remixing might be necessary.

7.4 Recommendation for UHPC Practice

7.4.1 Mix design

Based on the extensive study and multiple trial batches, the UNL UHPC 1900 mix is recommended as an economical and feasible mix with good performance to be used in highway bridge connections for NDOT. Table 7.2 shows the mix design of the recommended mix.

Table 7.2 Mix design of recommended UHPC mixes

Mix ID	Cement	Silica Fume	Slag	Water	Sand	Fiber	HRWR	w/b
UHPC 1900	1214	162	588	310	1612	266	55.6	0.178

The mix consists mainly of locally available raw materials in Nebraska. As UHPC is a very sensitive material, any changes in the source of the raw material could result in different performance. Changes in the mixing procedure or volume of batch also can affect the final performance characteristics. Trail batches are therefore strongly recommended to ensure appropriate fresh and hardened concrete behavior.

7.4.2 Batching

A pre-pour meeting including expected results, weather conditions during placement, batching procedures, placing method and sequence, quality control tests methods, and curing methods and procedures are recommended before every batch. A pre-pour inspection including examining the placement for cleanness (free of debris) and pre-wet to the SSD condition, mixer operation, raw materials condition and quantities, formwork condition, and the weather condition is also needed. To ensure a successful placement, the flow test should be performed every batch . Specimens for the compressive strength should be prepared once per pour and more often for larger pours (Ross, 2019).

7.4.2.1 Cement and cementitious materials

The powder materials should be stored appropriately to prevent moisture absorption. Materials should be examined to ensure free of any chunks of material.

7.4.2.2 Aggregate

The aggregate should be air-dried prior to batching. It is recommended to leave the aggregate air drying for a minimum of 24 hours, depending on how wet it is, and then measuring the moisture content. The moisture content should be no higher than 0.25% at the time of batching. Protection measures should be applied in windy conditions as the wind can blow the finer and lighter particles away, which will result in the change in aggregate gradation.

7.4.2.3 Water and chemical admixture

Water, ice, and chemical admixture(s) should be prepared right before the start of the mix to present evaporation. It is recommended to have ice to replace approximately 30% of the total water to prevent the excessive heat of the mix due to the extensive mix time. The ice can be directly placed into the mixer, while the admixture should be premixed with water right before placing it into the mixer to help its dispersion.

7.4.2.4 Fiber

Fibers should have no sign of rust prior to batching. Special care when handling the fibers is needed to prevent injury from the needle-like fibers. It is recommended to wear rip-resistant latex industrial nitrile glove under the normal work glove when handling the fiber.

7.4.3 Mixing

As mentioned before, UHPC performance can be greatly affected by the mixing procedure. To obtain desired characteristics, specific mixing procedure need to be followed. The air-dried fine aggregate and silica fume are first loaded into the mixer and mixed for three minutes, followed by cement and slag loaded into the mixer and mixed for another three minutes. Approximately 60 % of the premixed liquids (water and HRWR) loaded into the mixer in approximately 35 seconds. To reduce the temperature of the mix, approximately a third of the total water should be replaced by ice. It should be noted that some materials cluster could be observed at this stage. After approximately five minutes of mixing, the clusters start to disintegrate, and a minor change in the consistency of the concrete is observed. The remained premixed liquid (water and HRWR) is to be loaded into the mixer, while the mixer is mixing, in approximately 35-second duration. Approximately another ten minutes of mixing is generally needed to achieve a flowable and viscous consistency, as shown in Figure 6.11. As the consistency of the mixture depends on materials, mix design, as well as the mixing energy, which is influenced by the type of mixer and batch size, additional mixing time (up to eight more minutes) and slight adjustment of the HRWR dosage (up to 10%) might be applied until the desired consistency is reached. If the desired consistency is not observed after 18 minutes after the second portion of water introduced into the mixer, the mix should be deemed failed and disregarded.

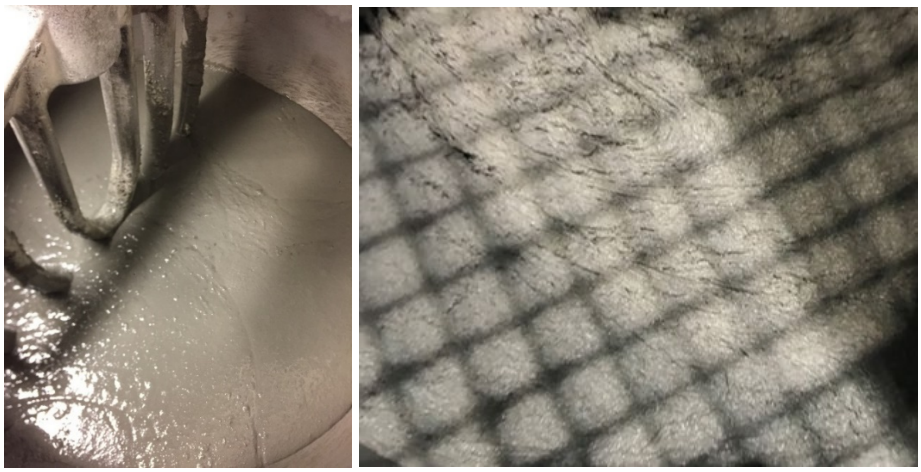

(a) Small (lab) mixer (b) Large (field) mixer

Figure 7.1 UHPC mixes with desired consistency

Finally, fibers are loaded while mixing and mix for three to five minutes, which includes the time spent loading the fibers.

7.4.4 Flow table test

The flow table test should be conducted immediately after the mixing process is completed. The flow table equipment must be leveled, dry and clean prior to being used for testing. The material should be allowed to flow for two minutes, and the long and short axis should be measured, the average is the reported flow. The flow need to be closely monitored if any adjustment in the mix is applied, or if a notable time is passed and a workability loss is observed, especially in hot days.

In the case of highly flowable mixes, to ensure fiber stability, the time that the UHPC takes to flow out of the flow table should not be less than 50 seconds. For mixes that flow out of the table in less than 50 seconds, it is suggested to keep the mixture in the mixer and keep mixing for a longer period until the measured flow is acceptable. For mixes with a high dosage of HRWR admixture, this process can take up to 60 minutes.

7.4.5 Casting

UHPC is time-sensitive, once the concrete is ready and the required quality control tests are completed, it should be immediately placed. The temperature of the material should be kept above 50°F (10°C) and bellow 90°F (32°C) because the temperature can affect the early age strength of the concrete (Ross, 2019).

Due to its strong thixotropy natural, when UHPC is allowed to rest for just a few minutes, the internal structure of the concrete starts to build up and it can lose the self-consolidating ability. When this does appear, it is necessary to agitate the rested concrete to overcome the thixotropy. The agitation can be rodding, hand mixing or mechanical mixing (loading it back in the mixer). Furthermore, a thin layer called elephant skin (as shown in Figure 6.12) could appear on the surface when the UHPC is allowed to rest for only a short period, which could create issues during placement. To place another layer of UHPC on top of the one that was allowed to rest and to ensure appropriate homogeneity, rodding (until the thin layer disappears) on the surface of the rested concrete is necessary.

Figure 7.2 Elephant skin on the surface of UHPC allowed to rest

UHPC with the adequate flow is self-consolidating and thus does not require any internal or external vibration. However, as the casting procedure can be time-consuming and UHPC can lose its workability during the process. It is recommended to have the mix placed from both ends of the connection simultaneously. Efforts to ensure continuous placing is also strongly encouraged.

7.4.6 Specimen preparation

According to ASTM C1856, test specimens for compressive strength test should be cylinders with diameters of 3 in. (76.2 mm) and height of 6 in. (152.4 mm). The cylinders should be cast within 10 minutes after the mixing is completed. Because of the high viscosity of the material, cylinder molds must be tilted in approximately 45° and cast with one layer to avoid entrapped air on the bottom. For mixes with flow less than 9 in., the cylinders should be tapped on the sides (maximum of 30 times) to remove entrapped air. For stiffer mixes, additional consolidation may be required. After finishing, the operator should wait for approximately one minute before closing the cylinder lids, just so the air inside the concrete can be relieved. After that, cylinder molds should be covered to prevent moisture loss, and then carefully moved to a flat surface for appropriate curing.

As UHPC is expected to be much stronger than the recommended strength for sulfur capping or neoprene capping, all the test cylinders should be end ground prior to compressive strength testing.

7.5 Summary

Based on the unit cost and mix design, the cost analysis of the developed UNL UHPC mixes indicated that the unit cost of the mix is less than $\$700/yd^3$, which is approximately one-third of the proprietary UHPC mix. The chapter also demonstrated the technical feasibility of producing and using the developed material. To provide better guidance for NDOT and contractors, the chapter also includes details of recommended practices for UHPC production and handling during construction.

CHAPTER 8 CONCLUSIONS, AND RECOMMENDATIONS FOR FUTURE WORKS

8.1 Conclusions

The goal of the study is to evaluate the feasibility of developing an economic non-proprietary UHPC mix with locally available materials for possible use in different bridge applications in Nebraska. The research demonstrated that it is possible to develop a local UHPC mix that is both technical and economically feasible. Through the comprehensive laboratory study, the following conclusions can be drawn:

- UHPC can be successfully produced with the combination of a local fine silica sand (No. 10) sand, type I/II cement, slag, silica fume, modified polycarboxylate-based HRWR, and micro steel fiber;
- Based on the comprehensive evaluation of different design parameters, a mix design with 8% (by mass of binder) of silica fume, 30% (by mass of binder) of slag, and a total binder content of approximately 1900 pcy is recommended and the specific material and mix design can be found below in Table 8.1:

Table 8.1 Ingredients and mix design for the recommended UNL UHPC 1900 mix

	Type	Mass (lb/yd^3)
Sand	No.10 silica sand	1612
Cement	Type I/II	1214
Slag	Grade 100 Slag	588
Silica fume	Force10,000 densified microsilica	162
Fiber	Dramix OL 13/.20 micro steel fiber	266
HRWR	Premia 150	55.6

- Flow test and field-scale connection casting demonstrated that the developed UNL-UHPC mix has sufficient flowability and stability to ensure successful placing of bridge deck connection and other structural elements;
- The developed UNL-UHPC mix exhibits excellent mechanical properties with satisfactory strength (28-day strength at 17.8ksi and 56-day strength at 20.0ksi), and modulus of elasticity, Poisson's ratio, flexural strength, splitting strength, tensile strength, direct shear strength, slant shear strength, and bond strength comparable to commercial UHPC product;
- Because of the very different design compared to conventional concrete, equations for properties such as modulus of elasticity and splitting tensile strength from AASHTO LRFD might not be appropriate for predicting UHPC mechanical properties;
- The developed UNL-UHPC mix exhibits excellent durability properties including mass loss of less than 1% and RDM with no notable change based on freezing/thawing resistance test, very low chloride ion penetration based on surface resistivity test, and no cracking based on restrained shrinkage test;
- As high mixing energy is needed for UHPC, a high-shear pan mixer is recommended for field production, and special batching and mixing procedures need to be followed to ensure successful UHPC production;
- As the consistency of the mixture depends on materials, mix design, as well as the mixing energy, which is influenced by the type of mixer and batch size, additional mixing time

and slight adjustment of the HRWR dosage might be applied until the desired consistency is reached.

- A structural test with a field-scale UHPC bridge connection demonstrated that the developed UNL-UHPC mix could provide similar structural capacity compared to commercial UHPC.

8.2 Recommendations for Future Works

The present study leads to several recommendations for further study:

- Current UHPC production is time consuming with a total mixing time over 20 minutes, which could lead to potential issues in field construction. A study is needed to identify best practices for more efficient UHPC production. A mixer with higher mixing energy and a fiber dispenser are likely more desirable in UHPC production;
- UHPC mixtures require both high flowability and fiber stability; further study is needed to provide a better guideline for the desirable workability characteristics for different construction applications;
- Fiber stability is a key parameter that significantly affects the UHPC mechanical properties. Further study is needed to set up a test method for fiber stability during batching and casting;
- UHPC is a viscous material and tends to lose workability quickly. More work is needed to identify better measures to maintain sufficient workability for a longer period. Chemical admixtures, such as workability-retaining admixtures, might be a viable option.

REFERENCES

AASHTO TP 95. Standard Method of Test for Surface Resistivity Indication of Concrete's Ability to Resist Chloride Ion Penetration. *American Association of State Highway and Transportation Officials*, 2014.

AASHTO LRFD Bridge Design Specifications, American Association of State Highway and Transportation Officials. *American Association of State Highway and Transportation Officials*, 2017.

Alkaysi, M. and El-Tawil, S. Effects of Variations in the Mix Constituents of Ultra High Performance Concrete (UHPC) on Cost and Performance. *Material and Structures*, 2015, 49: 4185-4200.

Ambily, P. S., Ravisankar, K., Umarani, C., Dattatreya, J. K., and Iyer, N. R. Development of Ultra-High-Performance Geopolymer Concrete. *Magazine of Concrete Research - Institute of Civil Engineers,* 2014, 66: 82-89.

American Concrete Institute (ACI). Building Code Requirements for Structural Concrete: Commentary on Building Code Requirements for Structural Concrete Report. *American Concrete Institute ACI 318*, 2019.

American Concrete Institute (ACI). Ultra-High-Performance Concrete: An Emerging Technology Report. *American Concrete Institute ACI 239*, 2018.

American Petroleum Institute. Specification for Cement and Materials for Well Cementing. *American Petroleum Institute API* (Spec 10A), 2010.

ASTM C39, Standard Test Method for Compressive Strength of Cylindrical Concrete Specimens. *ASTM International*, 2018.

ASTM C128. Standard Test Methods for Relative Density (Specific Gravity) and Absorption of Fine Aggregate. *ASTM International*, 2015.

ASTM C136. Standard Test Method for Sieve Analysis of Fine and Coarse Aggregates. *ASTM International,* 2014.

ASTM C150. Standard Specification for Portland Cement. *ASTM International*, 2018.

ASTM C157. Standard Test Method for Length Change of Hardened Hydraulic – Cement Mortar and Concrete. *ASTM International*, 2014.

ASTM C191. Standard Test Method for Time of Setting of Hydraulic Cement by Vicat Needle. *ASTM international*, 2018.

ASTM C230. Standard Specification for Flow Table for Use in Test of hydraulic Cement. *ASTM International,* 2014.

ASTM C403. Standard Test Method for Time of Setting of Concrete Mixtures by Penetration Resistance. *ASTM International*, 2016.

ASTM C469, Standard Test Method for Static Modulus of Elasticity and Poisson's Ratio of Concrete in Compression. *ASTM International*, 2014.

ASTM C494. Standard Specification for Chemical Admixture for Concrete. *ASTM International*, 2017.

ASTM C496, Standard Test Method for Splitting Tensile Strength of Cylindrical Concrete Specimens. *ASTM International*, 2017.

ASTM C595. Standard Specification for Blended Hydraulic Cements. *ASTM International*, 2018.

ASTM C618. Standard Specification for Coal Fly Ash and Raw or Calcined Natural Pozzolan for Use in Concrete. *ASTM International,* 2017.

ASTM C666. Standard Test Method for Resistance of Concrete to Rapid Freezing and Thawing. *ASTM International*, 2015.

ASTM C882, Standard Test Method for Bond Strength of Epoxy-Resin Systems Used with Concrete by Slant Shear. *ASTM International* , 2013.

ASTM C989. Standard Specification for Slag Cement for use in Concrete and Mortar. *ASTM International*, 2018.

ASTM C1017. Standard Specification for Chemical Admixture for Use in Producing Flowing Concrete. *ASTM International,* 2013.

ASTM C1240. Standard Specification for Silica Fume Used in Cementitious Mixtures. *ASTM International*, 2015.

ASTM C1252. Standard Test Methods for Uncompacted Void Content of Fine Aggregate. *ASTM International*, 2012.

ASTM C1437. Standard Test Method for Flow of Hydraulic Cement Mortar. *ASTM International*, 2015.

ASTM C1581. Standard Test Method for Determining Age at Cracking and Induced Tensile Stress Characteristics of Mortar and Concrete under Restrained Shrinkage. *ASTM International*, 2009.

ASTM C1609. Standard Test Method for Flexural Performance of Fiber-Reinforced Concrete (Using Beam with Third-Point Loading). *ASTM International,* 2012.

ASTM C1856. Standard Practice for Fabricating and Testing Specimens of Ultra-High Performance Concrete. *ASTM International*, 2017.

Berry, M., Snidarich, R., Wood, C. Development of Non-Proprietary Ultra-High Performance Concrete. *The State of Montana Department of Transportation,* FHWA/MT-17010/8237-001, 2017.

Bonneau, O., Lachemi, M., Dallaire, E., Dugat, J. and Aitcin, P. Mechanical Properties and Durability of Two Industrial Reactive Powder Concretes. *ACI Materials Journal*, 1997, 94: 286-290.

California Department of Transportation, Notice to Bidders and Special Provision. Contract No. 06-0K4604, Project ID 0612000105, 2015.

Choi, M. S., Lee, J. S., Ryu, K. S., Koh, K. and Kwon S. H. Estimation of Rheological Properties of UHPC Using Mini Slump Test. *Construction and Building Materials,* 2016, 106: 632-639.

De Larrard, F. and Sedran, T. Optimization of Ultra-High-Performance Concrete by the Use of Particle Packing. *Cement and Concrete Research*, 1994, 24: 997-1009.

De Larrard, F. Concrete Mixture Proportioning a Scientific Approach. *E & FN Spon an Imprint of Routledge,* London and New York, 1999.

Diamond, S. and Sahu, S. Densified Silica Fume: Particle Sizes and Dispersion in Concrete. *Materials and Structures,* 2006, 39: 849-859.

Dils, J., Boel V. and De Schutter. G. Influence of Cement Type and Mixing Pressure on Air Content, Rheology and Mechanical Properties of UHPC. *Construction and Building Materials*, 2013, 41: 455-463.

District Department of Transportation, Special Provision for Ultra High Performance Concrete. SP60, 2014.

El-Tawil, S., Alkaysi, M., Naaman A., Hansen W. and Liu Z. Development, Characterization and Applications of a Non Proprietary Ultra High Performance Concrete for Highway Bridges. *Department of Civil and Environmental Engineering University of Michigan, Ann Arbor, Michigan*, 2016.

El-Tawil, S., Tai, Y., Meng, B., Hansen W. and Liu, Z. Commercial Production of Non-Proprietary Ultra-High Performance Concrete. *Michigan Department of Transportation* (RC-1670)*,* 2018.

Fedorsian, I. and Camoes, A. Effective Low-Energy Mixing Procedure to Develop High-Fluidity Cementitious Pastes. *Materia Rio de Janeiro,* 2016, 21(1): 11-17.

Fehling, E., and Leutbecher, T. (2011). "Design of UHPC Members," *9th Munich Construction Materials Seminar, UHPC: Materials, Design, and Practice.* Förderverein Baustoff-Forschung e.V., Munich, 24-25.

Georgia Department of Transportation, Special Provision. Project No. CSBRG-0007-00(159), 2015.

Ghafari, E., Bandarabadi, M., Costa, H. and Julio E. Prediction of Fresh and Hardened State Properties of UHPC: Comparative Study of Statistical Mixture Design and an Artificial Neural Network Model. *American Society of Civil Engineering,* 2015, 10.1061.

Graybeal, B. A. Material Property Characterization of Ultra-High Performance Concrete FHWA-HRT-06-103. Federal Highway Administration, 2006.

Graybeal, B. and Hartmann, J. Strength and Durability of Ultra High Performance Concrete. *Presented at In Concrete Bridge Conference*, 2003, n/a: 20-40.

Graybeal, B. Design and Construction of Field-Cast UHPC Connection. *Federal Highway Administration Tech Note* FHWA-HRT-14-084, 2014.

Graybeal, B. Development of Non-Proprietary Ultra High Performance Concrete for Use in the Highway Bridge Sector. *Federal Highway Administration,* FHWA –HRT-13-100, 2013.

Haber, Z.B., Graybeal, B.A., Nakashoji, B. and Fay, A., New, Simplified Deck-To-Girder Composite Connections Using UHPC. *National ABC Conference Proceedings*, Florida, USA, 2017, 1-10.

Haber Z. B., De la Varga, I., Graybeal, B., Nakashoji, B. and El-Helou, R. Properties and Behavior of UHPC-Class Materials. *Federal Highway Administration,* FHWA-HRT-18-036, 2018.

Holland T. C. Silica Fume User's Manual. *Federal Highway Administration* FHWA-IF-05-016, 2005.

Hunger, M. An Integral Design Concept for Ecological Self-Compacting Concrete. *Eindhoven University of Technology, Netherlands*, 2010.

Hunger, M. and Brouwers, J. Development of Self-Compacting Eco-Concrete. *Presented at 16th International Conference on Building Materials, Weimar, Germany,* 2006.

Iowa Departament of Transportation, Special Provisions for Ultra High Performance Concrete. SP-090112a, 2011.

Ikeda, S., Okamura, H., Kakuta, Y., Koyanagi, W., Tazawa, E., Tanabe, T., Nagataki, S., Machida, A. and Miura, T. Recommendation for Design and construction of High Performance Fiber Reinforced Cement Composites with Multiple Fine Cracks (HPFRCC). *Japan Society of Civil Engineers*, 2008, series 82.

Khayat, K. H. and Meng, W. Design and Performance of Stay-in-Place UHPC Prefabricated Panels for Infrastructure Construction. *Center for Transportation Infrastructure and Safety*, *US Department of Transportation,* 2014, Report N.: NUTC R320.

Kosmatka, S. H., Kerkhoff, B. and Panarese, W. C. Design and Control of Concrete Mixtures. United States of America: Portland Cement Association. 14th edition, 2002.

Lowke, D., Stengel, T., Schiebl, P., and Gehlen, C. Control of Rheology, Strength and Fibre Bond of UHPC with Additions- Effect of Particle Density and Addition Type. *3rd International Symposium on "UHPC and Nanotechnology or High Performance Construction Materials", Kassel*, 2012.

Precast/Prestressed Concrete Institute (PCI). Manual for Quality Control for Plants and Production of Structural Precast Concrete Products. *Precast/Prestressed Concrete Institute,* 4th edition, 1999, MNL-116.

Meng, W. Design and Performance of Cost-Effective Ultra-High Performance Concrete for Prefabricated Elements. *Missouri University of Science and Technology, Doctoral Dissertation,* 2017.

Meng, W. and Khayat, K. H. Mechanical Properties of Ultra-High-Performance Concrete Enhanced With Graphite Nanoplatelets and Carbon Nano Fibers. *In Composites Part B*, 2016,107: 113-122.

Meng, W. and Khayat, K. H. Improving Flexural Performance of Ultra-High Performance Concrete by Rheology Control of Suspending Mortar. *Composites Part B*, 2017 (a), 117: 26-34.

Meng, W., Valipour, M., and Khayat, K. H. Optimization and Performance of Cost-Effective Ultra-High Performance Concrete. *Materials and Structure,* 2017 (b). 50: n/a.

Michigan Department of Transportation, Special Provision for Michigan Ultra High Performance Concrete (MI-UHPC) For Field Cast Joints, n/a.

Muzenski, W. S. The Design of High performcane and Ultra-High Performance Fiber Reinforced Cementitious Composites with Nano Materials.*University of Wisconsin-Milwaukee. A Doctoral Dissertation,* 2015.

Naaman, A., and Wille, K. The Path to Ultra High Performance Fiber Reinforced Concrete (UHP-FRC): Five Decades of Progress. *In proceedings of Hipermat 2012, 3rd International Symposium: Ultra High Performance Concrete and Nanotechnogy in Construction, Germany,* 2012.

National Precast Concrete Association (NPCA). Ultra-High Performance Concrete (UHPC) – Guide to Manufacturing Architectural Precast UHPC Elements NCPA, n/a.

New York State Department of Transportation, Precast Concrete Deck System Construction - Option 2. D262307, 2013.

Ross, A. UHPC Quality Control, Ensuring a Quality Product. *Second International Interactive Symposium on UHPC*, 2019.

Roy, M., Hollmann, C. and Wille, K. Influence of Volume Fraction and Orientation of Fibers on the Pullout Behavior of Reinforcement Bar Embedded in Ultra High Performance Concrete. *Construction and Building Materials*, 2017, 146: 582-593.

Sakai, E., Akinori, N., Daimon, M., Aizawa, K. and Kato, H. Influence of Superplasticizer on the Fluidity of Cements with Different Amount of Aluminate Phase. *Second International Symposium on Ultra High Performance Concrete*, *Kassel, Germany,* 2008. 85-92.

Sbia, L. A., Peyvandi, A., Soroushian, P. and Balachandra, A. M. Optimization of Ultra-High-Performance Concrete with Nano- and Micro-Scale Reinforcement. *Cogent Engineering,* 2014, n/a: 1-11.

Schroefl, C., Gruber, M. and Plank, J. Structure Performance Relationship of Polycarboxylate Superplasticizers Based on Methacrylic Acid Ester in Ultra High Performance Concrete. *Second International Symposium on Ultra High Performance Concrete, Kassel, Germany,* 2008, n/a: 383-390.

Scott, A. D., Long, W. R., Moser R. D., Green, B. H., O'Daniel, J. L. and Williams, B. A. Impact of Steel Fibers Size and Shape on the Mechanical Propoerties of Ultra-High Performacne Concrete. *U. S. Army Corps of Engineers Washington*, 2015, (DC 20314-1000 ERDC/GSL TR-15-22).

Scrivener, K. L., Crumbie, A. K. and Laugesen, P. The Interfacial Transition Zone (ITZ) Between Cement Paste and Aggregate in Concrete. *Interface Science,* 2004, 12(4): 411-421.

Shi, C., Wu, Z., Xiao, J., Wang, D., Huang, Z. and Fang, Z. A Review on Ultra High Performance Concrete: Part I. Raw Materials and Mixture Design. *Construction and Building Materials*, 2015, 101: 741-751.

Wille, K., Naaman, A. E., and Parra-Montesinos, G. J. Ultra-High Performance Concrete with Compressive Strength Exceeding 150MPA (22KSi): A Simpler Way. *ACI Material Journal,* 2011 (a), n/a: 46-54.

Wille, K., Naaman, A. E., and El-Tawil, S. Optimizing Ultra-High-Performance Fiber-Reinforced Concrete, Mixtures with Twisted Fibers Exhibit Record Performance under Tensile Loading. *Concrete International*, 2011 (b), n/a: 35-41.

Wu, Z., Shi, C., Khayat, K. H., and Wan, S. Effect of Different Nanomaterials on Hardening and Performance of Ultra-High Strength Concrete (UHSC), *Cement and Concrete Composites*, 2016, 70: 24-34.

Yang, S. L., Millard, S. G., Soutsos, M. N., Barnett, S. J. and Le, T. T. Influence of Aggregate and Curing Regime on Mechanical Properties of Ultra High Performance Concrete. *Construction and Building Materials*, 2009, 23: 2291-2298.

Yu, R., Spiesz, P., and Browers, H. J. H. Effect of Nano-Silica on the Hydration and Microstructure development of Ultra-High Performance Concrete (UHPC) with a Low Binder Amount. *Construction and Building Materials*, 2014 (a), 65: 140-150.

Yu, R., Spiesz, P., and Browers, H. J. H. Mix design and Proprieties Assessment of Ultra-High Performance Fibre Reinforced Concrete (UHPFRC). *Cement and Concrete Research*, 2014 (b), 56: 29-39.

Yu, R., Spiesz, P., and Browers, H. J. H. Development of an Eco-Friendly Ultra-High Performance Concrete (UHPC) With Efficient Cement and Mineral Admixture Uses. *Cement and Concrete Composites,* 2015, 55: 383-394.

Yuan, J. and Graybeal, B. A. Bond Behavior of Reinforcing Steel in Ultra-High Performance Concrete. FHWA-HRT-14-090. Federal Highway Administration, 2014.

APPENDIX A DETAILED RESULTS AND ANALYSIS OF IMPACT OF DIFFERENT DESIGN PARAMETERS

A.1 Impact of Cement

As mentioned before, four different types of cement were included in Series 1 in order to investigate the impact of cement type on UHPC behavior. In addition to Type I/II cement, a locally-available Type IP cement that consists of 25% Class F fly ash and 75% Type I cement also was included. Type IP cement also has slightly higher fineness than Type I/II cement. Finally, a Class H oil well cement was used due to its lower fineness, which could potentially improve the particle packing of UHPC and reduce the C_3A content. Table A.1 shows the design of the mixes that were prepared with different types of cement.

Table A.1 Mix design of mixes prepared with different types of cement

Mix ID	Cement	Silica Fume	Slag	Water	Sand	Fiber	HRWR	w/b
I/II:SF8:S30:B1450	884	117	427	239	2131	266	50.0	0.192
IP:SF8:S30:B1450	902	120	436	244	2176	266	51.1	0.192
OWH:SF8:S30:B1500	921	123	446	229	2222	266	52.0	0.178

Note: All units are in pcy (1 pcy = 0.59 Kg/m^3)

Figure A.1 shows the flow and the compressive strength of Series 1 mixes with different types of cement.

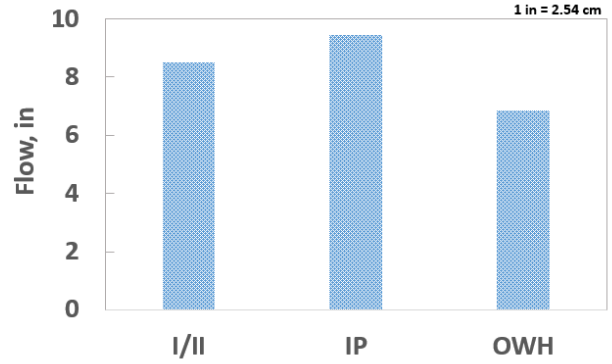

(a) Flow

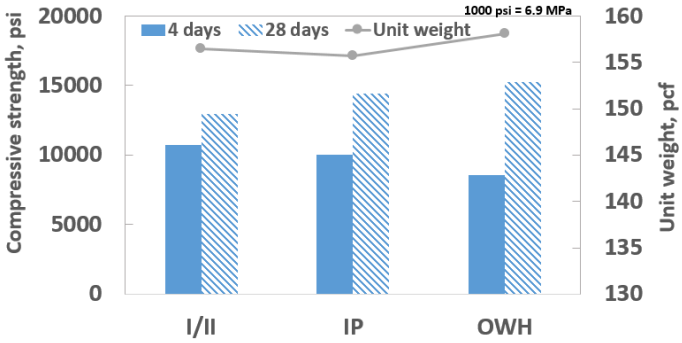

(b) Compressive strength and unit weight

Figure A.1 Impacts of cement type on UHPC performance

Results, as shown in Figure A.1(a), indicates that Type I/II and IP cement resulted in very similar flows. As mentioned before, IP cement consists of 25% Class F fly ash and 75% Type I.

However, although fly as, which can improve the flowability. However, the IP cement included in the study also has slightly finer particles compared to Type I/II, which increases the water demand and negatively impact the flowability. Due to the coarser particles of class H oil well cement, the use of this cement decreases the surface area, which leads to the lower water demand. Thus, a lower w/b can be used in mixes with oil well cement than those with other types of cement.

With the mixes analyzed, the different types of cement resulted in mixes with very similar compressive strengths, which led to the selection of Type I/II for further investigation due to its availability. Mix with Oil well cement presents a slightly higher compressive strength and higher unit weight compared to the other mixes. However, as its availability in Nebraska is limited, the cement was not included in further study. Note that several mixes with type III cement were also included in the preliminary study. As Type III cement has finer particles than the other types of cement that were analyzed, which increases the surface area and increases the water demand. With the same w/b, the mix with type III cement does not provide UHPC with acceptable workability. While it is not desirable to increase w/b, the use of type III cement was deemed not appropriate and was not included in further study.

A.2 Impact of Silica Fume

Series 2 evaluated the impact of the content of silica fume in the UHPC mixes. Because of its very fine particle size, it is believed that silica fume helps to provide denser particle packing (Holland, 2005), which, in turn, leads to increased strength. However, silica fume can also have a negative effect on the flowability due to its fineness. Low flowability can result in extensive entrapped air during the casting process, which will reduce the compressive strength. Therefore, the amount of silica fume should be well controlled. Thus, in Series 2, a series of mixes with silica fume content increased gradually from 4% to 15% by the mass of the binder were prepared. The mix designs of Series 2 mixes are presented in Table A.2.

Table A.2 Mix design of mixes prepared with different contents of silica fume

Mix ID	Cement	Silica Fume	Fly ash	Water	Sand	Fiber	HRWR	w/b
I/II:SF4:FA20:B1450	1108	58	295	247	2130	264	46.4	0.191
I/II:SF6:FA20:B1450	1076	87	294	250	2123	260	47.7	0.195
I/II:SF8:FA20:B1450	1049	117	294	247	2132	261	51.2	0.194
I/II:SF10:FA20:B1450	997	143	287	233	2081	260	46.4	0.186
I/II:SF12:FA20:B1450	987	175	293	236	2119	260	63.4	0.193
I/II:SF15:FA20:B1450	928	215	288	230	2098	260	65.7	0.193

Note: All units are in pcy (1 pcy = 0.59 Kg/m^3)

The results from fresh and hardened concrete properties are shown in Figure A.2.

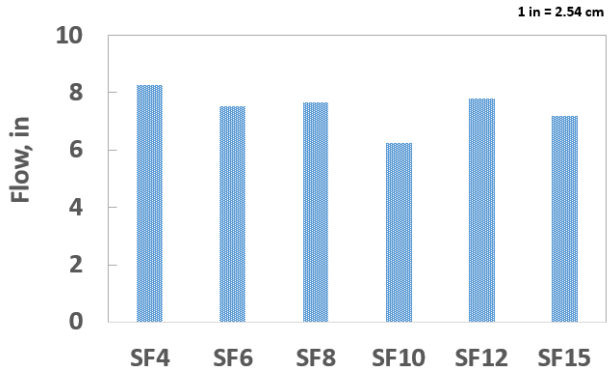

(a) Flow

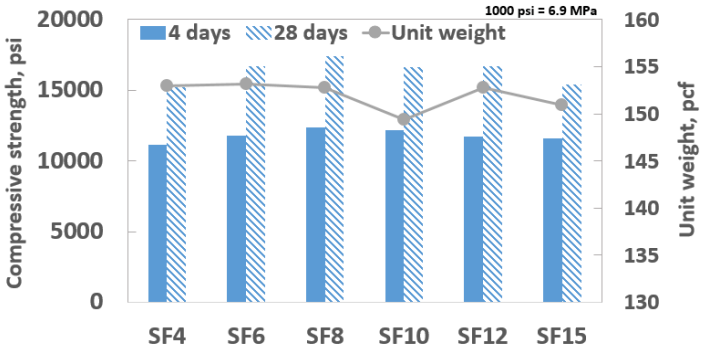

(b) Compressive strength and unit weight

Figure A.2 Impact of silica fume content on UHPC performance

Results, as shown in Figure A. 2, indicates that the flow decreased slightly with the silica fume content increased, and the compressive strength increased but started to drop after 8%. While it is generally believed that silica fume helps to provide denser particle packing, which leads to increased strength, it also has a negative impact on the flowability because of the very fine particles. Unit weights of concrete with silica fume content ranging between 4% and 8% are higher than those of concrete with the silica fume content ranging between 10% and 15%. The reduction in the unit weight is likely due to the entrapment of air in the mixes with slightly lower flowability. Lower flowability can result in the entrapment of air during the casting process, which will adversely affect the compressive strength. Based on the results, the most appropriate dosage of this material for the matrix was 8%.

In addition to the content of silica fume, to evaluate the impact of densified and un-densified silica fume on the fresh and hardened properties of UHPC, four additional mixes were prepared. Table A.3 presents the designs of the mixes, which include two mixes with 8% of densified silica fume and two mixes with 8% un-densified silica fume.

Table A.3 Mix design of the mixes prepared with densified and un-densified silica fumes

Mix ID	Cement	Silica Fume	Fly ash	Slag	Water	Sand	Fiber	HRWR	w/b
I/II:SF8:FA20:B1450	1049	117	294	0	247	2132	261	51.2	0.194
I/II:UndSF8:FA20:B1450	1050	118	295	0	244	2135	250	51.3	0.191
I/II:SF8:S42:B1450	711	121	0	603	240	2200	266	50.3	0.192
I/II:UndSF8:S42:B1400	691	118	0	586	234	2130	266	48.9	0.192

Figure A.3 shows the results of a comparison of the impacts of the un-densified and the densified silica fume on the flow and compressive strength of the UHPC.

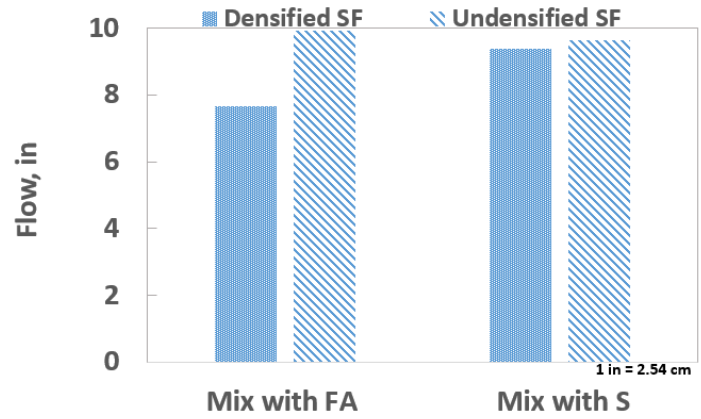

(a) Flow

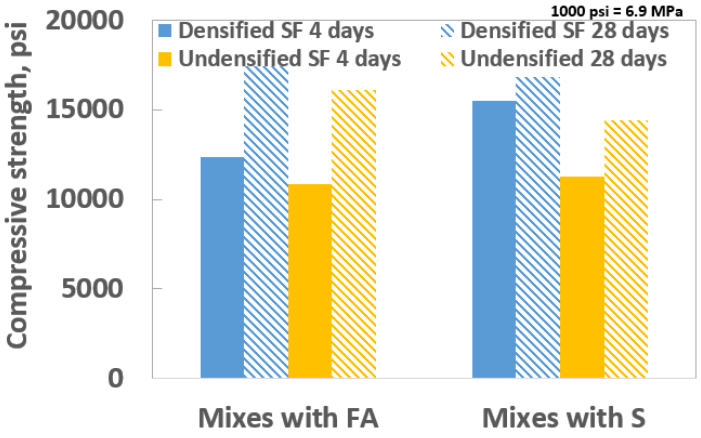

(b) Compressive strength

Figure A.3 Comparison of effects of un-densified and densified silica fume on the performance of the UHPC

Results showed that the use of un-densified silica fume resulted in concrete with higher or similar flows than those of the densified silica fume. However, when comparing the impacts of the two types of silica fumes on the compressive strength, it is apparent that the strength was reduced when the un-densified silica fume was used. This result led to the conclusion that the un-densified silica fume might have disturbed the packing of the UHPC and therefore, was not used in further study.

A.3 Impact of Fly Ash

The effect of fly ash on UHPC properties was evaluated in Series 3 mixes. The spherical particle shape of fly ash is believed to help concrete flow. Moreover, the pozzolanic reaction of fly ash could potentially improve the long-term strength of the developed UHPC mixes. However, because fly ash is an industrial byproduct, and coal-burning power plants have undergone some major changes during the last decade due to changes in regulations made by the Environmental

Protection Agency (EPA), the batch-to-batch variation of fly ash products tends to be high, which sometimes causes the issue of inconsistency.

Table A.4 shows the mix design of a series of mixes that were prepared with the fly ash content increasing gradually from 8% to 20% by mass of total binder.

Table A.4 Mix design of mixes prepared with fly ash

Mix ID	Cement	Silica Fume	Fly ash	Water	Sand	Fiber	HRWR	w/b
I/II:SF15:FA8:B1550	1183	232	130	261	1980	265	56.0	0.194
I/II:SF15:FA10:B1550	1157	231	154	260	1977	265	56.0	0.194
I/II:SF15:FA15:B1550	1086	233	233	262	1988	265	56.0	0.194
I/II:SF15:FA20:B1450	928	215	288	230	2098	260	65.7	0.193

Note: All units are in pcy (1 pcy = 0.59 Kg/m^3)

Figure A.4 shows the results of the impact in the UHPC mixes with different fly ash contents.

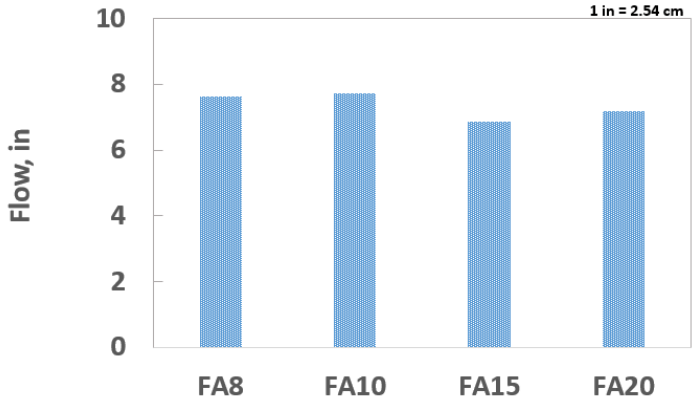

(a) Flow

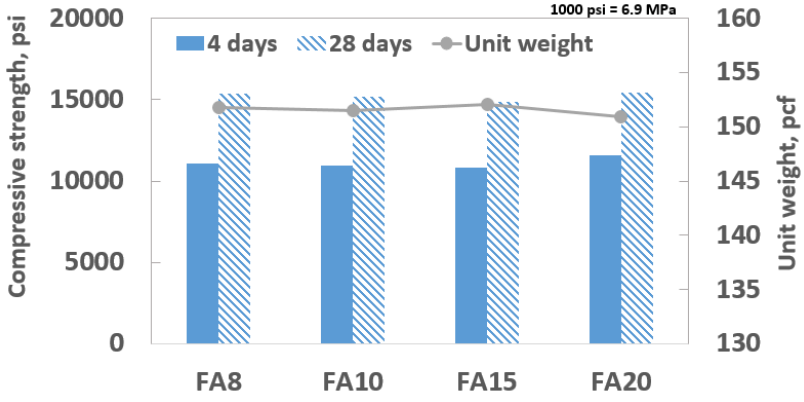

(b) Compressive strength and unit weight

Figure A.4 Impact of fly ash on UHPC performance

Figure A.4 indicates that, within the range of different fly ash content included in this study, the increase of fly ash content did not significantly affect UHPC performance. The flow and the

compressive strength slightly decreased as the fly ash content increased from 10% to 15%. However, the strength remained approximately the same.

A.4 Impact of Slag

Unlike fly ash, slag has rough and angular-shaped particles that are similar to cement, and therefore might not necessarily improve the flow. However, it is a more reactive and consistent material than fly ash and it potentially could result in better UHPC performance. Table A.5 presents the design of a series of mixes prepared with slag content increasing gradually from 20% to 42%, by mass of binder.

Table A.5 Mix design of mixes prepared with slag

Mix ID	Cement	Silica Fume	Slag	Water	Sand	Fiber	HRWR	w/b
I/II:SF8:S20:B1500	1064	119	299	245	2164	250	51.9	0.190
I/II:SF8:S30:B1450	906	117	427	239	2131	266	50.1	0.192
I/II:SF8:S42:B1450	711	121	603	240	2200	266	50.3	0.192

Note: All units are in pcy (1 pcy = 0.59 Kg/m^3)

Figure A.5 shows the results of the impact of slag content on UHPC performance.

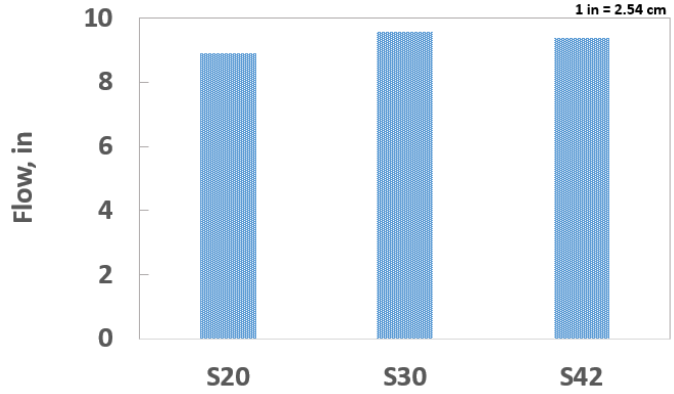

(a) Flow

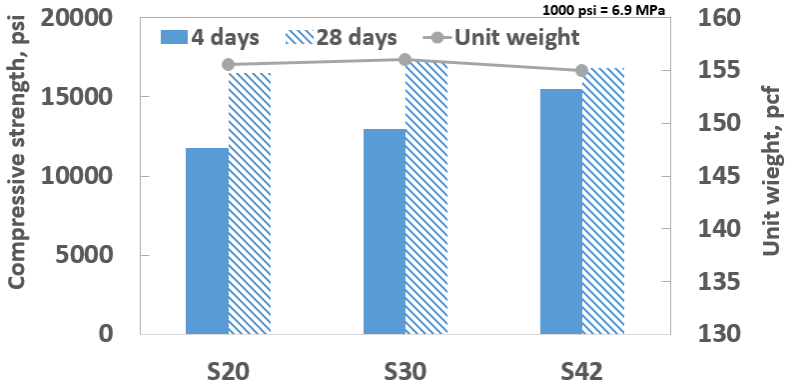

(b) Compressive strength

Figure A.5 Impact of slag on UHPC performance

Figure A.5 shows that the flow of UHPC increased when the slag content increased from 20% to 30% and then decreased when the content increased from 30% to 42%. Similar results were observed for the compressive strength of the UHPC. As the content of slag increased, the content of cement decreased, which could lead to insufficient cement content for the pozzolanic reaction of slag and the negative impact on strength. Results indicated that the most appropriate content of slag in the mix analyzed was 30%.

Comparing two similar mixes with fly ash (I/II:SF8:FA22:S0:QP0:SS) and with slag I/II:SF8:FA0:S23:QP0:SS, the use of slag improved flowability is improved, even with a rougher particle surface. Results indicated that the addition of slag could have resulted in an optimized packing. However, the slag and fly ash produced concrete with very similar 28-day compressive strength.

A.5 Impact of Quartz Powder

Quartz powder is a very fine filler that can impact the overall particle packing. Table A.6 presents the design of the mixes prepared with the fly ash replaced with quartz powder. Note that quartz powder is here considered as a part of binder due to its very fine particles.

Table A.6 Mix design of mixes prepared with quartz powder

Mix ID	Cement	Silica Fume	Quartz powder	Water	Sand	Fiber	HRWR	w/b
I/II:SF15:QP8:B1550	1202	236	132	265	2021	265	50.0	0.191
I/II:SF15:QP10:B1550	1159	232	155	261	1980	265	50.0	0.191
I/II:SF15:QP15:B1550	1075	230	230	259	1968	265	50.0	0.192

Note: All units are in pcy (1 pcy = 0.59 Kg/m^3)

Figure A.6 presents the results of the impact in the UHPC behavior when quartz powder was used.

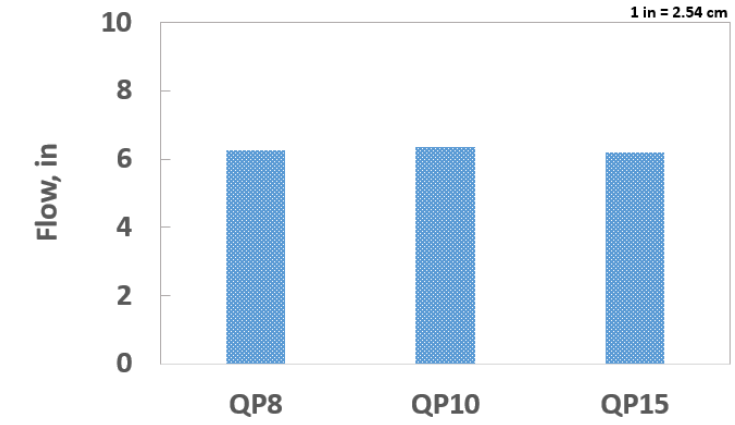

(a) Flow

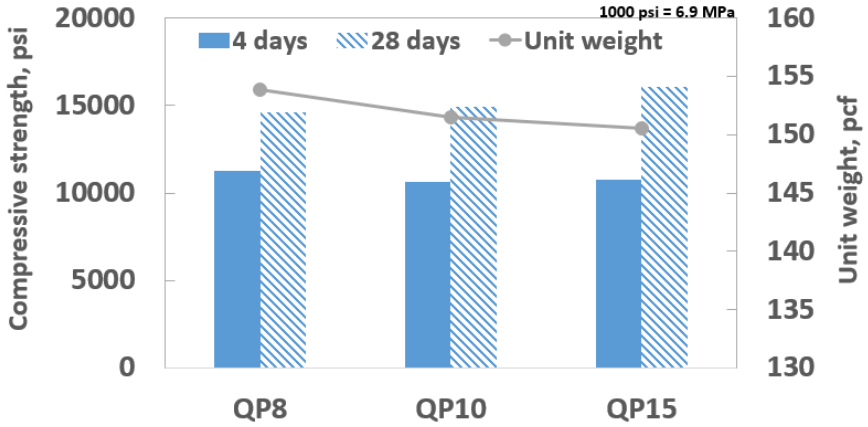

(b) Compressive strength

Figure A.6 Impact of quartz powder on UHPC performance

Figure A. 6 shows that the increase of the quartz powder content did not affect the overall flowability of the UHPC. However, the 28-day strength slightly increased when the quartz powder content increased. These results indicated that the packing density of the UHPC could have slightly improved as the amount of quartz powder increased.

When mixes with fly ash were compared to mixes with quartz powder, it was observed that the flow was reduced when quartz powder replaced the fly ash. This reduction was expected because of the spherical shape of fly ash particles and the fine particle size of quartz powder. Regarding the compressive strength, no significant improvement was observed when the quartz powder replaced the fly ash.

As the combination of silica fume, an additional SCMs (fly ash or slag) and the filler (quartz powder) could result in optimum packing, an additional series was prepared. Table A.7 shows the mix designs of three mixes prepared with slag and quartz powder.

Table A.7 Mix design of the mixes prepared with slag and quartz powder

Mix ID	Cement	Silica Fume	Slag	Quartz powder	Water	Sand	Fiber	HRWR	w/b
I/II:SF7:S23:QP16:B2000	1175	138	388	327	278	1637	266	58.0	0.157
I/II:SF13:S21:QP16:B1900	1025	242	341	316	259	1582	266	58.0	0.156
I/II:SF17:S20:QP17:B1900	958	319	319	319	256	1597	266	58.0	0.155

Figure A.7 shows the impact in the UHPC when slag and quartz powder was used. As shown in the figure, the flow of mixes is improved when slag is introduced in mixes with quartz powder. However, no clear impact on strength was observed.

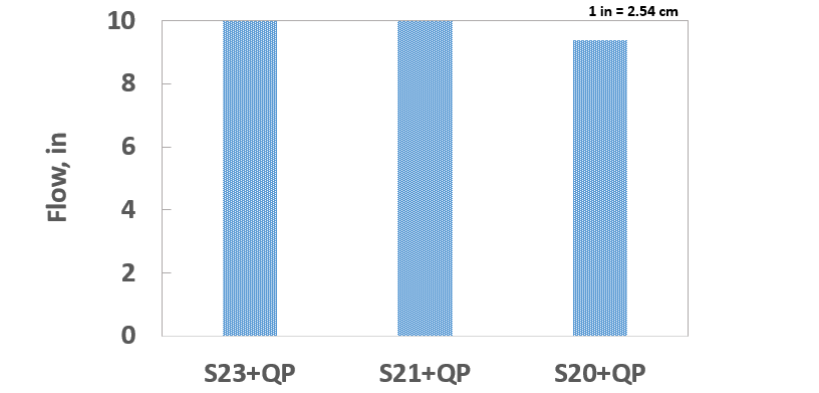

(a) Flow

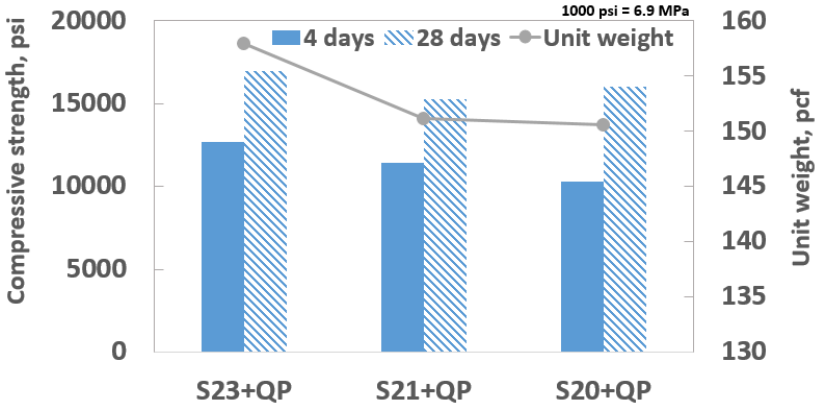

(b) Compressive strength

Figure A.7 Impact of slag and quartz powder in UHPC performance

A.6 Impact of Total Binder Content

Like in any concrete, cement paste is necessary to fill the voids of the aggregate matrix and to coat the aggregate particles and fibers, thereby minimizing the friction between the aggregate and the fiber. According to Naaman and Wille (2010), when rigid fibers are used, the particles tend to interact and often make the flow more difficult. According to Hu (2005), since the paste is the only phase inside a concrete mixture that can provide flowability, the excess paste is needed to reduce the friction between the particles and the fibers, those to provide concrete with sufficient workability. The excess paste is defined by the total paste volume subtracted by the portion that fills up the voids among aggregate particles.

As the content of binder increases, the excess paste is increased. Thus, it is essential to evaluate the impact of the total content of the binder on the performance of the UHPC to identify the appropriate binder content. Mixes with different cement types were prepared with a graduated increase of binder content ranging from 1450 to 2050 pcy (860 to 1216 Kg/m^3). Table A. 8 presents the design of the mixes prepared with different binder contents.

Table A.8 Mix design of mixes prepared with different total binder contents

Mix ID	Cement	Silica Fume	Slag	Water	Sand	Fiber	HRWR	w/b
I/II:SF8:S30:B1450	884	117	427	239	2131	266	50.1	0.192
I/II:SF8:S30:B1650	1035	138	501	280	1863	266	58.7	0.192
I/II:SF8:S30:B1900	1175	156	569	318	1559	266	66.6	0.192
IP:SF8:S30:B1450	902	120	436	244	2176	266	51.1	0.192
IP:SF8:S30:B1700	1065	141	516	288	1862	266	60.3	0.192
IP:SF8:S30:B1900	1182	157	573	319	1498	266	67.0	0.191
OWH:SF8:S30:B1500	921	123	446	229	2222	266	52.2	0.178
OWH:SF8:S30:B1750	1094	145	529	238	1913	266	62.0	0.159
OWH:SF8:S30:B2050	1281	171	621	278	1624	266	72.6	0.159

Note: All units are in pcy (1 pcy = 0.59 Kg/m^3)

The results of the impact of the binder content in the flow and compressive strength of UHPC are shown in Figure A.8.

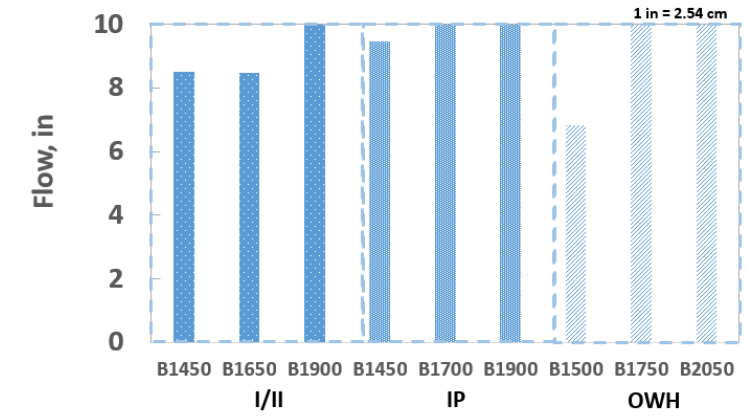

(a) Flow

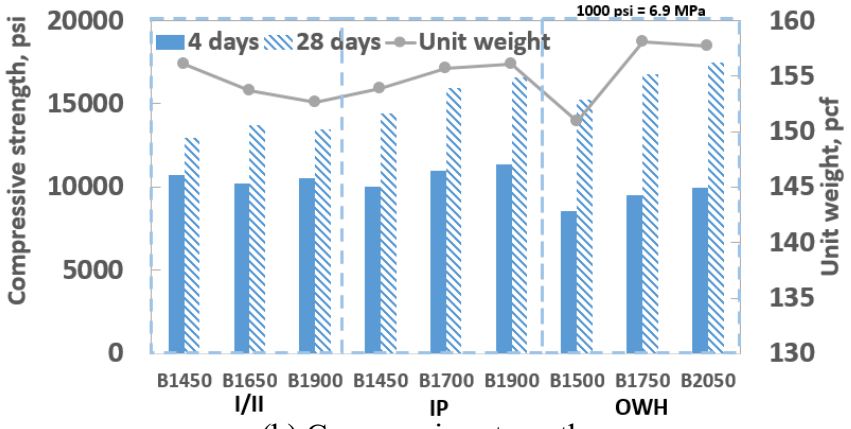

(b) Compressive strength

Figure A.8 Impact of total binder content on UHPC performance

As expected, results showed that as the binder content increases, the paste content of the concrete is increased, which leads to a more flowable UHPC. Similarly, the compressive strength of the mixes with all the three different types of cement increased when the binder increased.

A.7 Impact of HRWR Dosage

The impact of the HRWR content was studied with mixes prepared with different cement types. The HRWR admixture is important to provide UHPC with an appropriate flow. However, an excessive amount of HRWR can result in fiber segregation issues and chemical incompatibility (El-Tawil et al., 2018). Table A.9 presents the mix design of mixes with different HRWR percentage. Mixes prepared with type I/II and type IP cements with gradually reduced HRWR content yet the water content remained approximately the same, thus, the mixes are with slightly reduced w/b. Mixes with oil well cement were prepared with gradually reduced HRWR dosage yet maintain the same w/b.

Table A.9 Mix design of mixes prepared with different HRWR dosage

Mix ID	Cement	Silica Fume	Slag	Water	Sand	Fiber	HRWR	w/b
I/II:SF8:S30:B1900:HRWR3.4%	1179	157	571	301	1565	266	64.6	0.182
I/II:SF8:S30:B1900:HRWR2.8%	1172	156	576	300	1498	266	54.0	0.177
I/II:SF8:S30:B1900:HRWR2.3%	1156	154	560	295	1534	266	42.9	0.174
IP:SF8:S30:B1900:HRWR3.5%	1182	157	573	319	1498	266	67.0	0.191
IP:SF8:S30:B1900:HRWR2.4%	1185	158	574	320	1502	266	45.7	0.184
OWH:SF8:S30:B2050:HRWR3.5%	1281	171	621	278	1624	266	72.6	0.159
OWH:SF8:S30:B2100:HRWR2.9%	1291	172	626	289	1638	266	61.4	0.159
OWH:SF8:S30:B2050:HRWR2.4%	1277	170	617	293	1619	266	49.2	0.159

Figure A.9 shows the impact of the reduction of HRWR dosage on the flow and compressive strength of UHPC.

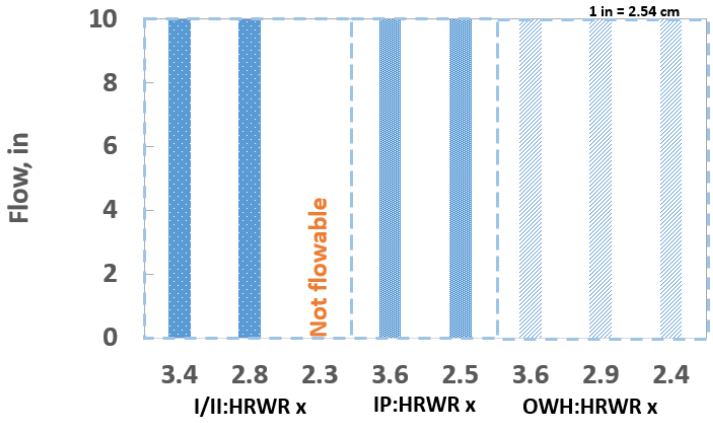

(a) Flow

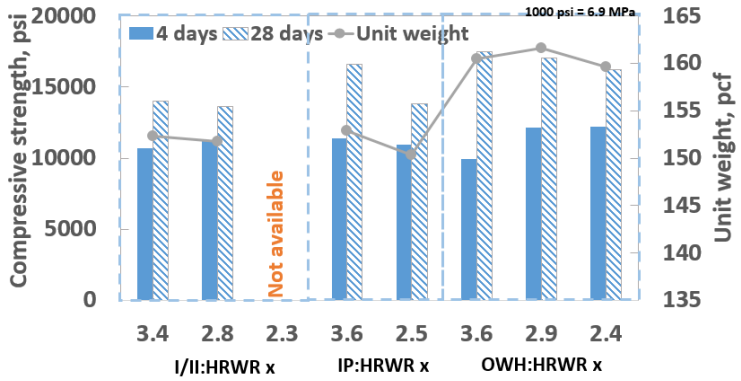

(b) Compressive strength

Figure A.9 Impact of HRWR dosage on UHPC performance

As shown in Figure A.9 (a), as all mixes achieve a 10 in. flow within two minutes, with the exception of I/II:SF8:S30:B1900:HRWR2.3%, which did not flow, the reduction of HRWR dosage in mixes prepared with the three different types of cement has no significant impact on the flow of the concrete. The mix that was not able to flow indicated that there is a minimum amount of HRWR in order to achieve acceptable workability. Similarly, Figure A.9 (b) shows that a slight reduction of compressive strengths can be observed with the reduced HRWR dosage.

APPENDIX B DETAILED RESULTS AND ANALYSIS OF IMPACT OF MIXER TYPE

Sufficient mixing energy is essential to properly disperse UHPC materials. Since a fairly large amount of HRWR is normally used in UHPC, and it takes time to be in effect, an extended mixing time compared to conventional concrete is generally necessary to produce concrete with the desired consistency, which is normally determined by visual examination of the fresh UHPC. In order to evaluate the impact of the mixer and mixing energy on the consistency and performance of UHPC, mixes were prepared using two different mixers, i.e., small (lab) and large (field) batches. The volumes of the small and large batches were 0.16 ft^3 (0.0045 m^3) and approximately 2.0 ft^3 (0.06 m^3), respectively. Table B.1 shows the mix design of the mixtures used for this comparison. Note that for each pair of small and large batches under comparison, the mix design could be slightly different as they were all adjusted based on the yield of the actual mix. For some of the mixes, w/b was adjusted slightly to achieve the desired UHPC consistency based on visual examination. Air detraining admixture was added into the large batch mix of design I/II:SF8:S30:B1900:HRWR2.8% to release excess air present in UHPC mix, and possibly improve the mechanical properties.

Table B.10 Mix design of mixes prepared with different mixers

Mix ID	Batch	Cement	Silica Fume	Slag	Water	Sand	Fiber	HRWR	Air detrainer	w/b
I/II:SF8:S30:B1450: HRWR3.5% (B1450)	Small	884	117	427	239	2131	266	50.1	0	0.192
	Large*	885	117	428	242	2133	266	55.0	0	0.196
I/II:SF8:S30:B1800: HRWR3.5% (B1700)	Small	1107	147	536	299	1991	266	62.7	0	0.192
	Large	1070	143	518	289	1925	266	60.6	0	0.191
I/II:SF8:S30:B1900: HRWR3.4%(B1900-A)	Small	1179	157	571	301	1565	266	64.6	0	0.182
	Large	1207	161	585	309	1603	266	66.1	0	0.182
I/II:SF8:S30:B1900: HRWR2.8% (B1900-B)	Small	1172	156	576	300	1498	266	54.0	0	0.177
	Large	1214	162	588	310	1612	266	55.6	1.4	0.178

Note: All units are in pcy (1 pcy = 0.59 Kg/m^3)
* HRWR3.9%

Figure B.2 presented the comparison of the flow and the 28 days compressive strength of mixes prepared with small-batch mixes and large batches mixes.

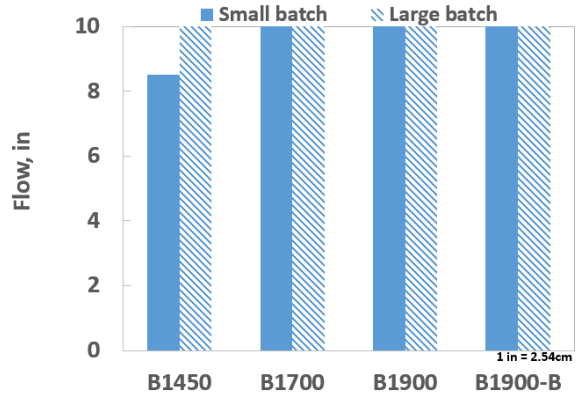

(a) Flow

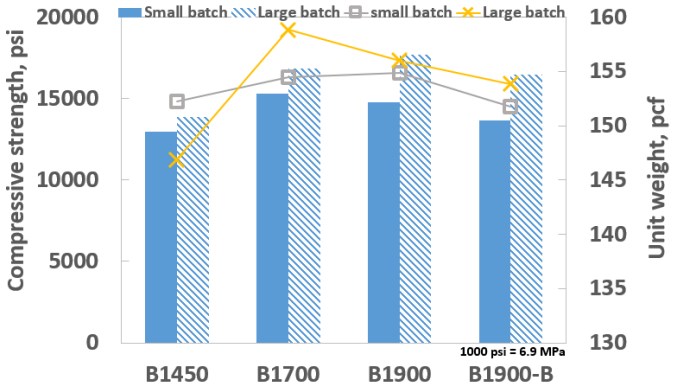

(b) Compressive strength

Figure B.1 Impact of mixers on UHPC performance

Figure B.2 also shows that, although the mixers have different input energies, with sufficient mixing time, UHPC prepared in small and large mixers resulted in a similar flow. However, mixtures prepared with the small batches present slightly lower compressive strength compared to those prepared with large batches. The large batch mixes had an average of approximately 750 psi (5.2 MPa) higher compressive strength than the small-batch mixes with the exception of I/II/SF8:S30:B1450:LB that had the water content increased when prepared in the large batch. The difference is likely due to the higher paddle rotating mixing speed associated with the much smaller distances that the small mixer paddles traveled when compared to large mixer paddles. The larger speed of the small mixer is necessary for the concrete to achieve the desired consistency. However, as shown in Figure B.2, the high rotating speed may also entrap more air during the mixing process, thus reducing the unit weight of the mixes. Figure B.3 shows the surfaces of cylinders prepared with the same mix design yet different sizes of mixers. It is clear that a good amount of air bubbles can be observed with cylinders prepared with a small mixer, which can result in lower compressive strength.

(a) Specimens mixed in small-batch mixer (b) Specimens mixed in large-batch mixer

Figure B.2 Surfaces of specimens prepared with different mixers

APPENDIX C DETAILED MECHANICAL PROPERTIES TEST RESULTS

C.1 Compressive Strength

Detailed test results of the compressive strength of the developed three UHPC mixes and commercial UHPC from 4-day to 56-day are presented in Table C.1.

Table C.1 Detailed compressive strength test results of UHPC mixes at different ages

Age (Days)			4	7	28	56
Compressive Strength (psi)	UHPC 1500	#1	10,276	11,614	13,705	15,629
		#2	9,789	12,732	14,010	16,260
		#3	-	-	14,192	-
		Avg.	10,033	12,173	13,969	15,944
	UHPC 1700	#1	10,437	13,541	17,063	17,473
		#2	12,149	13,269	16,925	16,922
		#3	-	-	16,475	-
		Avg.	11,293	13,405	16,821	17,198
	UHPC 1900	#1	11,906	13,527	17145	19,380
		#2	12,067	14,712	17771	20,484
		#3	-	-	18,099	-
		Avg.	11,986	14,119	17,672	19,932
	Commercial	#1	11,979	16,667	24,439	27,546
		#2	11,674	16,019	21,344	26,992
		#3	10,754	15,555	24,230	24,307
		Avg.	11,826	16,343	23,338	27,268

For quality control purposes, the repeatability of the mixing procedures was evaluated by comparing the strength growth of UHPC 1900 mixes prepared in two separate batches, namely UHPC 1900-A and UHPC 1900-B. For each batch, nine cylinders were used for compressive strength at 4, 7, 28, and 56 days. Figure 4.5 shows the average compressive strength versus the age of UHPC of the two batches. No significant difference between the two batches was observed, which indicates adequate repeatability of mixing procedures.

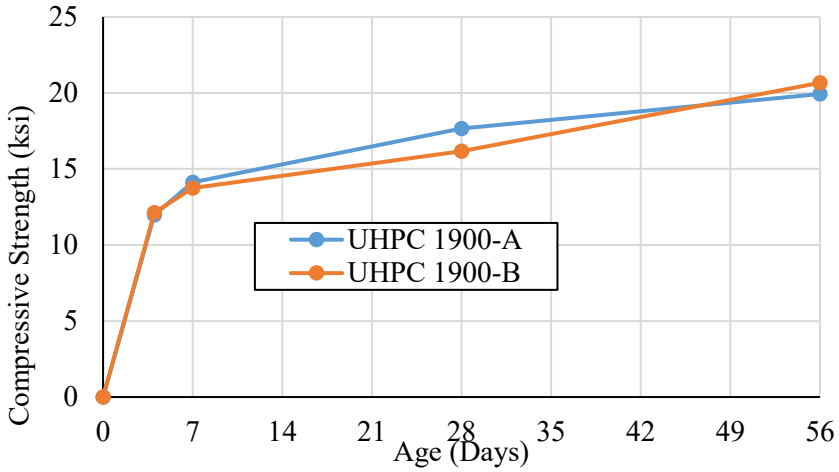

Figure C.1 Average compressive strength of UHPC from two different batches

C.2 Modulus of Elasticity and Poisson's Ratio

Detailed test results of the modulus of elasticity and Poisson's ratio of the developed three UHPC mixes and commercial UHPC from 4-day to 56-day are presented in Table C. 2 and C.3 respectively.

Table C.2 Detailed modulus of elasticity test results from different UHPC mixes

Mix	f'_c (ksi)	No.	MOE (ksi)	Average. MOE (ksi)	COV (%)	FHWA	AASHTO LRFD 2017
UHPC 1450	15.94*	1	6619	6560	1.3	5709	7096
		2	6461				
		3	6602				
UHPC 1700	17	1	6725	6613	2.0	5896	7249
		2	6643				
		3	6470				
UHPC 1900	17.67	1	6343	6377	4.4	6011	7342
		2	6112				
		3	6675				
Commercial	23.34	1	8173	8173	0.8	6908	8687
		2	8238				
		3	8109				

* 56 days compressive strength

Table C.3 Detailed Poisson's ratio test results from different UHPC mixes

Mix	f'_c (ksi)	No.	Poisson's Ratio	Average Poisson's Ratio	COV (%)
UHPC 1450	15.94*	1	0.27	0.26	3.2
		2	0.26		
		3	0.25		
UHPC 1700	17	1	0.25	0.26	2.2
		2	0.26		
		3	0.26		
UHPC 1900	17.67	1	0.25	0.26	3.4
		2	0.25		
		3	0.27		
Commercial	23.34	1	0.22	0.22	1.3
		2	0.22		
		3	0.22		

* 56 days compressive strength

C.3 Flexural Strength Test

Detailed flexure strength test results and cross-section of a representative beam from each of the three developed UHPC mixes and a commercial UHPC mix are presented in Figure C.2 to C.5.

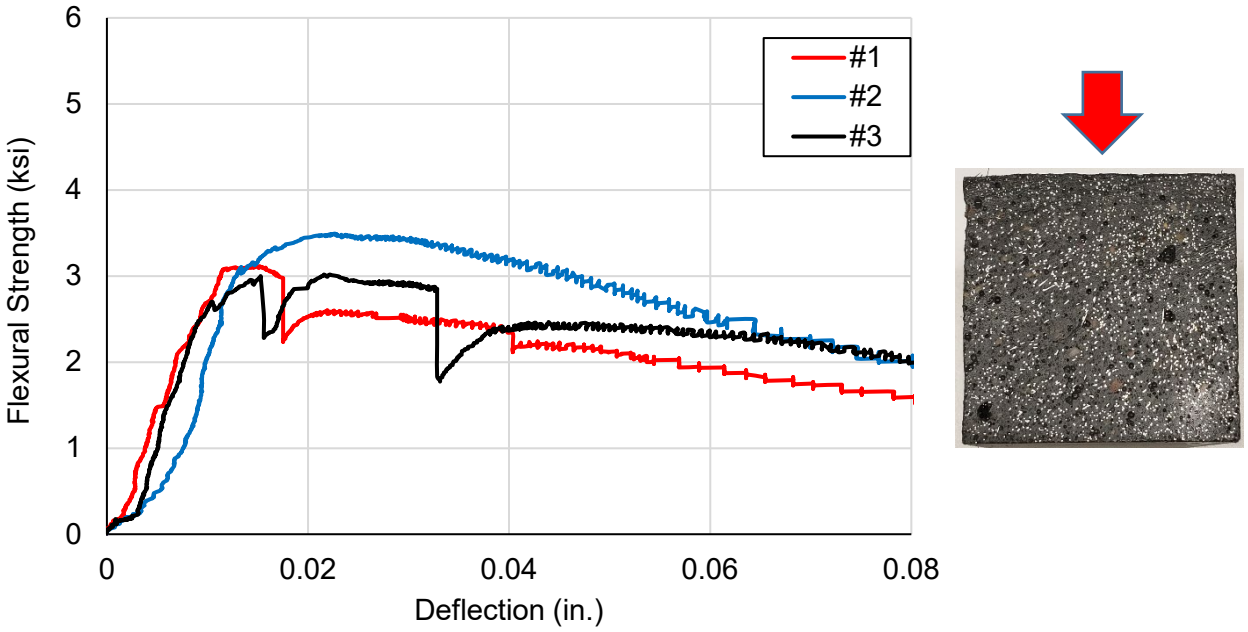

Figure C.1 Flexure strength test results for UHPC 1450 mix

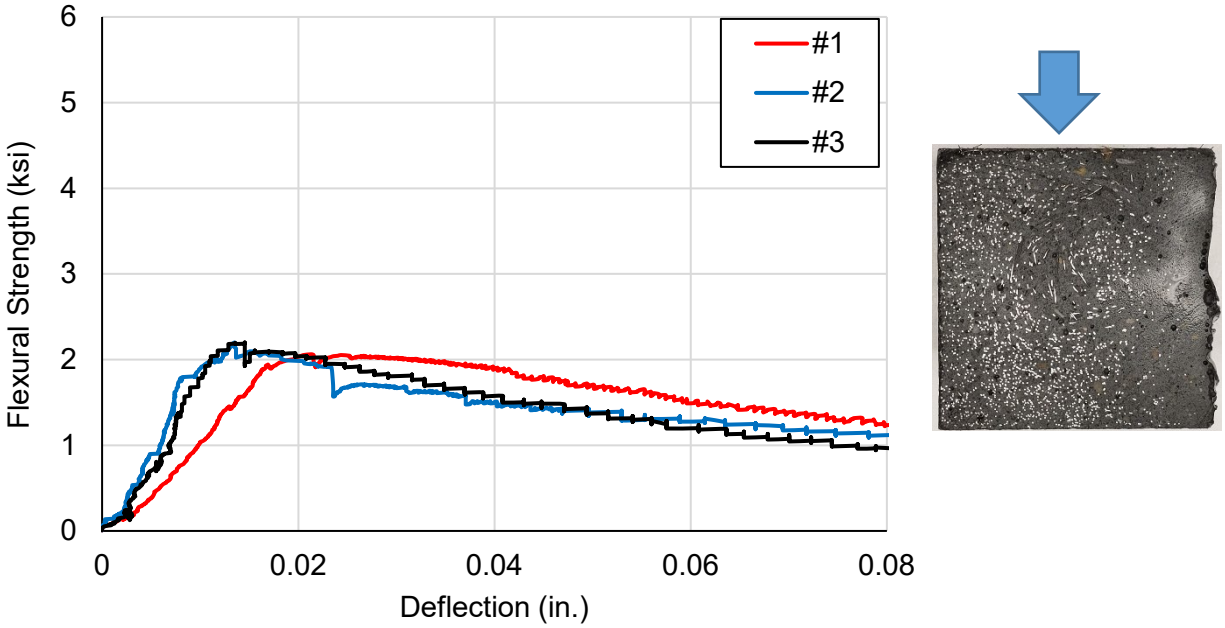

Figure C.2 Flexure strength test results for UHPC 1700 mix

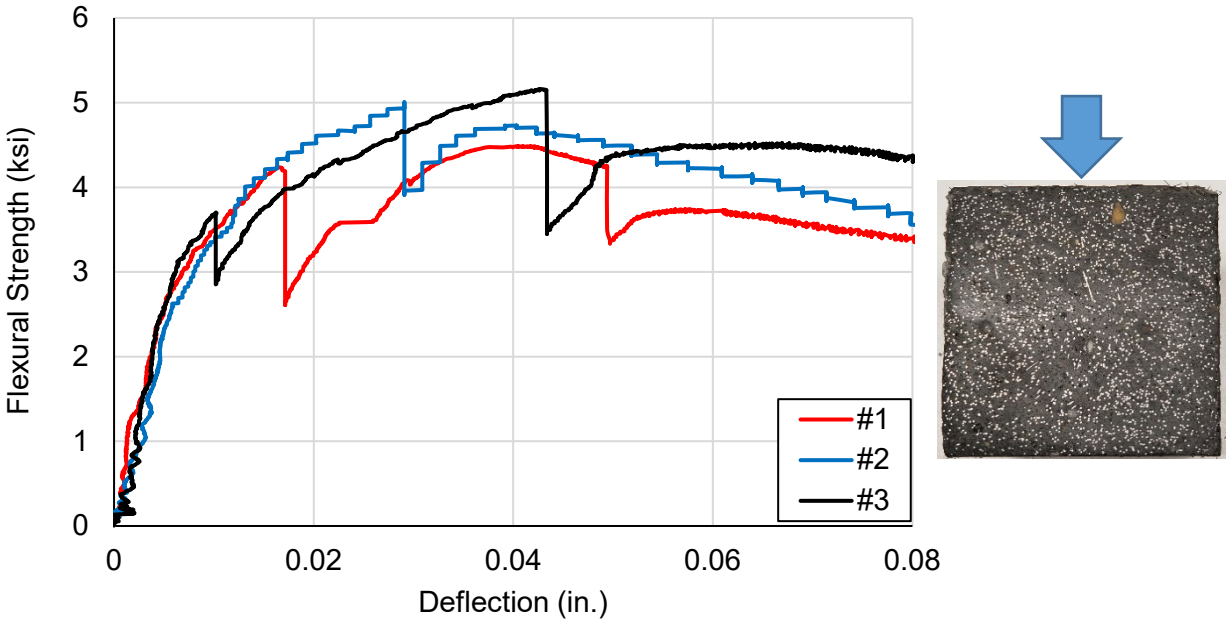

Figure C.3 Flexure strength test results for UHPC 1900 mix

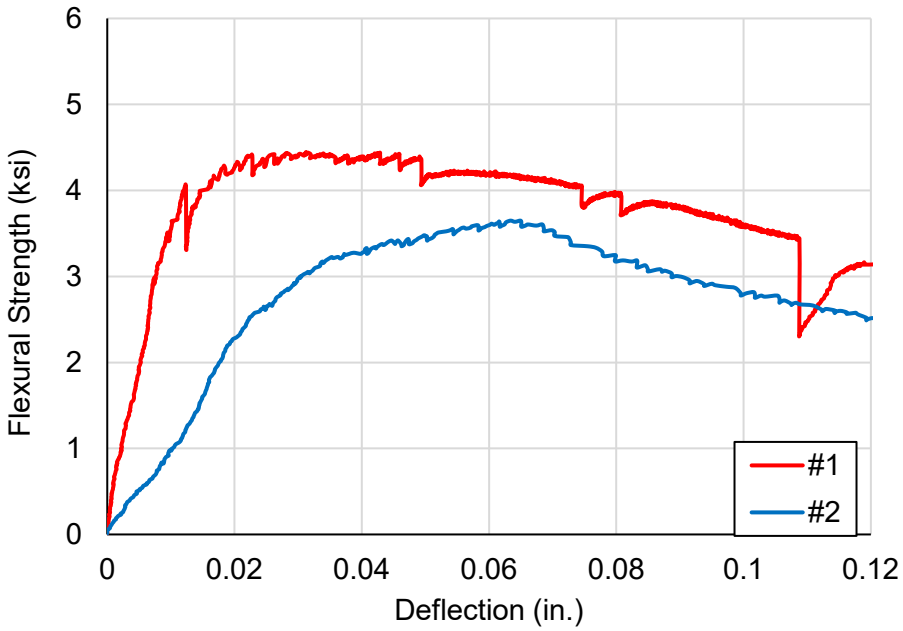

Figure C.4 Flexure strength test results for commercial UHPC mix

Details of key parameters from the flexural strength tests are presented in Table C. 5.

Table C.4 Flexural test results compared to ACI-318-19 limits

	ACI Minimum	UHPC 1450	UHPC 1700	UHPC 1900	Commercial
Flexural Strength at First Crack, psi	1500	2320	1260	3040	2820
Peak Flexural Strength, psi	2000	3210	2150	4880	4050
Peak Flexural Strength, % of First Crack Strength	125%	138%	171%	161%	144%
Residual at L/300, % of First Crack Strength	90%	113%	300%	157%	136%
Residual at L/150, % of First Crack Strength	75%	81%	199%	131%	113%

Failure modes from each of the tested specimens are shown in Figure C.6. As shown in the figure, all beams fractured inside the middle third of the span (±5%); therefore, all results are valid.

(a) UHPC 1500 (b) UHPC 1700 (c) UHPC 1900

Figure C.5 Flexural specimen failure modes

C.4 Splitting Tensile Strength Test

Detailed 28-day splitting tensile strength test results from each of the three developed UHPC mixes and a commercial UHPC mix are presented in Figure C.2 to C.5.

Table C.5 Splitting tensile test results of different mixes

Mix Design	Specimen No.	Maximum Tensile Strength (ksi)	Avg. Tensile Strength (ksi)	COV%
UHPC 1450*	#1	2.26	1.95	16.41
	#2	1.98		
	#3	1.62		
UHPC 1700	#1	2.09	1.88	11.48
	#2	1.66		
	#3	1.89		
UHPC 1900	#1	1.93	1.93	10.28
	#2	1.74		
	#3	2.13		
Commercial	#1	2.08	2.40	11.84
	#2	2.49		
	#3	2.63		

* Tested at 56-day instead of 28-day

C.5 Direct Shear Test

Detailed 28-day direct shear test results from each of the three developed UHPC mixes and a commercial UHPC mix are presented in Table C.7.

Table C.6 Direct shear test results of different mixes

Mix Design	Specimen No.	Shear stress (Ksi)	Avg. Shear Stress (Ksi)	COV %
UHPC 1450	#1	5.18	5.23	5.51
	#2	5.05		
	#3	5.05		
	#4	5.65		
UHPC 1700	#1	5.28	4.77	9.62
	#2	4.39		
	#3	4.37		
	#4	5.03		
UHPC 1900	#1	5.93	5.67	5.57
	#2	5.64		
	#3	5.24		
	#4	5.89		
Commercial	#1	4.79	5.95	17.69
	#2	6.23		
	#3	6.84		

*Measured at 56-day instead of 28-day

Typical failure mode from the direct shear test is shown in Figure C. 8. As shown in the figure, all specimens failed in double shear failure mode.

Figure C.7 Direct shear test failure mode

C.6 Slant Shear Test

Detailed 28-day slant shear test results from each of the three developed UHPC mixes and a commercial UHPC mix with as-cut and deep grooved surfaces are presented in Table C.7 and C.8 respectively.

Table C.2 As-Cut surface texture slant shear test results

Mix Design	Specimen No.	Type of Failure	Interface Shear Resistance (Ksi)		COV %
			Resistance	Average	
UHPC 1450[1]	#1	Interface Break	4.65	4.34	10.1
	#2		4.03		
	#3		1.40[2]		
UHPC 1700	#1		3.72	3.79	2.46
	#2		3.75		
	#3		3.89		
UHPC 1900	#1		3.40	3.59	7.74
	#2		3.91		
	#3		3.46		
Commercial	#1		4.27	4.12	4.10
	#2		4.15		
	#3		3.94		

[1] Measured at 56-day instead of 28-day

[2] The specimen failed at a low value with bond failure and is not taken in the average

Table C.3 Deep grooved surface texture slant shear test results

Mix Design	Specimen No.	Type of Failure	Interface Shear Resistance (Ksi)		COV %
			Resistance	Average	
UHPC 1450	#1	CC Failure	4.19	4.63	8.37
	#2		4.77		
	#3*		4.92		
UHPC 1700	#1		5.00	4.79	7.35
	#2		4.97		
	#3		4.38		
UHPC 1900	#1		4.46	4.72	4.95
	#2		4.87		
	#3		4.84		
Commercial	#1		4.57	4.47	3.31
	#2		4.30		
	#3		4.54		

*Tested at 56-day instead of 28-day

C.7 Bond Strength Test

The failure mode of the bond strength test of the commercial UHPC mix and the developed UHPC 1900 mix are presented in Figures C. 9 and C. 10, respectively.

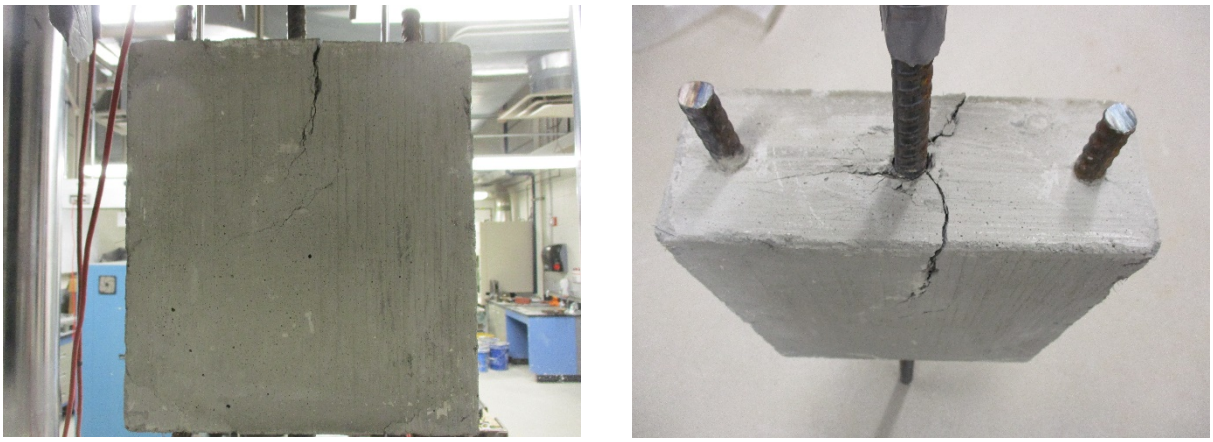

(a) Specimen #1

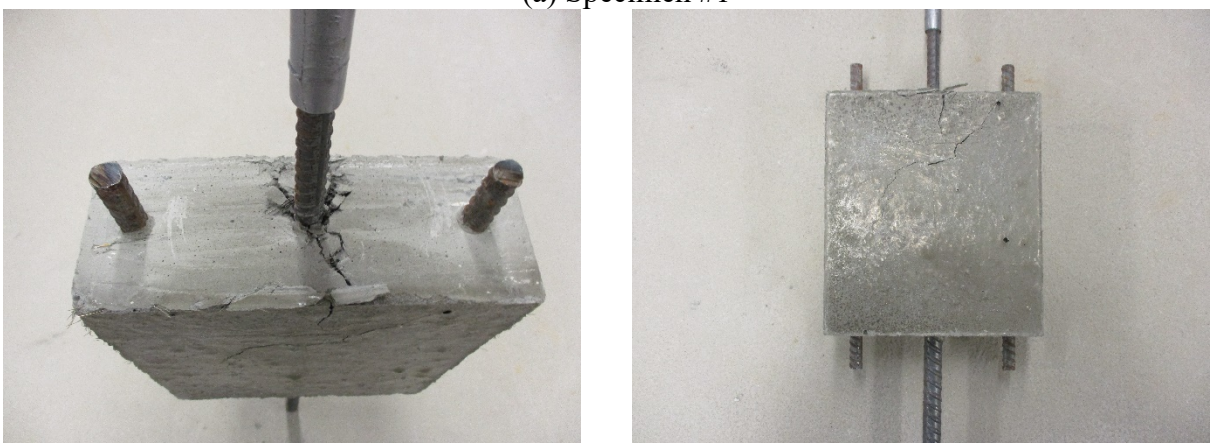

(b) Specimen #2

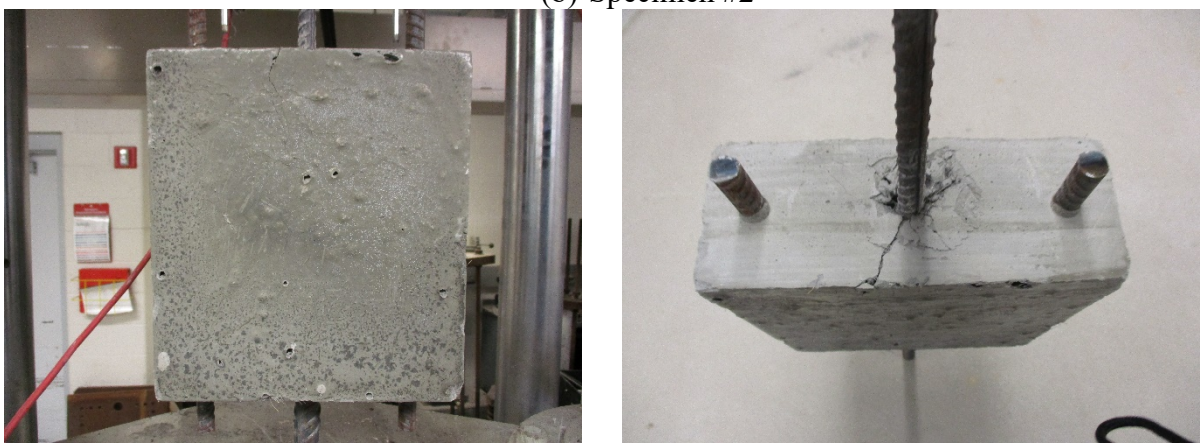

(c) Specimen #3

Figure C.8 Bond strength test results of commercial UHPC mix specimens

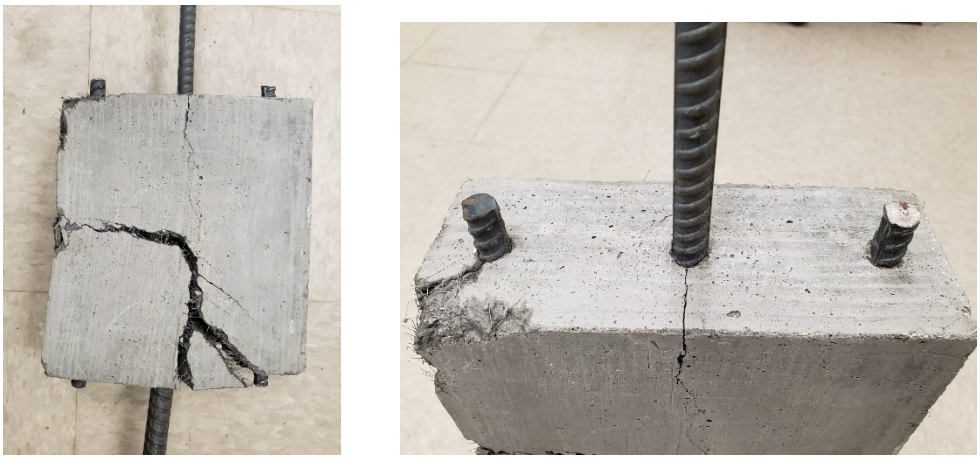

(a) Specimen #1

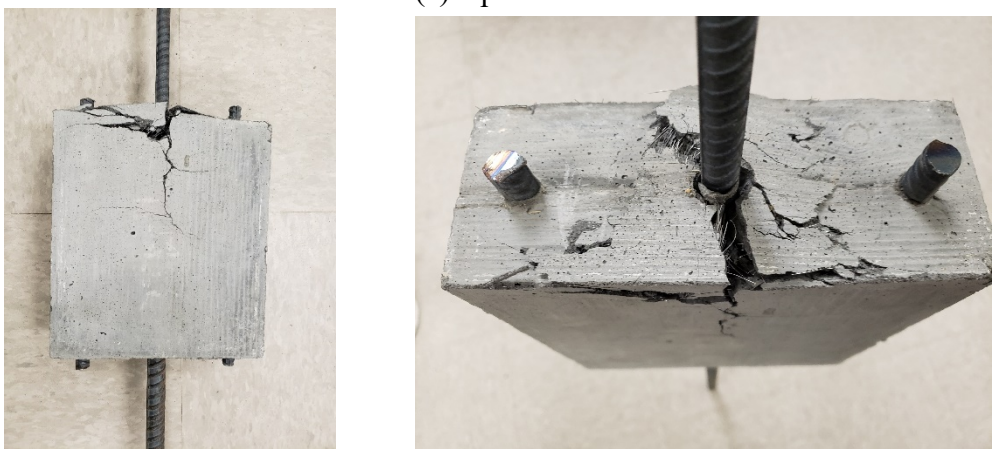

(b) Specimen #2

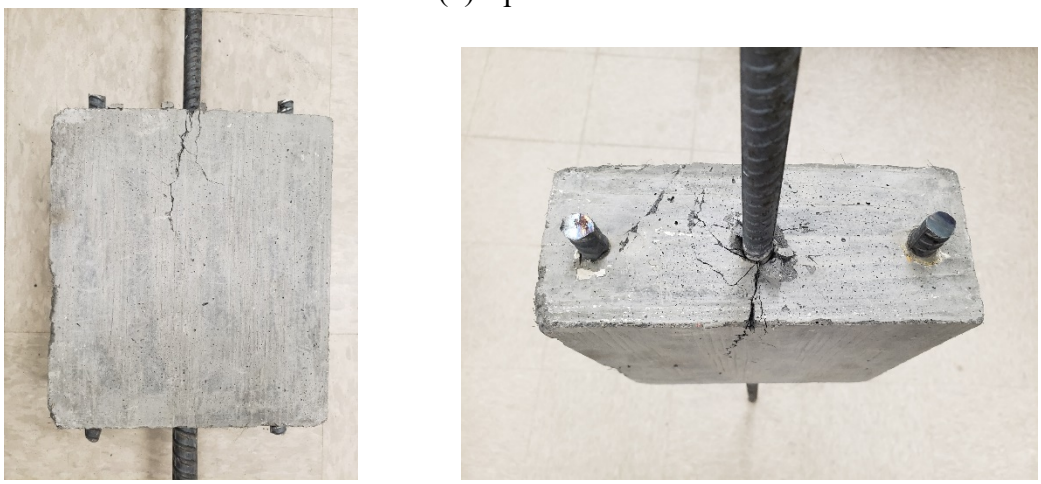

(c) Specimen #3

Figure C.9 Bond strength test results of UHPC 1900 mix specimens

APPENDIX D. STUDY OF IMPACT OF CURING ON MECHANICAL PROPERTIES

Since concrete compressive strength is highly depended on the type of curing method used, the effect of different curing procedures was evaluated with specimens from the UHPC 1900 mix. In addition to the standard curing method, two accelerated curing procedures were investigated with the intention of simulating the effect of heat curing in a standard precast plant.

According to the PCI Architectural Quality Control Manual, an oven curing method procedure was used on one set of specimens. After the specimens were cast in plastic molds, they were immediately covered and placed at the room temperature (73ºF) for 6 hours until the initial set. Specimens were then moved to an oven with temperature was preset at 90º F. After one hour, the temperature was increased by 15ºF/hour for three hours until the oven temperature reaches 135º F. The specimens were left at 135º F for 9 hours, followed by the temperature reduced in intervals of 10ºF/hour until the oven temperature reached 90ºF. After one hour at 90ºF, the cylinders were removed from the oven, stripped out, and allowed to cool down and then placed in lime saturated water at 73ºF till the day of testing.

Following steam curing procedure presented on report No. FHWA-HRT-13-060, a hot bath method curing procedure was applied on another set of specimens. After the specimens were cast in plastic molds, they were immediately covered and left at the room temperature (73ºF) for 6 hours until the initial set. Plastic molds were then carefully removed, and specimens were submerged in a hot water bath with a constant water temperature of 182ºF. After 58 hours, the specimens were removed out from the water and left to cool down in air at 73ºF then placed in lime saturated water at 73ºF till the day of testing. Figure D.1 illustrates the temperature setting profile for the oven and hot bath accelerated curing methods.

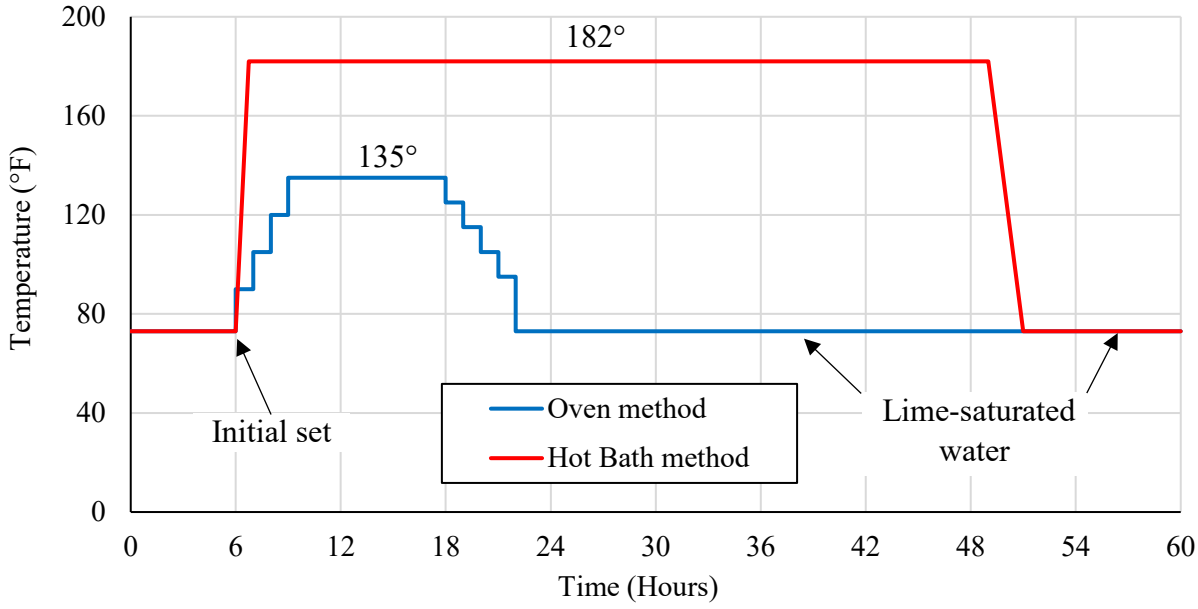

Figure D.1 Temperature setting profiles for oven and hot bath accelerated curing methods

The average compressive strength results at 1, 4, 7, and 28 days from the two above-mentioned accelerated curing procedures, and the standard curing method are presented in Figure D.2. Results indicate that the accelerated curing procedures result in approximately 68% and 119% higher 1-day compressive strength than standard curing procedures for the oven and hot bath

curing procedures, respectively. However, with the two accelerated curing method, the strength growth slows down after 4-day. The hot bath method cylinders achieved 21.25 ksi at 28-day, which is 20% higher than the standard cured method.

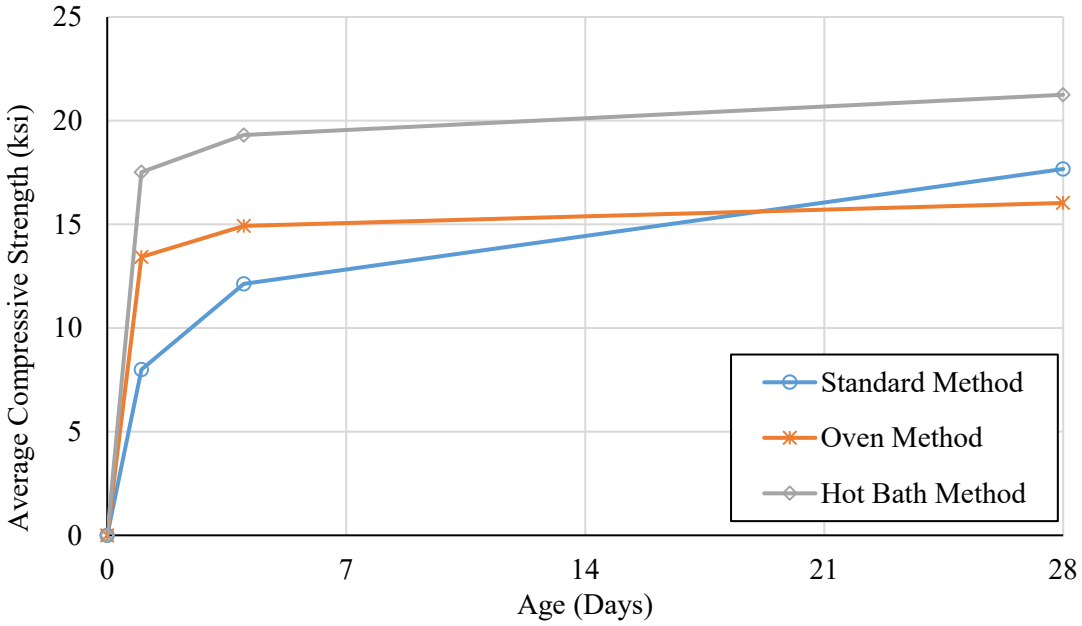

Figure D.2 Effect of curing procedures on UHPC compressive strength

APPENDIX E. STUDY OF IMPACT OF FIBER STABILITY ON MECHANICAL PROPERTIES

To evaluate the extent of the impact of mix stability to fiber distribution and mechanical properties, two sets (three specimens each) of 3×3×14in. flexural strength test prisms were prepared with high fiber stability (UHPC 1900-B) mix. The first three specimens were tested according to ASTM C78 by turning the test specimen on its side with respect to the specimen position when casted. The other three specimens were tested in the as-cast direction, without turning to its side. The flexural test was conducted following the same procedure as detailed in section 3.4 and the failure mode of all tested specimens results of the flexural strength test are shown in Figure E.1. As shown in the figure, all beams fractured inside the middle third of the span (±5%); therefore, all results are valid.

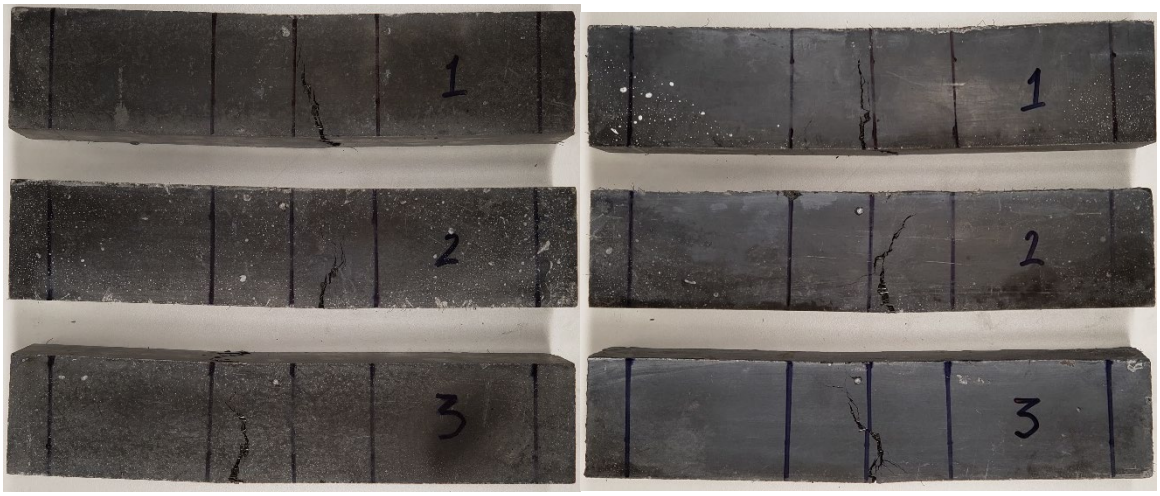

(a) Side Orientation (b) As-Cast Orientation

Figure E.1 Failure modes of flexural strength test specimens of UHPC 1900-B mix tested at two different orientations

As the key parameters as summarized in Table E.1, there is no significant difference in first cracking and peak flexural strengths.

Table E.1 Effect of specimen orientation on flexural strength of UHPC 1900-B mix

Specimen orientation	f'_c (ksi)	Flexural strength at first crack (ksi)	Peak flexural strength (ksi)
Side	16.16	3.04	4.88
As-Cast		3.39	4.90

Detailed flexural strength test data, together with the representative cross section from test specimens, showing fiber orientation at mid-span are shown in Figure E. 2.

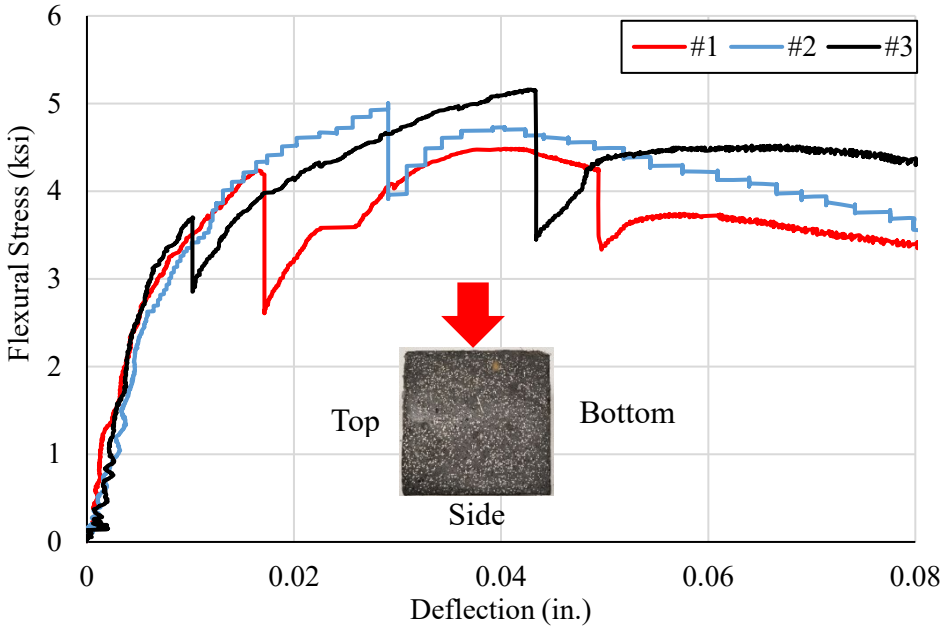

(a) Side

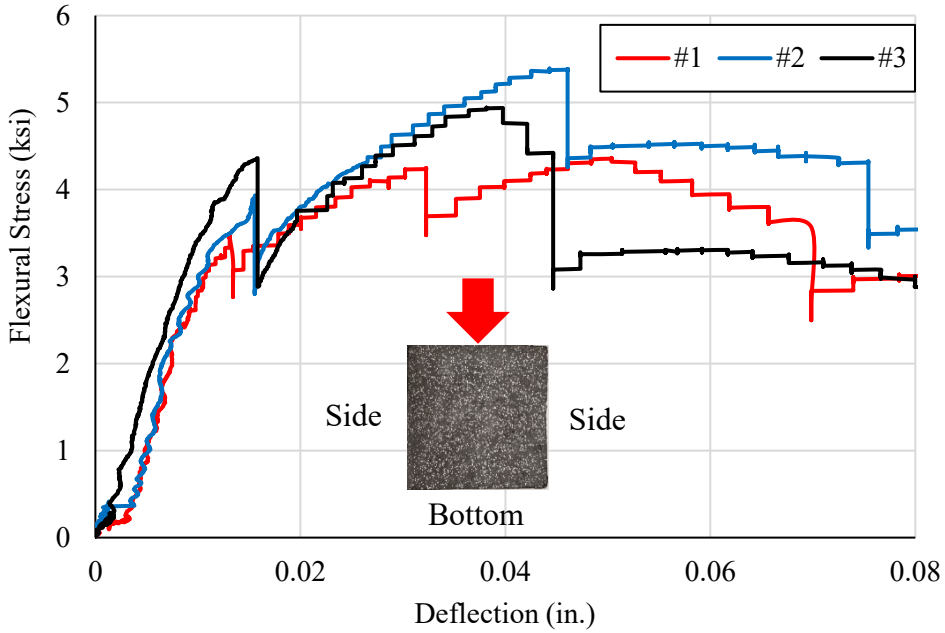

(b) As Cast

Figure E.2 Flexural strength results of different specimen orientation for high stability mix

With the low stability mix (UHPC 1900-A), three specimens were tested according to ASTM C78 by turning the test specimen on its side with respect to the specimen position when casted. As shown in Figure E.3, all beams fractured inside the middle third of the span (±5%); therefore, all results are valid.

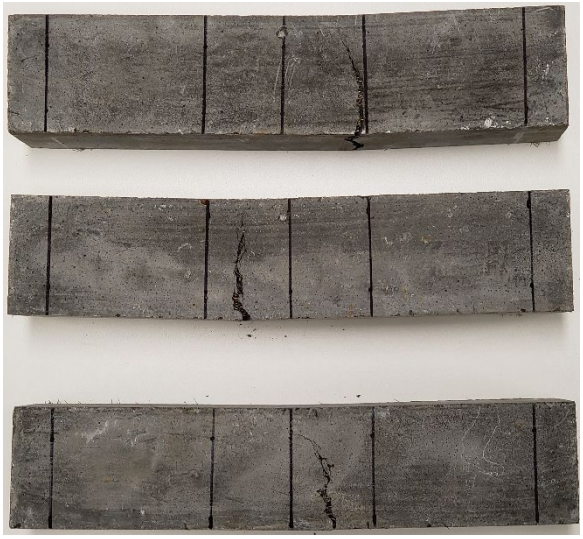

Figure E.3 UHPC 1900-A flexural specimens failure modes

Results, as summarized in Table E.2, indicated that while the mix still satisfied the minimum first crack and peak strengths of 1.5 ksi and 2 ksi, the first crack and peak strengths of UHPC 1900-A are reduced by 37% and 54%, respectively, compared to the more stable mix (UHPC 1900-B).

Table E.2 Effect of stability on flexural strength of UHPC 1900 mix

Mix	Flowability	f'_c (ksi)	Flexural strength at first crack (ksi)	Peak flexural strength (ksi)
UHPC 1900-A	High	17.67	1.91	2.26
UHPC 1900-B	Low	16.16	3.04	4.88

Figure E.4 provided detailed test results as well as the representative cross-section, in which fiber segregation was clearly observed.

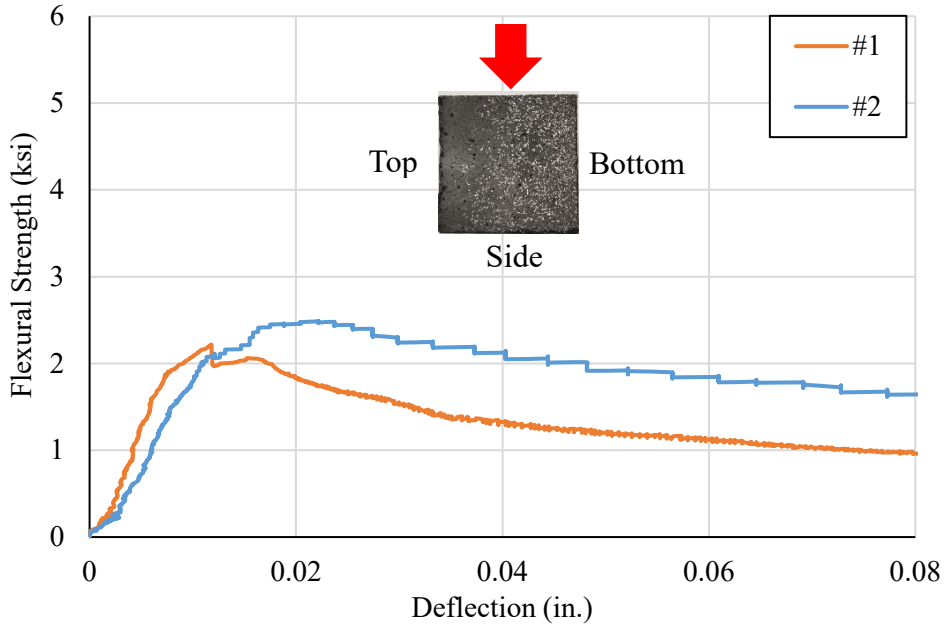

Figure E.1 Flexural strength results of high flowability UHPC 1900 mix (UHPC 1900-A)

Eight 2x2x6 in. direct shear prisms were prepared and tested with the same procedures as previously discussed. As illustrated in Figure E.5, results showed that with the low stability mix (UHPC 1900-A), the direct shear strength o is reduced by 30% compared to the high stability mix, which has the direct shear strength comparable to the commercial UHPC mix.

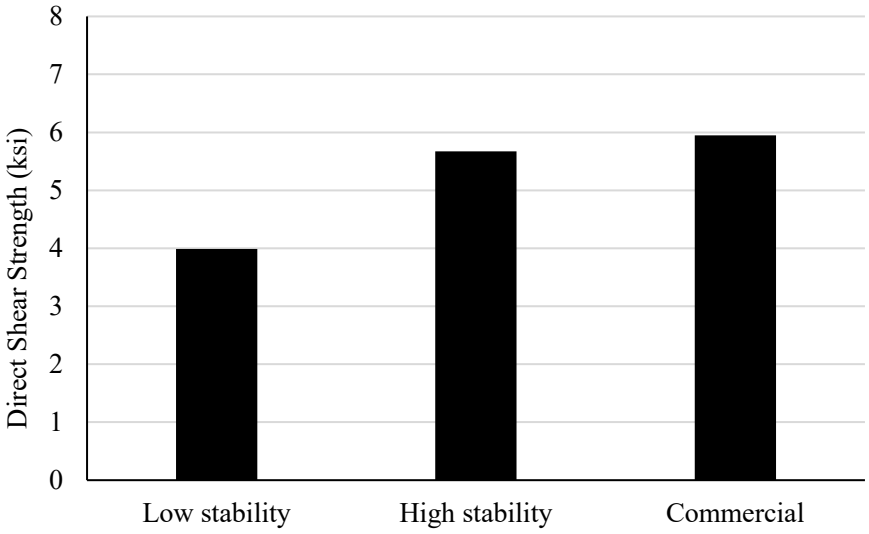

Figure E.2 Effect of stability on direct shear test results of UHPC 1900 Mix

Results indicated that mix stability is the key parameter that significantly affects the UHPC mechanical properties. Further study is needed to set up workability criteria to prevent undesired fiber stability issues during batching and casting.